Aus der Klinik für Kardiologie
der Medizinischen Fakultät Charité – Universitätsmedizin Berlin

DISSERTATION

Left ventricular strain analysis with cardiovascular magnetic resonance feature tracking (CMR-FT): a study in Landrace pigs
-
Analyse der linksventrikulären Strain mittels kardiovaskulärer Magnetresonanztomographie (CMR-FT): eine Studie an Landrassenschweinen

zur Erlangung des akademischen Grades
Doctor medicinae (Dr. med.)

vorgelegt der Medizinischen Fakultät
Charité – Universitätsmedizin Berlin

von

Alessandro Faragli

aus Alessandria (Italien)

Datum der Promotion: 25.06.2023

Summary

Abbreviations

List of abbreviations

2Ch	two chambers
3Ch	three chambers
4Ch	four chambers
avg	average
bpm	beats per minute
BSA	body surface area
BL	baseline
bSSFP	balanced steady-state free precession
CI	cardiac index
CAD	coronary artery disease
CMR	cardiac magnetic resonance
CMR-FT	cardiac magnetic resonance feature tracking
CO	cardiac output
CPO	cardiac power output
DENSE	displacement encoding with stimulated echoes
Dob	dobutamine
DP	diastolic pressure
Ees	end-systolic elastance
EDV	end-diastolic volume
ESPVR	end-systolic pressure volume relationship
ESV	end-systolic volume

FiO_2	fraction of inspired oxygen
GCS	global circumferential strain
GCSi	global circumferential strain indexed for mAOP
GCSw	global circumferential strain indexed for meridional Wall Stress
GLS	global longitudinal strain
GLSi	global longitudinal strain indexed for mAOP
GLSw	global longitudinal strain indexed for meridional Wall Stress
GRS	global radial strain
GRSi	global radial strain indexed for mAOP
GRSw	global radial strain indexed for meridional Wall Stress
HCM	hypertrophic cardiomyopathy
HF	heart failure
HFpEF	heart failure with preserved ejection fraction
HR	heart rate
ICC	intraclass correlation coefficient
LV	left ventricle / left ventricular
LVEF	left ventricular ejection fraction
LVESD	left ventricular end-systolic diameter
LVP	left ventricular pressure
LVP_{sys}	left ventricular pressure during systole
mAOP	mean aortic pressure
MRI	magnetic resonance imaging
PWT	posterior wall thickness

SAX	short axis
SD	standard deviation
SENC	strain-encoded imaging
SP	systolic pressure
STE	speckle tracking echocardiography
SV	stroke volume
SVR	systemic vascular resistance
TR	repetition time
TE	echo time
Ver	verapamil

1 Zusammenfassung

Hintergrund: Die Bildgebung bei linksventrikulärer (LV) Strain ist eine validierte Bildgebungstechnik, die in der Lage ist, die myokardiale Funktion zu quantifizieren. Während die echokardiographische Beurteilung des LV-Strain eine etablierte klinische Routine ist, ist die Analyse des LV-Strain mittels kardiovaskulärer Magnetresonanz (CMR) stattdessen eine neu aufkommende Methode. Im Besonderen ist die CMR-Feature Tracking (CMR-FT) eine vielversprechende Gewebeverfolgungstechnik, die für die Beurteilung der myokardialen Bewegung und Deformation entwickelt wurde. Inwieweit der systolische LV-Strain der CMR-FT die mechanische Funktion des Herzens widerspiegelt, muss jedoch noch vollständig verstanden werden. Aus diesem Grund war es das Ziel unserer Studie, die nicht-invasive CMR-FT LV-Strain mit invasiven hämodynamischen Parametern zu vergleichen, die für die mechanische Funktion des Herzens repräsentativ sind, wie z.B. Herzindex (CI), Herzleistung (CPO) und end-systolische Elastanz (Ees), indem sie bei verschiedenen inotropen Zuständen analysiert wurden.

Methoden: Zehn gesunde Landrace-Schweine wurden intubiert, mechanisch beatmet und in die 3-Tesla-MRT-Einrichtung transportiert. Nach den Basislinienmessungen (BL) wurden zwei Schritte durchgeführt: I) dobutamininduzierte Hyperkontraktilität (Dob) und II) verapamilinduzierte Hypokontraktilität (Ver). In jedem Schritt wurden MRT-Bilder in Kurzachsen- (SAX), 2Ch, 3Ch und 4Ch-Ansicht aufgenommen. Die Software MEDIS wurde zur Beurteilung der globalen Längs- (GLS), Zirkumferentiell- (GCS) und Radial Strain (GRS) verwendet. Die zum Nachweis einer relativen Änderung der BL-Strain erforderliche Probengröße wurde berechnet.

Ergebnisse: Dob erhöhte signifikant die Herzfrequenz, CI, CPO und Ees, während Ver sie

verringerte. GLS, GCS und GRS stiegen dementsprechend (im absoluten Wert) während der Dob-Infusion an, während GLS und GCS (im absoluten Wert) während der Ver abnahmen. Die lineare Regressionsanalyse zeigte eine mäßige Korrelation zwischen GLS, GCS und den hämodynamischen LV-Parametern, während GRS schlecht korrelierte. Die Indizierung globaler Strain Parameter für indirekte Messungen der Nachlast, wie z.B. mittlerer Aortendruck oder Wandspannung, verbesserte diese Korrelationen signifikant.

Schlussfolgerungen: Die globale Längs- und Zirkumferentiell Strain korreliert mäßig mit LV-invasiven Parametern wie der kardialen Leistung, dem kardialen Index und der end-systolischen Elastanz unter verschiedenen inotropen Zuständen. Die Indexierung von Strain Parametern für indirekte Messungen der Nachlast verbessert diese Korrelation erheblich. Die CMR-FT-LV-Strain kann in der klinischen Routine ein nützliches Instrument zur Charakterisierung der LV-Hämodynamik bei Patienten mit unterschiedlichem Grad der LV-Dysfunktion sein.

2 Abstract

Background: Left ventricular (LV) strain imaging is a validated imaging technique able to quantify myocardial function. While the assessment of LV strain is an established clinical routine in echocardiography, cardiovascular magnetic resonance (CMR) LV strain analysis is, instead, a newly emerging method. In specific, CMR feature tracking (CMR-FT) is a promising tracking technique for tissue developed for evaluating myocardial movement and deformation. However, to what extent CMR-FT LV systolic strain reflects the LV mechanical function of the heart still needs to be fully understood. For this reason, the aim of our study was to compare the non-invasive CMR-FT LV strain against invasive hemodynamic parameters representative of the mechanical function of the heart. This includes the cardiac index (CI), cardiac power output (CPO) and end-systolic elastance (Ees), and the data was compared by analyzing them at different inotropic states (hypercontractility and hypocontractility).

Methods: Ten healthy Landrace pigs were instrumented, intubated, mechanically ventilated, and transported to the 3-Tesla MRI facility. After baseline measurements (BL), two steps were performed: I) dobutamine-induced hyper-contractility (Dob) and II) verapamil-induced hypocontractility (Ver). At each step, MRI images were acquired at short axis (SAX), 2Ch, 3Ch and 4Ch views. The software MEDIS was utilized to assess the LV mechanical parameters such as global longitudinal strain (GLS), global circumferential strain (GCS) and global radial strain (GRS). Additionally, we calculated the sample size required for the detection of a relative change in baseline strain.

Results: Dob demonstrated a noteworthy increased heart rate, CI, CPO and Ees, while Ver decreased them. GLS, GCS and GRS accordingly increased (in absolute value) during Dob infusion, while GLS and GCS decreased (in absolute value) during Ver. Linear regression analysis demonstrated a moderate correlation between GLS, GCS and LV hemodynamic parameters, while GRS correlated poorly. The correlations were significantly improved by indexing global strain parameters for indirect afterload measures such as mean aortic pressure or wall stress.

Conclusions: Global longitudinal and circumferential strain moderately correlate with LV invasive parameters such as cardiac power output, cardiac index and end-systolic elastance under various inotropic states. Indexing strain parameters for indirect afterload measures greatly improves this correlation. CMR FT LV strain imaging may be a useful tool in the clinical routine to characterize the LV hemodynamics in patients experiencing different degrees of LV dysfunction.

3 Synopsis

3.1 Introduction

Left ventricular ejection fraction (LVEF) currently represents the most utilized parameter in the cardiology clinics for identifying the function of the heart[3, 4, 5]. Even if easy and fast to assess even with a simple echocardiography, changes in LVEF generally happen late in myocardial diseases, due to several intrinsic limitations of this parameter[3-7].

LVEF estimates only the global function of the ventricle and is not able to identify localized myocardial alterations[3, 6]. Indeed, patients presenting regional dysfunctions, such as hypokinetic segments, may still have a normal LVEF[8]. Another clear disadvantage is that LVEF, being a pure systolic parameter, does not provide any information on the relaxation of the ventricle and on the diastolic function[3, 6]. Eventually LVEF is dependent on the preload and afterload, being not optimal for the assessment of the intrinsic heart contractility[3, 6]. In other words, LVEF alone does not allow to reproduce and to fully understand the mechanical contraction of the heart[9, 10].

The mechanical action of the myocardium cannot be explained with LVEF only, due to the complex movements that the heart performs[11-13]. In specific, the cardiac base pushes towards the apex, the ventricular walls contract following an inward direction while the base and the apex produce a rotational movement in opposite directions[11-13]. From an anatomical point of view, the subendocardial fibers are the ones producing the longitudinal shortening and torsion, expressed as the clockwise rotation of the apex and the counterclockwise rotation of the base[11-13]. The mid-wall layer is, instead, responsible thanks to the circumferentially oriented fibers to the circumferential rotation, while the epicardial fibers are responsible for the longitudinal stretching of the apical counterclockwise rotation and of the

basal clockwise rotation[11-13]. For a better characterization of myocardial deformation in different cardiovascular diseases, several imaging techniques have been developed in the past years, ranging from echocardiography to cardiovascular magnetic resonance (CMR)[14-16]. Pathologic wall motion abnormalities can be simply detected visually with both echocardiography and CMR, however, are often difficult to be fully interpreted being highly subjective and poorly reproducible[17].

For this reason, myocardial strain has been proposed in the past decades as an innovative method able to quantitatively assess the regional and global myocardial function and the deformation ability of the heart both in systole and in diastole, avoiding as much as possible geometric assumptions[3, 8, 17, 18]. Myocardial strain can identify the longitudinal and circumferential shortening together with radial thickening and torsion, describing at its best the mechanical movements of the heart[17]. Myocardial strain can be defined as a measure of the degree of deformation of a myocardial segment from its initial length (L_0, usually in end diastole) to its maximum length (L, usually in end systole). It is generally expressed as a percentage with the following formula: myocardial strain: $L - L_0 / L_0$[17].

Originally strain imaging has been derived by echocardiographic tissue Doppler myocardial velocities[19], but more recently speckle tracking echocardiography (STE) has become the most preferred and widest available echocardiographic technique, mainly because it can be easily performed with standard B-Mode images[6, 20]. Numerous studies have shown that LV strain measured through STE is useful for the diagnosis of several pathologies, identifying subclinical myocardial regional changes, in various patients' populations[20-25]. Some studies showed even the impact of LV strain as a marker of prognosis in cardiovascular pathologies such as heart failure with preserved EF (HFpEF), coronary artery disease (CAD), diabetes mellitus, hypertensive heart disease and hypertrophic cardiomyopathy (HCM)[20, 26-33].

In the past years, CMR has emerged as an extremely valid technique to assess the heart function and morphology in a more complex way than the standard echocardiography, and strain has been widely studied and developed by using various MRI methodologies[15, 17, 34]. The most validated technique to assess myocardial strain is CMR tagging[18, 35, 36], a method that was first developed by the group of Zerhouni et al[37]. The method is based on an acquisition phase in which magnetic labels or tags are orthogonally over-imposed to the myocardium at the start of the cine sequences. The subsequent deformation and movement of such lines is analyzed throughout the cardiac cycle detecting myocardial deformation[37, 38]. However, the main limitations of CMR tagging are given by tag fading and by the low spatial resolution, due to reduced number and density of tag lines, producing a reduced accuracy in thin myocardial walls[37, 38]. More advanced techniques of CMR tagging, such as displacement encoding with stimulated echoes (DENSE) or strain-encoded imaging (SENC) have been developed in the past years to improve the reliability of the method, however, have mainly remained research tools without obtaining a large spread in the clinical routine[17]. The main reason is that basic or advanced CMR tagging require long dedicated acquisition sequence and mostly time-consuming post processing work through specific software solutions[17].

A relatively new approach, CMR tissue tracking, has recently attracted interest in the cardiovascular imaging field[15]. Tissue tracking has developed as a new strategy to detect myocardial motion and deformation and it has been appeared to be precise in the detection of myocardial movement and function by utilizing basic steady-state free procession sequences[33, 34, 39-41]. CMR feature tracking (CMR-FT) is a relatively new technique that focuses on the contouring of the endocardium and epicardium, allowing the contrast between the myocardium and the blood pool to be identified and it then can be applied to routinely

acquired cine CMR images [42, 43]. CMR-FT estimates global longitudinal strain (GLS) from at least two long-axis cine images while global circumferential (GCS) and global radial strains (GRS) are extracted from the short-axis cine images[42, 43]. It has been shown that the CMR-FT is comparable to speckle tracking for assessing myocardial strain[44]. Moreover, CMR-FT has been also validated against myocardial CMR tagging technique for the assessment of regional myocardial motion in humans showing promising results by being simpler and faster than tagging techniques, that need instead a laborious post-processing analysis [45-47].

Nonetheless, even CMR-FT myocardial strain has not entered completely the routine assessment of the myocardial function in CMR and LVEF is still the most utilized parameter[20]. One reason is driven by the lack of studies investigating the physiological validation of CMR-FT against hemodynamic invasive measurements[17, 48]. Moreover, also LV strain is known to present the same limitation as LVEF, being a load-dependent measurement and is not able to depict optimally myocardial contractility[8, 20].

Load-independent measurements are generally achieved through hemodynamic catheterization and, in specific, with the analysis of pressure-volume loops[49]. In facts, the invasive assessment of end-systolic elastance (Ees) represents the gold standard method for assessment of the contractile function of the heart[49]. To assess the LV systolic function and dysfunction and cardiac reserve invasively measured parameters such as cardiac index (CI) or cardiac power output (CPO) represent some of the most accurate[50, 51]. CPO has been shown to be effective in identifying the mechanical function of the heart. It couples cardiac work with the response of the vasculature, providing an assessment of the intraventricular flow. On other words, it explains the mechanical function of the heart much more than any other hemodynamic parameter[50, 52]. Eventually, CPO has been shown to be a useful clinical parameter able to predict the prognosis of heart failure patients[53, 54].

However, whether CMR-FT LV strain reflects the hemodynamic parameters and is able to describe the mechanical function of the myocardium above has not been yet investigated. Even less is known of the behaviour of CMR-FT strain during different inotropic states, such as hyper- or hypocontractility states, or during stress and ischemia.

For this reason, the primary aim of the current study was to compare CMR-FT LV strain parameters with invasively measured hemodynamic parameters such as CI, CPO and the Ees under various inotropic states in pigs. Since data on CMR-FT LV strain in large animals such as Landrace pigs are lacking, a secondary aim of our study was to evaluate the inter- and intra-observer reproducibility of CMR-FT derived strain measurements necessary to calculate the sample size and aimed to define the number of animals needed for future studies.

3.2 Methods

The experimental study was approved by the ethical committee of Berlin, Germany (G0138/17), and is conformed to the “European Convention for the Protection of Vertebrate Animals used for Experimental and other Scientific Purposes” (Council of Europe No 123, Strasbourg 1985).

Experimental setup and protocol

The experimental setup is displayed in Figure 1.

Figure 1. The experimental setup. This panel represents the experimental setting and setup. The Landrace pigs were instrumented with a closed chest procedure in the operating

room (A) (B) and were then transported to the MRI where anesthesia and monitoring was kept during the whole experiment (C) (D). This Figure refers to the published article by Faragli et al[1].

Ten (n=10) female Landrace pigs (51±10 kg) were sedated and intubated on the day of the experiment. To achieve the goal of a deep sedation to obtain a stable, hemodynamics, the anaesthesia was set with fentanyl, midazolam, ketamine and pancuronium and a low dose of isofluorane. Pigs were invasively ventilated (Cato, Dräger Medical, Germany) with a FiO2 of 0.5, an I: E-ratio of 1:1.5, a positive end-expiratory pressure of 5 mmHg and a tidal volume of 10 ml kg-1. The respiratory rate was kept at an end-expiratory carbon dioxide partial pressure of 35-45 mmHg. Respiratory gases, heart rate (HR), and invasively derived arterial blood pressure were continuously monitored. Body temperature was measured with a sublingual thermometer and was maintained at 38°C during CMR imaging through air ventilation or, if needed, infusion of cold saline solution. An acute instrumental examination of the animal occurred, closed chest, and then transported to the MRI facility for examination. The protocol consisted in baseline measurements (BL) and in two different steps: I) Dobutamine-stress (Dob), defined also as hypercontractility, and II) verapamil-induced cardiovascular depression (Ver), defined as hypocontractility. MRI images were acquired in the short axis (SAX), 2Ch, 3Ch and 4Ch views at each protocol step.

The pharmacologic protocol was established in a previous a small pilot study (data not shown), with the goal of obtaining an optimal titration of dobutamine and verapamil. During this study data were assessed by LV invasive conductance measurements in line with previous publications from our study group [55]. The infusion of dobutamine was titrated to achieve the 25% increase in heart rate compared to baseline values and verapamil was

administered with the aim of decreasing the cardiac index (CI) to 25% of the original value. For each experiment, Verapamil was given in repeated 2.5 mg boluses to avoid significant hypotension that would cause hemodynamic instability. For this reason, CI was continuously assessed in real-time. In case CI was not decreased as expected, a further bolus was administered. A wash-out period of 30 minutes was performed between the different protocol steps. At the end of the protocol the animals were transported back to the operating room for sacrifice. As standard procedure, 80 mmol bolus of potassium was injected to sacrifice the animal into the coronary artery.

Cardiac magnetic resonance image acquisition and analysis

The CMR images were acquired using a 3T MRI scanner (Ingenia, Philips Healthcare, Best, The Netherlands) composed of an anterior- and a built-in posterior coil element. Up to 30 coil elements were employed and adjusted on the individual anatomy of the animals. All the animals were scanned with identical imaging protocols. The research protocol initially included the first scout to determine cardiac imaging planes. All the cine images were acquired using the ECG-gated balanced steady-state free precession (bSSFP) sequence obtained in three LV long-axis (two-chamber, three-chamber, and four-chamber) planes. The short-axis (SAX) slices encompassing the entire LV were stacked through the ventricular two-chamber and four-chamber planes. The following imaging parameters were utilized: repetition time (TR) = 2.9 ms, echo time (TE) = 1.45 ms, flip angle = 45°, measured voxel size = 1.9 × 1.9 × 8.0 mm3, reconstructed voxel size 1.0 x 1.0 x 8mm^3, and 40 cardiac phases.

All the acquired images were analyzed offline through a commercially available software (Medis Suite, version 3.1, Leiden, The Netherlands). The image analysis was based on the

CMR consensus document for the quantification of LV function[56]. A blinding of the data was conducted by assigning a numeric code to the exported images at the different measurements' steps. By doing so the observers were blinded.

In the SAX view, the endocardial borders of the LV were traced manually on all slices of each cardiac phase. The Simpson method of disks summation was utilized to calculate the volumes, by multiplying slice thickness (8mm) by the sum of the cross-sectional area. The Simpson method was utilized also to calculate the left ventricular ejection fraction (LVEF). The LV outflow tract, the papillary muscles and the trabeculations are included as part of the LV blood volume. The ascending aorta was outlined in all the acquired images allowing flow calculation in the corresponding velocity-encoded phase images. The average flow velocity (cm/s) was multiplied by the vessel area (cm2) to obtain the measurement of flow (ml/s). Then flow was utilized to calculate the cardiac cycle and obtain stroke volume (SV). Cardiac output (CO) was indirectly calculated as the product of SV and HR.

Concerning strain 2Ch, 3Ch and 4Ch cine images, and respectively, 3 preselected mid-ventricle slices from SAX images were utilized for the analysis. The endocardial and epicardial contours previously drawn with QMass version 8.1 were transferred to QStrain RE version 2.0. Here, after the application of the tissue tracking algorithm, endocardial and/or epicardial borders were detected in the cardiac cycle (Figure 2A, 2D). The long-axis cine images were utilized to compute GLS strain, instead the short-axis images were utilized for the GLS and GRS strain (Figure 2B, 2E). Global strain was obtained by averaging the calculated systolic peak strain according to the American Heart Association 17 segments model, excluding the apex[57]. GCS was obtained from averaging circumferential strain for 6 basal, 6 mid and 4 apical segmental individual values; GLS as obtained from 2Ch, 3Ch and

4Ch averaging 6 basal, 6 mid and 4 apical segments and by using a bull-eye view (Figure 2C, 2F, 2G, 2H, 2I).

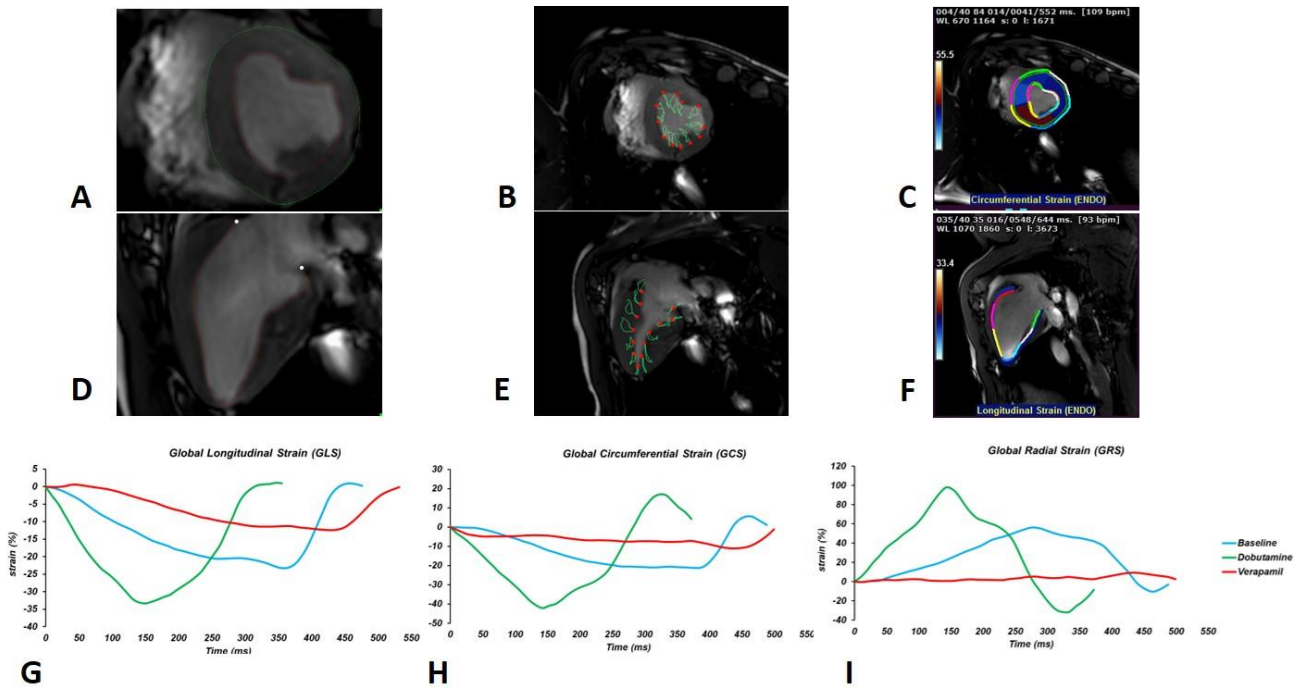

Figure 2. Measuring global strain analysis via Qstrain software and representative LV strain curves obtained from one animal. This figure shows the steps needed to obtain the global strain values of one pig. Displayed in Figure (A) are the endocardial and epicardial contouring in short axis; (B) the circumferential measured strain by Qstrain; (C) the end-systole time-to-peak circumferential strain; (D) the endocardial contouring in longitudinal axis; (E) the longitudinal strain measured by Qstrain; (F) the end-systole time-to-peak longitudinal strain; and the (G) GLS, (H) GCS, and (I) GRS curves during BL, Dob and Ver (mean values of all segments). This Figure refers to the published article by Faragli et al[2].

Hemodynamic parameters

Systolic (SP) and diastolic (DP) blood pressure and mean aortic pressure (mAOP) were measured invasively with a pressure sensing catheter placed in the carotid artery for the entire protocol study. The systemic vascular resistance (SVR) was calculated in the following manner:

$$(1)\, SVR_{mmHg/L} = \frac{Mean\ Arterial\ Pressure\ (MAP) - Right\ Atrial\ Pressure}{Cardiac\ Output\ (CO)}$$

Cardiac power outpt (CPO) was calculated as follows:

$$(2) CPO = \frac{CO \times mAOP}{451}$$

Cardiac index (CI) was calculated as follows:

$$(3) CI = \frac{CO}{BSA}$$

End-systolic elastance (Ees) was calculated as follows:

$$(4) Ees = \frac{LVP_{sys}}{V_{LVP_{max}} - V_0}$$

where:

$$LVP_{sys} = \frac{2}{3} Systolic\ Blood\ Pressure + \frac{1}{3} Diastolic\ Blood\ Pressure$$

$$V_{LVP_{max}} = End\text{–}Systolic\ Volume$$

$$V_0 = 0$$

as already described in the study by Kelly et al[58].

GLS, GCS and GRS were indexed to the indirect measure of afterload, namely mAOP by adapting the formula published by Rhea et al [59]:

$$(5)\frac{Global\ Strain \times mAOP}{avg(mAOP)}$$

where Global Strain equated to the global value obtained from either longitudinal (GLSi), circumferential (GCSi) or radial (GRSi) strain and avg(mAOP) was the respective average of the mAOP measured for each step of the protocol, namely at baseline, dobutamine and verapamil.

The calculation of meridional wall stress was obtained via the following formula[60]:

$$(6)LV\ wall\ stress = \frac{(0.334 \times LVP_{sys} \times LVESD)}{PWT \times [1 + PWT/LVESD]}$$

where LVESD = left ventricular end-systolic diameter, PWT = posterior wall thickness and LVP_{sys}= left ventricular pressure at systole, as already described in the work by Reichek et al[60].

Consequently, GLS, GCS and GRS were indexed to the above-defined wall stress utilizing the formula of the work by Reichek et al[60] as following:

$$(7)Global\ Strain\ indexed = \frac{Global\ Strain \times LV\ wall\ stress}{avg(LV\ wall\ stress)}$$

where Global Strain was obtained by indexing the global value of either longitudinal strain (GLSw), or circumferential strain (GCSw) or radial strain (GRSw). The calculated average (LV wall stress) was calculated for each protocol step, meaning at baseline, dobutamine and for verapamil (Table 1).

Statistical analysis, reproducibility and sample size

All data analysed are presented as mean ± SD. To understand whether the data were normally distributed the Shapiro-Wilk test was utilized. The Wilcoxon test was used for the

non-parametric variables. A p-value of <0.05 was defined as statistically significant. Linear regression analysis was utilized to assess the relationship between strain and hemodynamic data. The specific conditions (baseline, dobutamine, verapamil) were included as regressors in the linear regression model. The slopes were compared to see if the linear corelations differed significantly. If the slopes were not different, the intercept was compared, as previously described in the work by Weaver and Wuensch[61]. The data between groups measured at different inotropic states were analysed by utilizing the one-way ANOVA for repeated measurements. Post-hoc testing was calculated by Tukey's test. For statistical calculations, the software Sigmastat (Version 4.0, Systat Software, Inc) and SPSS (Version 23.0, IBM, Armonk, NY) were utilized.

The inter- and intra-observer reproducibility analysis was quantified by using intra-class correlation coefficient (ICC) and displayed with Bland-Altman plots[62]. The agreement was considered excellent in case of ICC >0.74, good for ICC 0.60–0.74, fair for ICC 0.40–0.59, and poor for ICC <0.40[43]. After 4 weeks of interval, the intra-observer data analysis was repeated. All the operators performed the measurements two times, and the averaged calculated values were taken.

The study sample size needed to detect a 5, 8 and 10% relative change in strain with a power of 80% and a significance of 5% was calculated with the following formula[63]:

$$(8) n = f(\alpha, P)\, \sigma^2\, 2 / \delta$$

where n represents the calculated sample size, α represents the significance level, P the required study power and f the calculated value of the factor needed for different values of α and P (f = 10.5 for α = 0.05 and p = 0.080), with σ representing the standard deviation of

differences in measurements between studies or observers and δ the desired difference to be found. The sample size calculation was only performed for baseline measurements.

3.3 Results

Systemic hemodynamics

The dose of dobutamine necessary to provide a 25% increase in HR was 6.4 ± 2.5 µg/kg/min, while 5 ± 2 mg of verapamil was needed to decrease CI of at least 25% from baseline.

Concerning systemic hemodynamics, a significant increase in heart rate (HR) during Dob administration (106 ± 15 to 146 ± 12 bpm) accompanied by a significant decrease during Ver (98 ± 19 bpm) was observed. Dob raised significantly baseline CO (6 ± 1 to 9 ± 2 L/min) and LV EF (59 ± 8 to 77 ± 7 %), while Verapamil decreased both significantly (4 ± 1 L/min and 39 ± 9 %). Systemic vascular resistance (SVR) significantly decreased with Dob (15 ± 5 to 11 ± 4 dyn*s*cm^{-5}) and increased during Ver (19 ± 9 dyn*s*cm^{-5}). Mean aortic pressure (mAOP) did not decrease significantly during Dob (90 ± 12 to 98 ± 19 mmHg), but significantly fell during Ver (70 ± 10 mmHg). Wall stress increased significantly during Dob (0.12 ± 0.02 to 0.16 ± 0.04 mmHg) and decreased during Ver (0.10 ± 0.02 mmHg). Cardiac power output (CPO) increased by Dob administration (1.2 ± 0.3 to 2.0 ± 0.6 W) and decreased significantly during Ver (0.7 ± 0.2 W). A similar effect was observed for CI with a significant rise during Dob (2.5 ± 0.2 to 3.8 ± 0.5 L/min/m^2) and fall during Ver (1.7 ± 0.7 L/min/m^2).

End-systolic elastance (Ees), representing the slope of the end-systolic pressure-volume relationship (EPSVR) increased significantly during Dob and decreased during Ver administration (Figure 3).

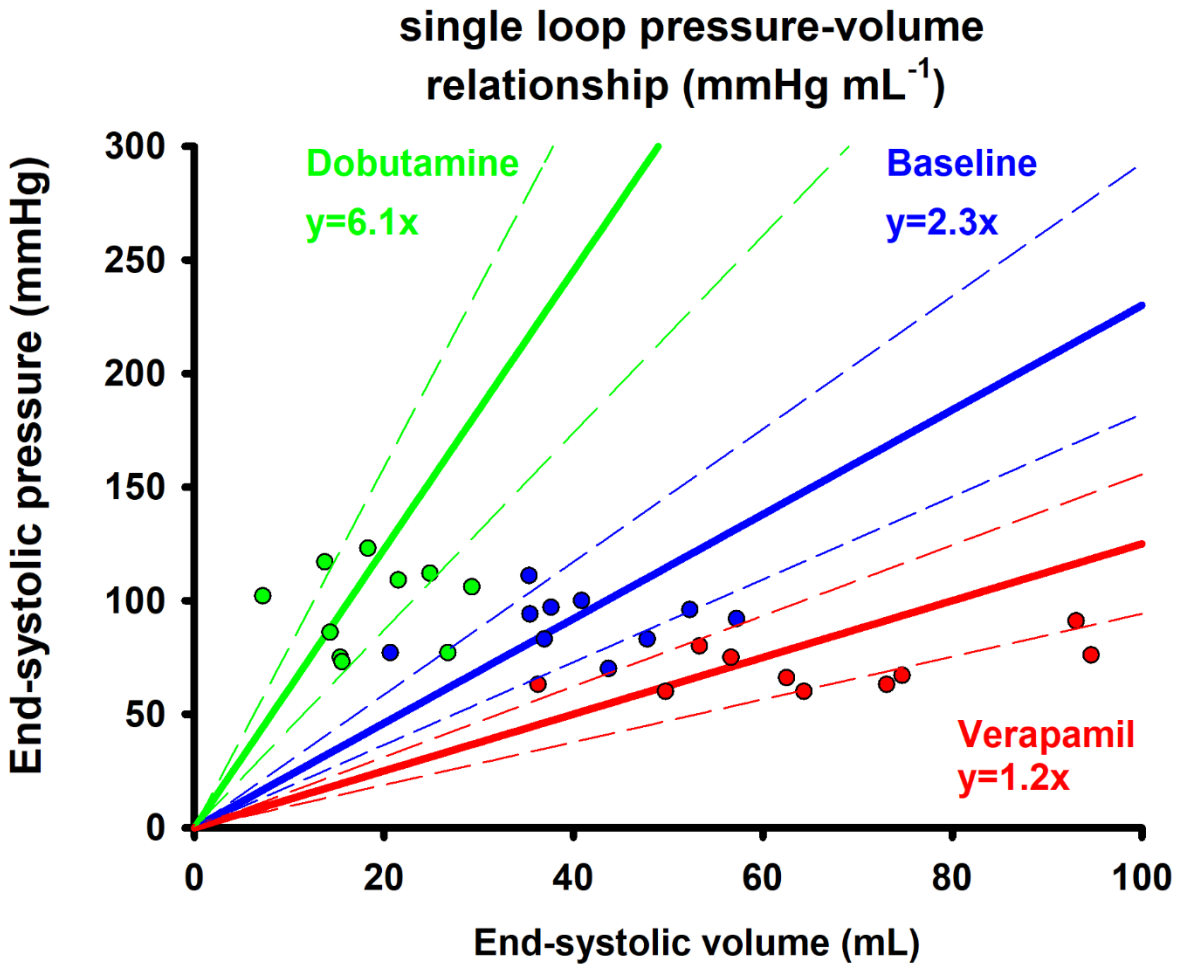

Figure 3. End-systolic pressure-volume relationship averaged for baseline, dobutamine and verapamil steps. A single-loop obtained from the end-systolic pressure-volume relationship (ESPVR) has been plotted under different inotropic states. The average ESPVR during dobutamine infusion is represented through the lines (green), at baseline (blue) and during verapamil (red). An increase in ESPVR with dobutamine and a decrease with verapamil are observed. Each animal is plotted in the data (n=10). The dashed lines are

representative of the 95% confidence intervals. This Figure refers to the published article by Faragli et al[2].

Global strain parameters

Global strain parameters are shown in Table 1A. Global longitudinal strain (GLS) and global circumferential strain (GCS) increased significantly during Dob, while a relevant decrease was observed during Ver. Global radial strain (GRS) was not significantly decreased during, while was decreased during Ver infusion.

Adjusting global strain parameters for mAOP (Table 1B) or for meridional wall stress (Table 1C) did not change the effects induced by Dob and Ver described above.

A.	**Baseline**	**Dobutamine**	**Verapamil**
GLS (%)	-23 ± 4	-45 ± 9*	-16 ± 3*, §
GCS (%)	-31 ± 8	-53 ± 10*	-17 ± 5*, §
GRS (%)	72 ± 19	88 ± 36	30 ± 12*, §
B.	**Baseline**	**Dobutamine**	**Verapamil**
GLSi (%)	-23 ± 4	-45 ± 10*	-16 ± 4*, §
GCSi (%)	-30 ± 8	-52 ± 8*	-16 ± 5*, §
GRSi (%)	71 ± 19	84 ± 23	30 ± 13*, §
C.	**Baseline**	**Dobutamine**	**Verapamil**
GLSw (%)	-23 ± 5	-44 ± 10*	-16 ± 3*, §
GCSw (%)	-31 ± 9	-52 ± 13*	-17 ± 17*, §

GRSw (%)	71 ±20	90 ±54	35 ±27*, §

Table 1. Global strain and adjusted global strain value measured under different variable force states. (A) Global strain values (B), global strain adjusted for mean aortic pressure (mAOP) and (C) global strain adjusted for meridional wall stress are displayed during BL, Dob and Ver states. N=10; *p<0.05 vs. BL; §p<0.05 vs. Dob. Dob = dobutamine; GLS = global longitudinal strain; GCS = global circumferential strain; GRS = global radial strain; GLSi = global longitudinal strain indexed for mAOP; GCSi = global circumferential strain indexed for mAOP; GRSi = global radial strain indexed for mAOP; GLSw = global longitudinal strain indexed for Wall Stress; GCSw = global circumferential strain indexed for Wall Stress; GRSi = global radial strain indexed for Wall Stress; mAOP = mean aortic pressure; Ver = verapamil.

Correlation between global strain, ejection fraction and hemodynamic parameters

Linear regression analysis demonstrated a moderate correlation between GLS, GCS and CPO, while only a weak correlation was observed between GRS and CPO (Figure 4A). s Similarly, between GLS, GCS and CI (Figure 4B) a moderate correlation was observed, while GRS poorly performed. A same observation could be drawn for GLS, GCS and Ees where a moderate correlation was found, while a poor one was observed in the correlation of GRS and Ees (Figure 4C).

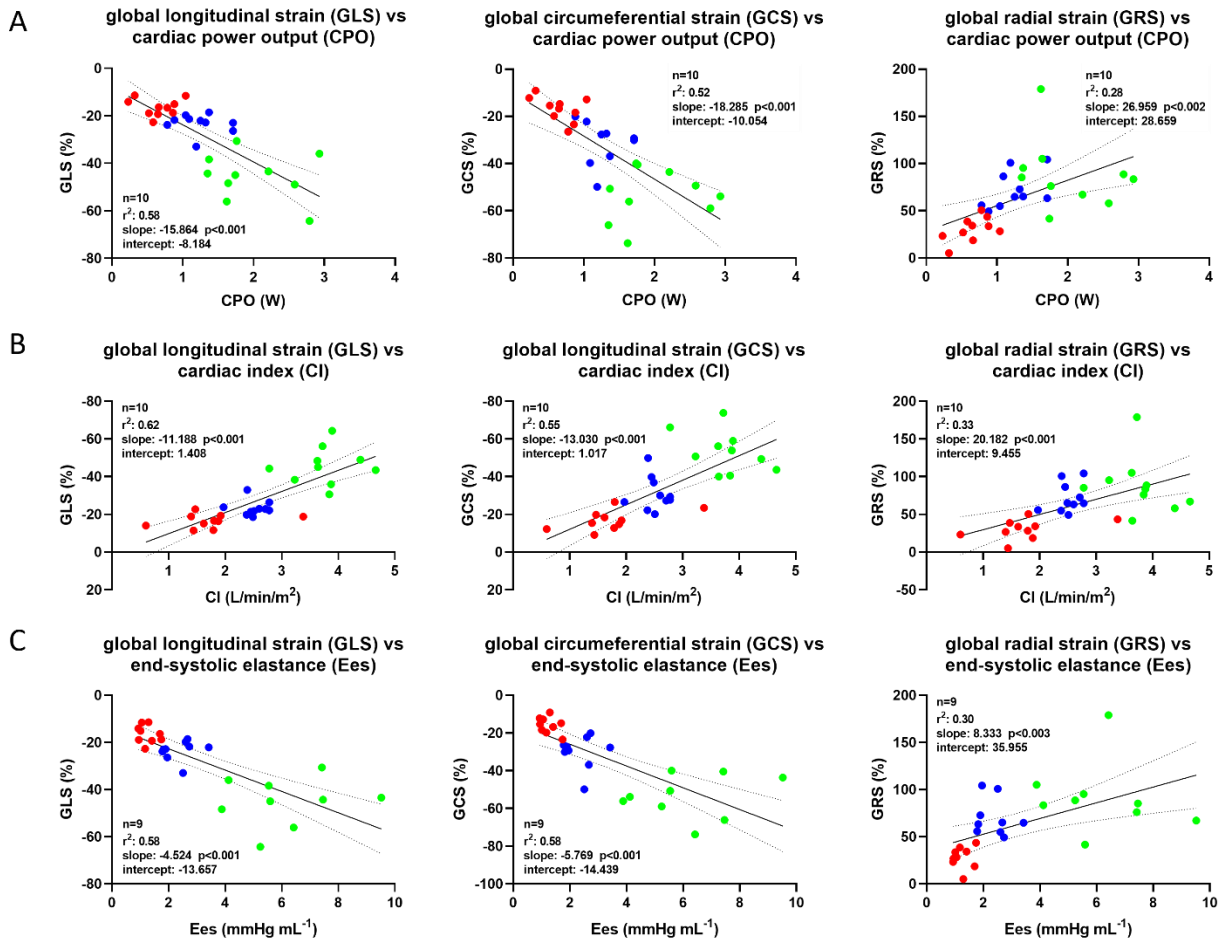

Figure 4. Correlation between global strain and invasive hemodynamic parameters. This panel displays the linear correlation analysis between invasive hemodynamic parameters and global strain values at different inotropic states. The linear regression analysis shows a moderate correlation between GLS and GCS against CPO (A), CI (B) and Ees (C). The correlation between invasive parameters and GRS was found to be poor (A-C). Blue points address BL, green ones' address Dob, and red ones' address Ver (n=10). BL = baseline; CI = cardiac index; CPO = cardiac power output; Dob = dobutamine; Ees = end-systolic elastance; GLS = global longitudinal strain; GCS = global circumferential strain; GRS

= global radial strain; Ver = verapamil. This Figure refers to the published article by Faragli et al[2].

By adjusting global strain parameters for mAOP or for wall stress the correlations with CPO (Figure 5A and 6A), with CI (Figure 5B and 6B) as well as with Ees (Figure 5C and 6C) improved. By analysing LVEF, we found a moderate correlation with CI and CPO (r^2 = 0.81 and r^2 = 0.69, respectively), comparable with the one obtained in GLSw with CI and CPO (r^2 = 0.74 and r^2 = 0.72, respectively). Moreover, GLSw moderately correlated with Ees in the same way as LVEF correlated with Ees (r^2 = 0.74 versus r^2 = 0.74). All the correlations were statistically different with a $p<0.0001$.

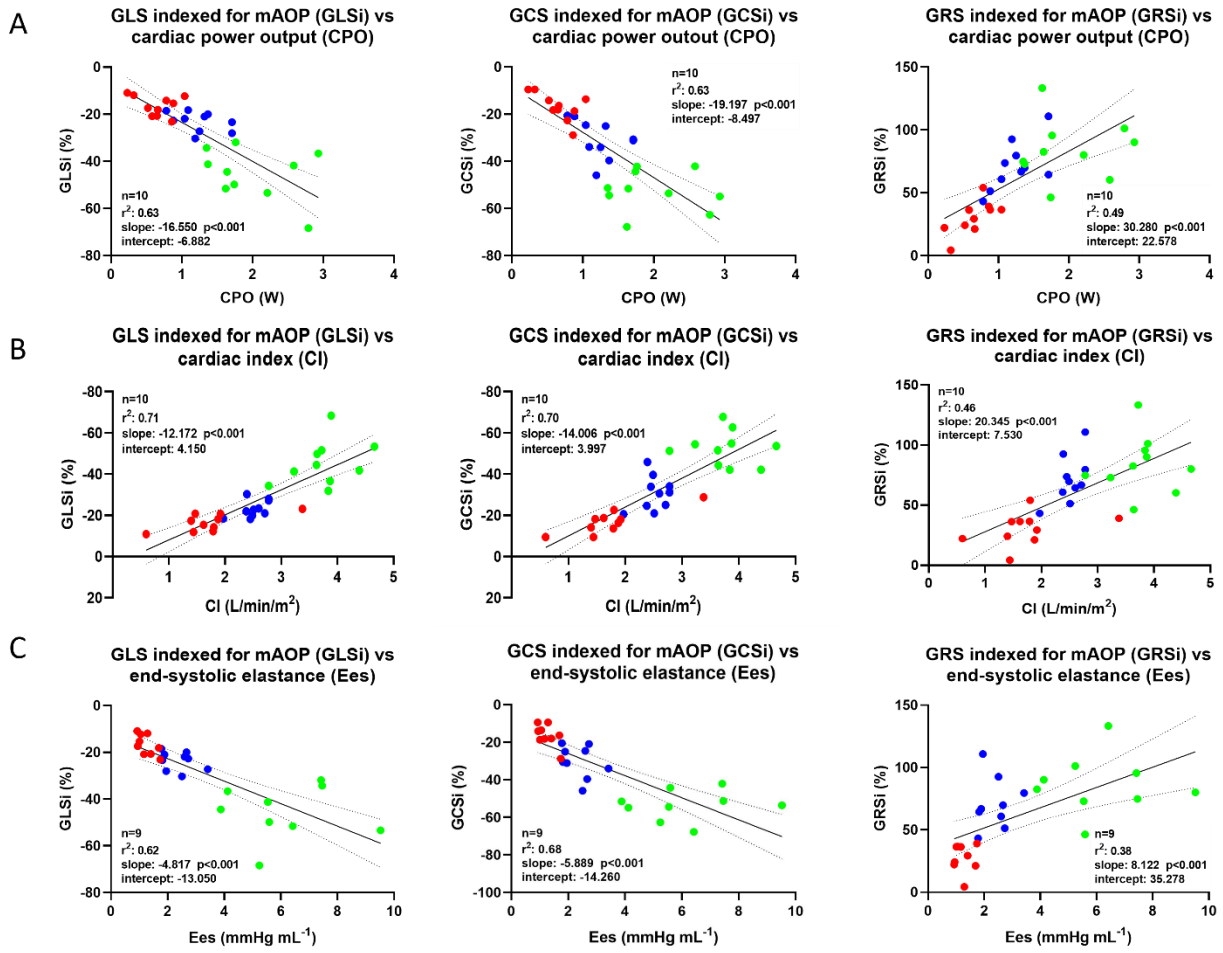

Figure 5. Correlation between global strain adjusted for mean aortic pressure and invasive hemodynamic parameters. This panel displays the linear correlation analysis between invasive hemodynamic parameters and global strain values indexed for mAOP at different inotropic states. The linear regression analysis between GLSi, GCSi, GRSi and CPO (A), CI (B), and Ees (C) improves after indexing global strain for mAOP. Blue points address BL, green ones' address Dob, and red ones' address Ver (n=10). BL = baseline; CI = cardiac index; CPO = cardiac power output; Dob = dobutamine; Ees = end-systolic elastance; GLSi = global longitudinal strain indexed for mAOP; GCSi = global circumferential

strain indexed for mAOP; GRSi = global radial strain indexed for mAOP; mAOP = mean aortic pressure; Ver = verapamil. This Figure refers to the published article by Faragli et al[2].

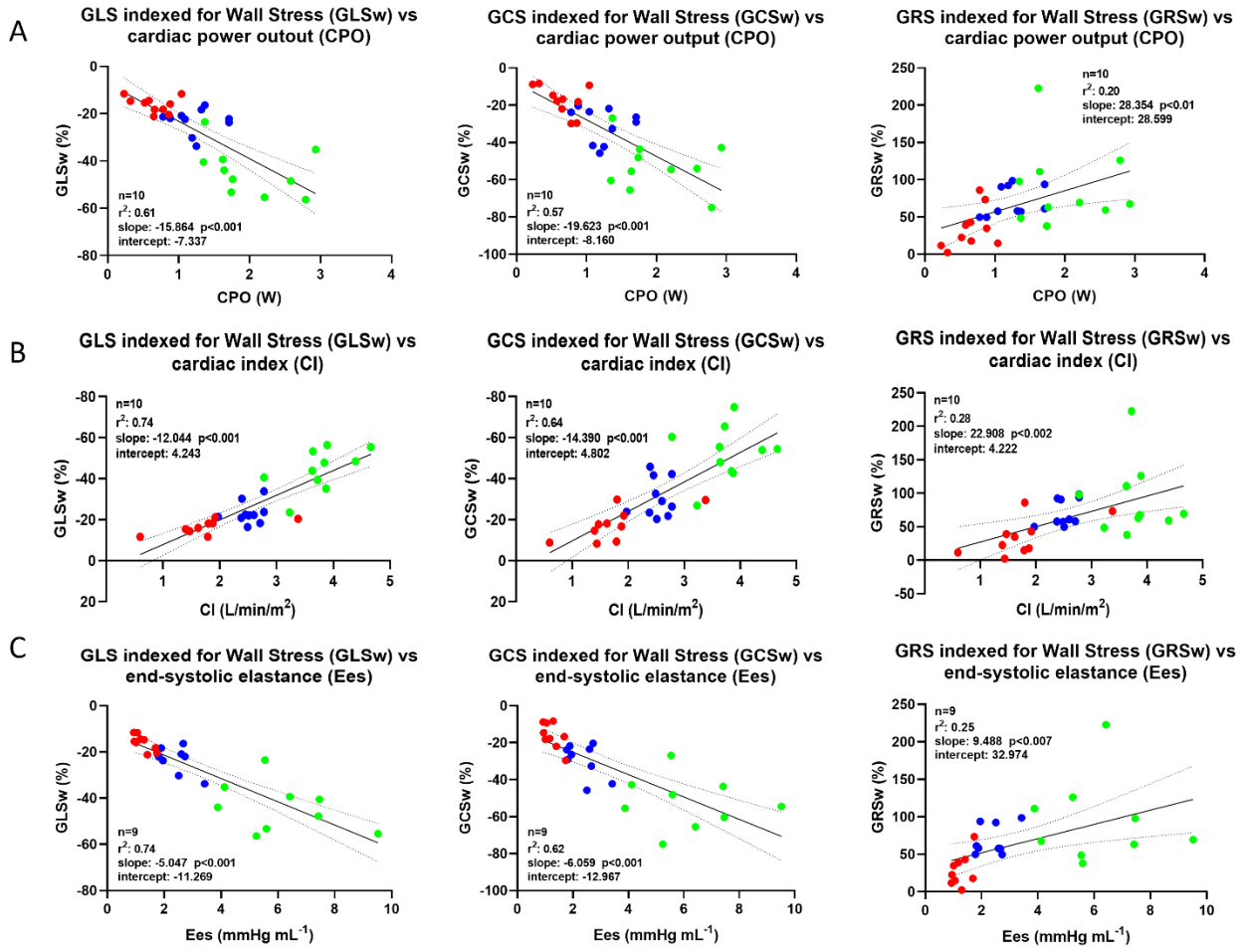

Figure 6. Correlation between global strain adjusted for wall stress and invasive hemodynamic parameters. Linear regression analysis between GLSw, GCSw, GRSw and CPO (A), CI (B), and Ees (C) improves after indexing strain values for meridional Wall Stress. Blue points address BL, green ones' address Dob, and red ones' address Ver (n=10). BL = baseline; CI = cardiac index; CPO = cardiac power output; Dob = dobutamine; Ees = end-systolic elastance; GLSw = global longitudinal strain indexed for Wall Stress; GCSw = global

circumferential strain indexed for Wall Stress; GRSw = global radial strain indexed for Wall Stress; Ver = verapamil. This Figure refers to the published article by Faragli et al[2].

Relative changes of mechanics between baseline, dobutamine and verapamil

Relative changes in global LV strain parameters, defined as non-invasive cardiac mechanics, and hemodynamic parameters were plotted in comparison to baseline (Figure 7).

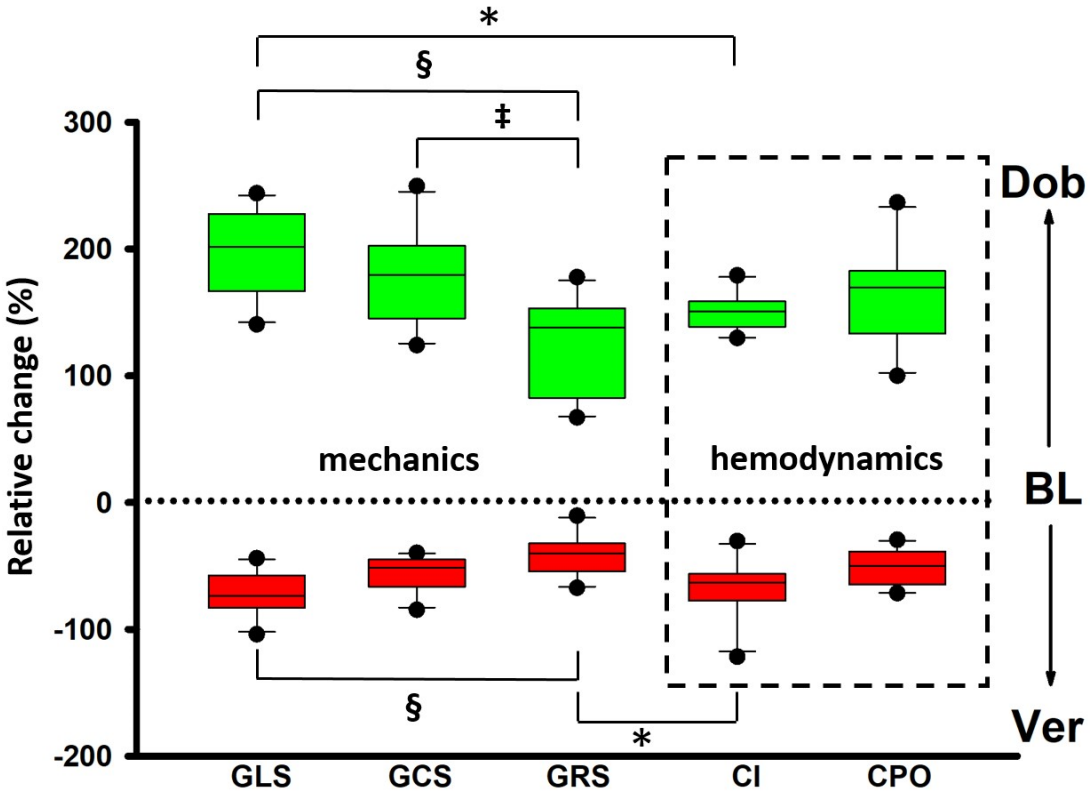

Figure 7. Graphical representation of the relative change of global strain values and cardiac mechanics parameters during baseline, dobutamine and verapamil steps. Global strain value and relative change of invasive hemodynamic parameters (dashed box)

are plotted from baseline (BL, dashed horizontal line) to dobutamine (Dob, green boxes) and from BL to verapamil (Ver, red boxes), respectively. N=10; *p<0.05 vs CI, §p<0.05 vs GLS, ‡p<0.05 vs GCS. BL = baseline; CI = cardiac index; CPO = cardiac power output; Dob = dobutamine; GLS = global longitudinal strain; GCS = global circumferential strain; GRS = global radial strain; Ver = verapamil. This Figure refers to the published article by Faragli et al[2].

Among global strain values, GLS was found to have a higher relative change than for example GRS both at Dob and Ver. GCS was found different for Dob only. Dob effects were found to be more prominent in GLS than by CI, while the impact of Ver on GRS was negligible, if compared to CI. The effect of Dob and Ver on the other mechanic and hemodynamic parameters was comparable.

Inter-observer and intra-observer reproducibility

Table 2 shows the CMR-FT derived strain parameters, which were obtained by two independent researchers.

Measurements obtained by two observers

(inter-observer level)

		First observer	**Second observer**
BL	GLS (%)	-26.1 ± 5	-25.1 ± 4
	GCS (%)	-32.7 ± 8	-30.4 ± 6
	GRS (%)	73.3 ± 9	51.5 ± 17
Dob	GLS (%)	-45.1 ± 11*	-40.6 ± 7 *
	GCS (%)	-55.1 ± 12	-54.7 ± 10 *
	GRS (%)	103.0 ± 20	101.8 ± 14 *
Ver	GLS (%)	-20.8 ± 6 §	-17.3 ± 5 *, §
	GCS (%)	-18.6 ± 4 §	-21.0 ± 6 *, §
	GRS (%)	53.9 ± 10 §	29.1 ± 9 *, §

Measurements obtained by one observer

(intra-observer level)

		First measurement	**Second measurement**
BL	GLS (%)	-26.1 ± 5	-23.3 ± 4

	GCS (%)	-32.7 ± 8	-31.0 ± 8
	GRS (%)	73.3 ± 9	71.7 ± 19
Dob	GLS (%)	-45.1 ± 11 *	-45.6 ± 9 *
	GCS (%)	-55.1 ± 12	-53.3 ± 11 *
	GRS (%)	103.0 ± 20	87.9 ± 36
Ver	GLS (%)	-20.8 ± 6 §	-16.5 ± 3 *, §
	GCS (%)	-18.6 ± 4 §	-16.9 ± 5 *, §
	GRS (%)	53.9 ± 10 §	30.3 ± 13 *, §

Table 2. Global strain parameters obtained by two observers are displayed at different inotropic states. The measurements were taken twice, and the average values are shown. N=10; *p<0.05 vs. BL; §p<0.05 vs. Dob. BL = baseline; Dob = dobutamine; GLS = global longitudinal strain; GCS = global circumferential strain; GRS = global radial strain; Ver = verapamil.

The calculated mean differences ± SD, limits of agreement and ICC for strain parameters are presented in Table 3.

	Parameter	**Steps**	**Mean difference ± SD**	**Limits of Agreement**	**ICC (95% CI)**
Inter-observer variability	GLS	BL	-1.0 ± 3.0	-6.9 to 4.8	0.88 (0.57 – 0.97)
		Dob	-4.5 ± 10.0	-24.1 to 15.1	0.60 (-0.35 – 0.89)

		Ver	3.5 ± 4.2	-4.7 to 11.7	0.79 (0.10 – 0.95)
	GCS	BL	-2.2 ± 7.6	-17.2 to 12.6	0.66 (-0.21 – 0.92)
		Dob	-0.4 ± 11.5	-23.0 to 22.2	0.51 (-0.23 – 0.87)
		Ver	2.4 ± 3.4	-4.3 to 9.2	0.61 (-0.40 – 0.90)
	GRS	BL	21.7 ± 11.6	-0.9 to 44.5	0.80 (0.21 – 0.95)
		Dob	1.2 ± 29.6	-56.9 to 59.3	-1.60 (-9.47 – 0.35)
		Ver	24.7 ± 12.6	0.1 to 49.4	0.24 (-2.03 – 0.81)
Intra-observer variability	GLS	BL	2.8 ± 2.9	-2.8 to 8.5	0.81 (0.41 – 0.95)
		Dob	-0.4 ± 7.3	-14.8 to 14.0	0.87 (0.45 – 0.96)
		Ver	4.3 ± 4.3	-4.1 to 12.7	0.75 (0.01 – 0.94)
	GCS	BL	1.7 ± 1.5	-1.3 to 4.7	0.98 (0.77 – 0.99)
		Dob	1.8 ± 3.4	-4.8 to 8.4	0.97 (0.89 – 0.99)
		Ver	1.6 ± 1.4	-1.1 to 4.4	0.95 (0.36 – 0.99)
	GRS	BL	-1.5 ± 12.7	-26.4 to 23.3	0.79 (0.15 – 0.94)
		Dob	-15.1 ± 31.1	-76.0 to 45.8	0.62 (-0.50 – 0.90)
		Ver	-23.6 ± 15.7	-54.4 to 7.2	0.14 (-2.43 – 0.78)

Table 3. Inter-observer and intra-observer reproducibility analysis for GLS, GCS and GRS. The inter-observer and intra-observer variability data concerning the mean difference ± standard deviation, the limits of agreement and the intraclass correlation (ICC) during BL, Dob and Ver are shown. The measurements were taken twice, and the average values are displayed. N=10. BL = baseline; Dob = dobutamine; GLS = global longitudinal strain; GCS =

global circumferential strain; GRS = global radial strain; ICC = intraclass correlation coefficient; Ver = verapamil.

Analyzing the inter-observer variability, it was observed that the reproducibility for GLS during BL and Ver steps was excellent. For Dob, the observed reproducibility was found to be only good. With regards to the GCS analysis, a good reproducibility during BL and Ver steps was found; while during Dob, the reproducibility observed was only fair. For GRS, an excellent reproducibility during BL measurements was found, while for Dob and Ver steps the reproducibility was only poor. Regarding intra-observer analysis, the level of reproducibility for most measurements is excellent. GLS and GCS reproducibility was excellent for all the steps; GRS instead showed an excellent reproducibility only during BL, while during Dob was good and during Ver only poor. In Figures 8 and 9, Bland-Altman plots have been drawn to show the inter-observer and the intra-observer reproducibility of global strain parameters at BL, Dob and Ver steps (see Figures 8, 9).

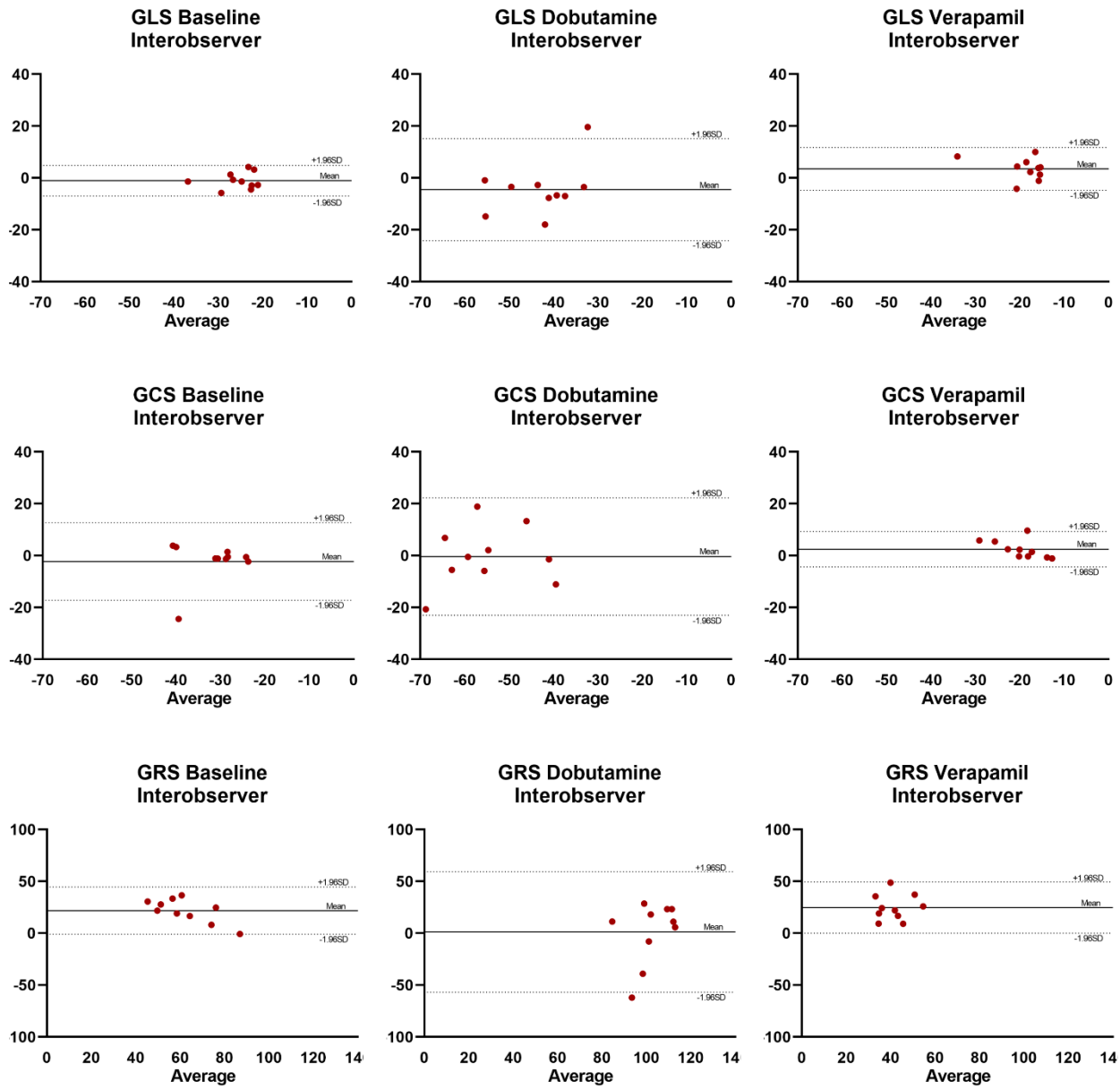

Figure 8. Brand-Altman plot showing reproducibility between observers of global strain values. Bland-Altman plots analyzing inter-observer reproducibility for GLS, GCS and GRS during BL, Dob and Ver are shown (n=10). GLS = global longitudinal strain; GCS = global circumferential strain; GRS = global radial strain. This Figure refers to the published article by Faragli et al[1].

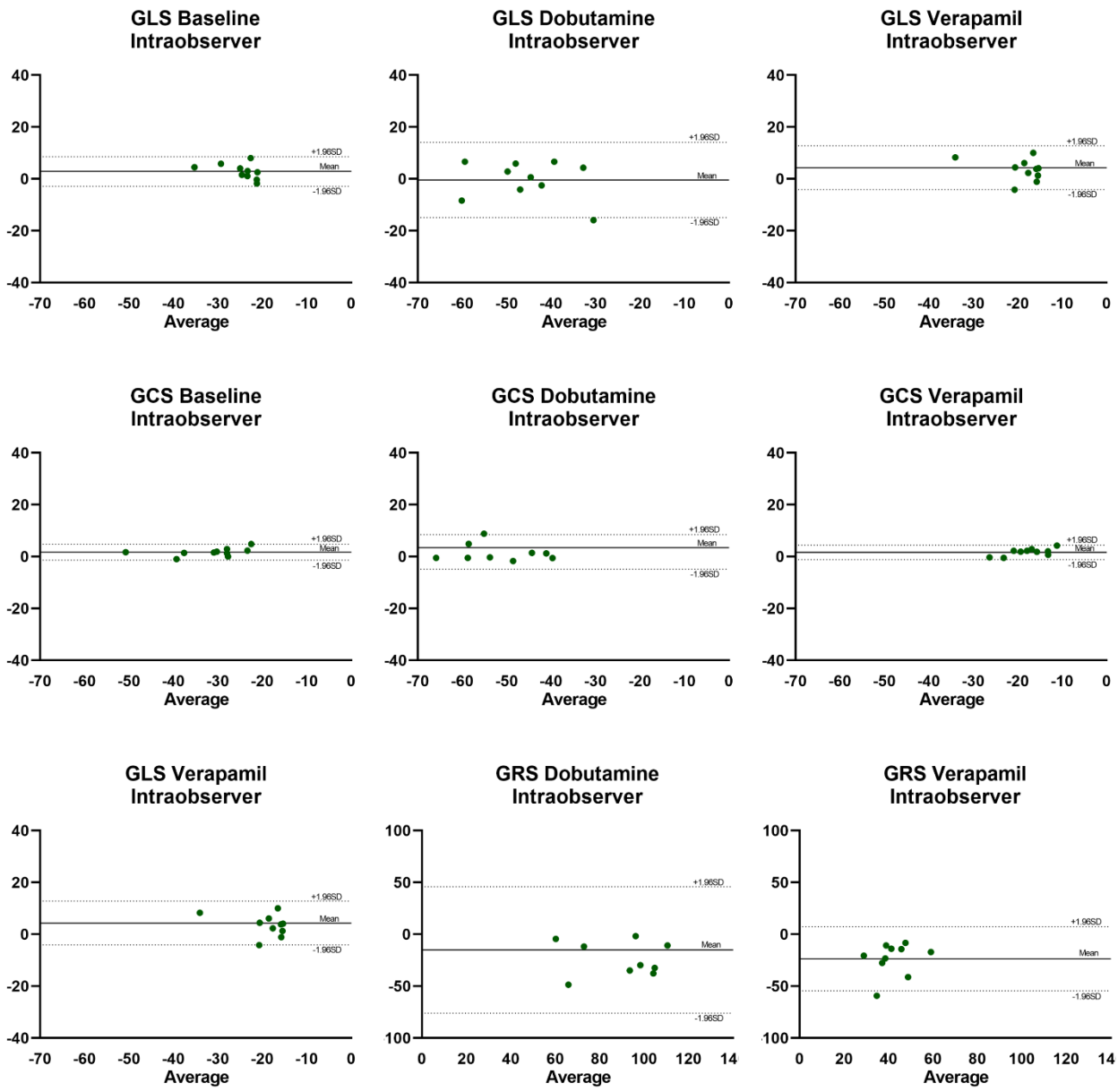

Figure 9. Bland-Altman showing the relationship reproducibility between observers of global strain values. Bland-Altman plots analyzing intra-observer reproducibility for GLS, GCS and GRS analysis during BL, Dob and Ver are shown (n=10). GLS = global longitudinal

strain; GCS = global circumferential strain; GRS = global radial strain. This Figure refers to the published article by Faragli et al[1].

Sample size

The required sample sizes calculated for each strain-derived parameter are represented in Table 4.

		Sample Size (n)		
	Mean difference ± SD pooled	**5%**	**10%**	**15%**
GLS	-1.08 ± 4.9	20	5	2
GCS	-2.27 ± 7.4	45	11	5
GRS	21.7 ± 17.9	NA	68	30

Table 4. Sample size calculation for global strain baseline values. The sample size was analyzed to detect the desired percentage relative change with 80% power and α error of 0.05. The mean difference is calculated from the inter-observer average difference analysis[1]. The pooled standard deviation has been calculated by applying Cohen formula: $SD_{pooled} = \sqrt{(SD_1^2 + SD_2^2)^{-1}}$. In the table are displayed the number of animals needed to detect a 5%, 10% and 15% change in GLS, GCS and GRS respectively. GLS = global longitudinal strain; GCS = global circumferential strain; GRS = global radial strain; SD = standard deviation; Ver = verapamil.

A relative 10% change in GLS in pigs requires five animals, as represented in Figure 10. Twenty pigs instead are required to detect a 5% change in GLS (power of 80% and α error of 0.05).

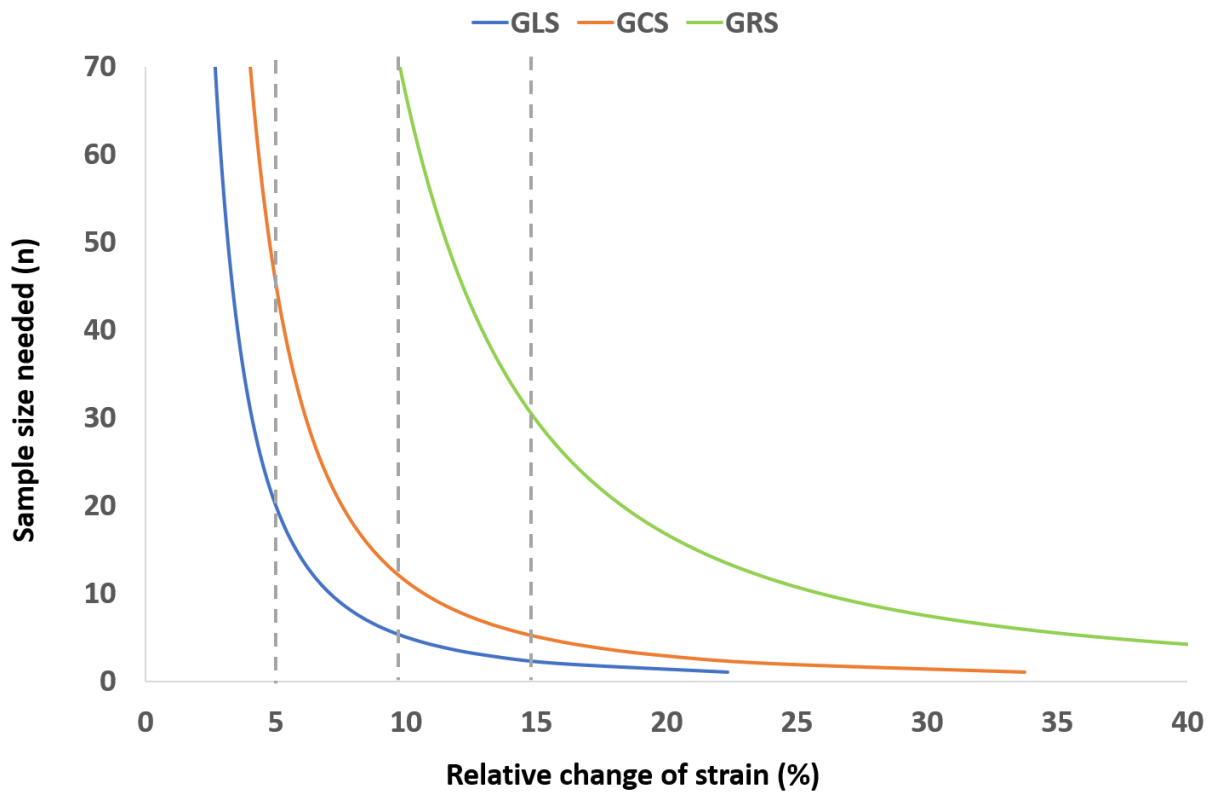

Figure 10. The sample size of the baseline global strain values visualized. Graphical representation of the sample size for GLS, GCS and GRS (baseline measurements) to detect the desired percentage relative change of strain (n=10). The calculation was performed aiming at the 80% power and α error of 0.05. GLS = global longitudinal strain; GCS = global circumferential strain; GRS = global radial strain. This Figure refers to the published article by Faragli et al[1].

3.4 Discussion

The main goal of the current study was to compare CMR-FT LV systolic strain to the invasively measured classical hemodynamic parameters[2]. The goal was to understand whether LV strain can reproduce the mechanical function of the heart[2]. To do so, we investigated LV strain under various inotropic states[2]. What we observed is that although a moderate correlation of global strain parameters against LV hemodynamics was found, by indexing strain parameters to indirect measures of afterload the correlation was improved[2].

Correlation between global strain, ejection fraction and LV hemodynamic parameters

The role of echocardiographic LV strain in the clinics is already established, and numerous studies have already shown its diagnostic and prognostic role in different patients' populations[9, 10, 21-25, 28, 29]. Cardiovascular magnetic resonance feature tracking (CMR-FT) strain analysis represents a relatively new accurate technique utilizing simple steady-state free procession sequences for assessing myocardial function and dysfunction [17, 33, 34, 39-41, 64]. CMR-FT been shown to predict major adverse cardiac events in ischemic or non-ischemic cardiomyopathy[37-39]. Nonetheless, due to the current lack of in vivo studies it is not known whether CMR-FT LV strain is able to reproduce accurately the mechanical function of the myocardium[65]. Whether CMR-FT LV strain is an effective tool for evaluating cardiac mechanics of the myocardium, and how these changes under different inotropic states, is still unclear because of the lack of research in this field.

In our study, we were able to show how CMR LV strain correlated with hemodynamic parameters describing the hydraulic and mechanical role of the heart as a pump[2] by

comparing it with invasively validated parameters such as cardiac power output (CPO) and cardiac index (CI)[49, 51, 52, 66].

Up to now, most of the in vivo studies concentrated on 2D and 3D STE[20], correlating for example the STE with the sonomicrometry in large animal models and showing good agreement between the techniques[20]. In an in vivo study on pigs, the group of Weidemann et al was able to show the ability of LV strain to reproduce the LV-contractility of pigs under various inotropic conditions and independently of heart rate[67]. An in vivo study, with a goal comparable to ours, is the one performed by Yotti et al[26]. The aim of the study was to show a correlation between echocardiographic assessed LV strain and invasive pressure-volume catheterization data[26]. In their study, circumferential strain correlated moderately, while longitudinal strain correlated poorly[26]. An interesting point raised by the study was that circumferential strain, unlike longitudinal strain, was not affected in patients with aortic stenosis or hypertension. This could be due to the lower load-dependency of circumferential strain or by the effect of afterload[26].

Another main goal of our study was to compare CMR-FT LV strain with one of the most accurate parameter of LV contractility, meaning the invasively measured end-systolic elastance (Ees)[2]. End-systolic elastance is a relatively load-independent parameter that represents the slope of the end-systolic pressure-volume relationship and can explain. the LV inotropic status[49]. Recently, Seeman et al. were able to assess Ees non-invasively via CMR imaging[68]. In our study, we were able to show a moderate to good correlation between both GLS, GCS, and Ees[2].

Relative change of mechanics under various inotropic states

To understand how global LV strain is able to reproduce the hemodynamic function and the mechanical contraction the myocardium, we analyzed the relative changes of global LV strain, CPO, CI and Ees between hypercontractility and hypocontractility compared to baseline, respectively (Figure 7). What we observed is that the impact of Dob and Ver was comparable between global strain and hemodynamic parameters, apart from two exceptions[62]. GLS changed relatively more during Dob induced hypercontractility if compared to CI. With Ver induced hypocontractility, instead, the relative changes of GRS were small if compared to CI, indicating in those cases a poor comparison between the two methods[62].

Inter-observer and intra-observer reproducibility

Concerning the reproducibility of LV strain, few studies analyzed it in animal models. Previously, a study from our group showed the high reproducibility of strain measurements through CMR-FT in a model of small animals (mice)[76, 77]. However, the main limitation of that study lies in the model, being too small to be able to translate to humans[76, 77].

Large animals, such as Landrace pigs, do present a cardiac anatomy and physiology extremely similar to humans. For this reason, we envisioned the importance of having data on Landrace pigs to establish the reproducibility of CMR-FT LV strain and this has been published as a sub-study of the presented experimental protocol[1]. The purpose of that study was to provides an analysis on the reproducibility of the CMR-FT LV strain and an analysis of the sample size needed to detect LV strain changes[1].

For global longitudinal and global circumferential strain, we found a good to excellent inter-observer reproducibility. Instead, radial strain, in line with the already published literature in human studies [78-81], to be poorly reproducible between repeated measurements, in specific

for the inter-observer measurements. As expected, the intra-observer reproducibility was higher than the inter-observer, and particularly good for circumferential strain. This was also in line with previously published studies [62, 82].

In the published study, we also had the ability to assess the reproducibility of the LV strain measurements under different inotropic states[1]. What it was observed was that during dobutamine infusion, a high increase in HR was achieved (mean 146 ± 12 bpm). This caused a lower reproducibility of the inter-observer and intra-observer measurements[1]. One explanation could be that the processed images were affected by a worse resolution due to the increased frame rate. A reduced precision of the measurement due to high heart rate has already been described in previous studies [63, 83]. In our model, lower heart rates such as during baseline and verapamil were associated with a greater reproducibility of all the global LV strain values[1].

Previous studies have shown that CMR-FT global circumferential strain achieved the best interobserver agreement[62], while global radial strain has the weakest one in agreement with our recent published study[1]. Even if previous studies identified a poorer reproducibility of longitudinal strain, probably due to a more difficult tracking of the basal segments at the level of the mitral annuls[62], in our published study longitudinal strain was found to be highly reproducible both for the inter- and the intra-observer measurements[1]. Nonetheless, one of the main causes of variability of strain values comes from the different software utilized of the analysis and because of a lack of contouring standardization[84].

Sample size

Since reproducibility has an influence on the sample size required to detect significant differences in strain parameters, group variance is key. The greater the variability, the larger

is the sample size needed. Sample size is fundamental to test the reliability of new imaging methods[85, 86], especially in the field of animal studies where the reduction of the number of animals needed per experiments is unvaluable[87]. By utilizing previously published sample sizes it is also possible to avoid pilot experiments or unnecessary replications[88]. In our cohort study, we were able to prove that if the effects of animal-to-animal variation on the measurement is eliminated or greatly reduced, the animals required to test hypotheses can be reduced[1].

3.5 Clinical applications

In the past years, LV strain measured through echocardiography has emerged as an important method to evaluate the clinical function of the heart better than LVEF[8, 17, 48]. Previous studies have already been shown that changes in LV strain may not strictly reflect the same alterations in LVEF, mainly given by geometric confounders, as for example an increased ventricular wall in diseases such as HCM[3, 89]. Measurable alterations in GLS may not necessarily affect LVEF that, in many cases, may still be normal[3, 89]. Moreover, since LVEF is a parameter of systolic function, LV strain may improve the understanding of the heart function in MRI being also an indicator of the diastolic phase[3].

LV strain slowly entered the CMR clinical routine, mainly because of the time-consuming post-processing analysis of the sequences, being mostly relegated to research purposes[48]. Even if the newly developed CMR-FT has the advantage of providing the physicians with a quick assessment, based on simple steady-state free precession sequences, allowing a potential use of LV strain for clinical routine[33, 34, 39-41], the main limitation of myocardial strain is given by its load-dependency[48, 59].

In this current study we were able to demonstrate that LV strain parameters measured with CMR-FT correlate moderately with hemodynamic parameters such as cardiac index (CI), cardiac power output (CPO), as well as a load-independent parameter that measures cardiac contractility, namely end-systolic elastance (Ees)[2]. Moreover, we were able to add a relevant piece of the puzzle through our study, since we were able to show that by indexing LV strain for indirect measures of afterload, such as mAOP as well as meridional wall stress, an improvement in the correlation between strain parameters and LV hemodynamics was observed[2]. For instance, by indexing GLS parameter for meridional wall stress, the

correlation against Ees was as good as the one between Ees and LVEF in reflecting LV contractility[2]. This shows how an indexed measure of GLS may be as useful as LVEF as a routine clinical assessment for CMR purposes. Our results suggest that even a simple non-invasive measurement of the blood pressure combined with LV strain may provide additional information on the heart contractility[2].

Eventually, the possible clinical applications of CMR-FT strain range among different pathologies such as for the assessment of CAD, diabetes mellitus, hypertensive heart disease and HCM patients[3, 17, 44]. However, the main clinical advantage of LV strain may be for the diagnosis and prognosis of chronic HF patients, and in specific for HFpEF ones, as already shown in previous studies[10]. HFpEF patients are a population presenting with heart failure symptoms like dyspnea, but with a normal LVEF[90]. LV strain may provide the missing information that clinicians need since those patients may present an alteration of the heart mechanics, that with the sole measurement of LVEF is not detectable[90].

3.6 Limitations

There are several limitations to the current study. One of them is related to the setting. Since animals were studied under general anaesthesia, necessary to reduce the animals' distress and to gather stable hemodynamic conditions, the results obtained may be influenced by the medications needed to maintain the animals anesthetized. Another limitation is given by the fact that due to conditions such as easier housing and milder behaviour, all the animals selected for the study were females. This creates a potential gender bias of the results. Concerning the analysis, only endocardial values were utilized. Endocardial strain has already been shown[90] to be the most relevant among the other layers (myocardial and epicardial) for the assessment of cardiac contraction, however, presenting only endocardial values may be perceived as a limitation. Regarding the analysis, software variability between the providers should be taken into account when considering the absolute strain values.

Eventually, even if the animals analysed were healthy ones, with a cardiovascular pathology, the induced conditions of conditions of hyper-contractility (stress) and hypo-contractility (ischemia) were induced, and we believe to be already representative enough for a potential clinical translation. Nonetheless, further research in this field is necessary in a clinical setting to prove our hypotheses. A final limitation is related to the sample size required to detect finer differences. Adding a 25% dropout rate before planning a study may provide more accurate results.

3.7 Conclusions

CMR-FT LV strain correlates with LV hemodynamics in pigs under hypercontractility and hypocontractility states. Indexing LV strain for circuitous measures of afterload progresses the correlation. In specific, GLS indexed for wall stress provides the best results being at least as good as LVEF in assessing LV contractility. CMR-FT LV strain may be easily integrated into the clinical CMR routine to characterize the LV mechanics of patients with various degrees of dysfunction adding a relevant information on top of LVEF.

3.8 Declarations

Ethics approval

Not applicable.

Consent for publication

Not applicable.

Competing interests

Apart from Alessandro Faragli, Heiner Post, Sebastian Kelle and Alessio Alogna, who declare to have received funding in the Funding section, none of the other authors reports a relationship with industry and other relevant entities – financial or otherwise – that might pose a conflict of interest in connection with the submitted article. The following authors report financial activities outside the submitted work: Burkert Pieske reports having received consultancy and lecture honoraria from Bayer Daiichi Sankyo, MSD, Novartis, Sanofi-Aventis, Stealth Peptides and Vifor Pharma; and editor honoraria from the Journal of the American College of Cardiology.

Funding

Alessandro Faragli, Heiner Post, Sebastian Kelle and Alessio Alogna received funding from DZHK (c) and by the BMBF (German Ministry of Education and Research). Sebastian Kelle is supported by a grant from Philips Healthcare.

Authors contribution

A.A., S.K., H.P. conceived the experiment, A.F., A.A., S.K., C.K., C.S. conducted the experiments, A.F., R.T., D.A., A.A., S.P., C.S., F.P.L.M., L.F. analyzed the results. All authors revised the manuscript.

4 Bibliography

1. Faragli A, Tanacli R, Kolp C, Lapinskas T, Stehning C, Schnackenburg B, Lo Muzio FP, Perna S, Pieske B, Nagel E, Post H, Kelle S and Alogna A. Cardiovascular magnetic resonance feature tracking in pigs: a reproducibility and sample size calculation study. *The International Journal of Cardiovascular Imaging*. 2020;36:703-712.
2. Faragli A, Tanacli R, Kolp C, Abawi D, Lapinskas T, Stehning C, Schnackenburg B, Lo Muzio FP, Fassina L, Pieske B, Nagel E, Post H, Kelle S and Alogna A. Cardiovascular magnetic resonance-derived left ventricular mechanics-strain, cardiac power and end-systolic elastance under various inotropic states in swine. *Journal of cardiovascular magnetic resonance : official journal of the Society for Cardiovascular Magnetic Resonance*. 2020;22:79.
3. Stokke TM, Hasselberg NE, Smedsrud MK, Sarvari SI, Haugaa KH, Smiseth OA, Edvardsen T and Remme EW. Geometry as a Confounder When Assessing Ventricular Systolic Function: Comparison Between Ejection Fraction and Strain. *Journal of the American College of Cardiology*. 2017;70:942-954.
4. Stanton T, Leano R and Marwick Thomas H. Prediction of All-Cause Mortality From Global Longitudinal Speckle Strain. *Circulation: Cardiovascular Imaging*. 2009;2:356-364.
5. Bellenger NG, Burgess MI, Ray SG, Lahiri A, Coats AJ, Cleland JG and Pennell DJ. Comparison of left ventricular ejection fraction and volumes in heart failure by echocardiography, radionuclide ventriculography and cardiovascular magnetic resonance; are they interchangeable? *European heart journal*. 2000;21:1387-96.
6. Salvo GD, Pergola V, Fadel B, Bulbul ZA and Caso P. Strain Echocardiography and Myocardial Mechanics: From Basics to Clinical Applications. *J Cardiovasc Echogr*. 2015;25:1-8.
7. Konstam MA and Abboud FM. Ejection Fraction: Misunderstood and Overrated (Changing the Paradigm in Categorizing Heart Failure). *Circulation*. 2017;135:717-719.
8. Salvo G, Pergola V, Fadel B, Bulbul Z and Caso P. Strain echocardiography and myocardial mechanics: From basics to clinical applications. 2015;25:1-8.
9. Stanton T, Leano R and Marwick TH. Prediction of all-cause mortality from global longitudinal speckle strain: comparison with ejection fraction and wall motion scoring. *Circulation Cardiovascular imaging*. 2009;2:356-64.
10. Stokke TM, Hasselberg NE, Smedsrud MK, Sarvari SI, Haugaa KH, Smiseth OA, Edvardsen T and Remme EW. Geometry as a Confounder When Assessing Ventricular Systolic Function: Comparison Between Ejection Fraction and Strain. *Journal of the American College of Cardiology*. 2017;70:942-954.
11. Buckberg G, Hoffman JI, Nanda NC, Coghlan C, Saleh S and Athanasuleas C. Ventricular torsion and untwisting: further insights into mechanics and timing interdependence: a viewpoint. *Echocardiography (Mount Kisco, NY)*. 2011;28:782-804.
12. Buckberg G, Hoffman JI, Mahajan A, Saleh S and Coghlan C. Cardiac mechanics revisited: the relationship of cardiac architecture to ventricular function. *Circulation*. 2008;118:2571-87.
13. Biswas M, Sudhakar S, Nanda NC, Buckberg G, Pradhan M, Roomi AU, Gorissen W and Houle H. Two- and three-dimensional speckle tracking echocardiography: clinical applications and future directions. *Echocardiography (Mount Kisco, NY)*. 2013;30:88-105.
14. Cheng S, Larson MG, McCabe EL, Osypiuk E, Lehman BT, Stanchev P, Aragam J, Benjamin EJ, Solomon SD and Vasan RS. Age- and sex-based reference limits and clinical correlates of myocardial

strain and synchrony: the Framingham Heart Study. *Circulation Cardiovascular imaging*. 2013;6:692-699.
15. Schuster A, Hor KN, Kowallick JT, Beerbaum P and Kutty S. Cardiovascular Magnetic Resonance Myocardial Feature Tracking. 2016;9:e004077.
16. Obokata M, Nagata Y, Wu VC, Kado Y, Kurabayashi M, Otsuji Y and Takeuchi M. Direct comparison of cardiac magnetic resonance feature tracking and 2D/3D echocardiography speckle tracking for evaluation of global left ventricular strain. *European heart journal cardiovascular Imaging*. 2016;17:525-32.
17. Scatteia A, Baritussio A and Bucciarelli-Ducci C. Strain imaging using cardiac magnetic resonance. *Heart failure reviews*. 2017;22:465-476.
18. Edvardsen T, Gerber BL, Garot J, Bluemke DA, Lima JAC and Smiseth OA. Quantitative Assessment of Intrinsic Regional Myocardial Deformation by Doppler Strain Rate Echocardiography in Humans. 2002;106:50-56.
19. Sutherland GR, Di Salvo G, Claus P, D'Hooge J and Bijnens B. Strain and strain rate imaging: a new clinical approach to quantifying regional myocardial function. *Journal of the American Society of Echocardiography*. 2004;17:788-802.
20. Amzulescu MS, De Craene M, Langet H, Pasquet A, Vancraeynest D, Pouleur AC, Vanoverschelde JL and Gerber BL. Myocardial strain imaging: review of general principles, validation, and sources of discrepancies. *European heart journal cardiovascular Imaging*. 2019;20:605-619.
21. Kraigher-Krainer E, Shah AM, Gupta DK, Santos A, Claggett B, Pieske B, Zile MR, Voors AA, Lefkowitz MP, Packer M, McMurray JJ, Solomon SD and Investigators P. Impaired systolic function by strain imaging in heart failure with preserved ejection fraction. *Journal of the American College of Cardiology*. 2014;63:447-56.
22. Hasselberg NE, Haugaa KH, Sarvari SI, Gullestad L, Andreassen AK, Smiseth OA and Edvardsen T. Left ventricular global longitudinal strain is associated with exercise capacity in failing hearts with preserved and reduced ejection fraction. *European heart journal cardiovascular Imaging*. 2015;16:217-224.
23. Smedsrud MK, Sarvari S, Haugaa KH, Gjesdal O, Orn S, Aaberge L, Smiseth OA and Edvardsen T. Duration of myocardial early systolic lengthening predicts the presence of significant coronary artery disease. *Journal of the American College of Cardiology*. 2012;60:1086-93.
24. Yang H, Sun JP, Lever HM, Popovic ZB, Drinko JK, Greenberg NL, Shiota T, Thomas JD and Garcia MJ. Use of strain imaging in detecting segmental dysfunction in patients with hypertrophic cardiomyopathy. *Journal of the American Society of Echocardiography : official publication of the American Society of Echocardiography*. 2003;16:233-9.
25. Fang ZY, Yuda S, Anderson V, Short L, Case C and Marwick TH. Echocardiographic detection of early diabetic myocardial disease. *Journal of the American College of Cardiology*. 2003;41:611-7.
26. Yotti R, Bermejo J, Benito Y, Sanz-Ruiz R, Ripoll C, Martinez-Legazpi P, del Villar CP, Elizaga J, Gonzalez-Mansilla A, Barrio A, Banares R and Fernandez-Aviles F. Validation of noninvasive indices of global systolic function in patients with normal and abnormal loading conditions: a simultaneous echocardiography pressure-volume catheterization study. *Circulation Cardiovascular imaging*. 2014;7:164-72.
27. Gorcsan J, 3rd and Tanaka H. Echocardiographic assessment of myocardial strain. *Journal of the American College of Cardiology*. 2011;58:1401-13.

28. Dahlslett T, Karlsen S, Grenne B, Eek C, Sjoli B, Skulstad H, Smiseth OA, Edvardsen T and Brunvand H. Early assessment of strain echocardiography can accurately exclude significant coronary artery stenosis in suspected non-ST-segment elevation acute coronary syndrome. *Journal of the American Society of Echocardiography : official publication of the American Society of Echocardiography*. 2014;27:512-9.
29. Ng AC, Sitges M, Pham PN, Tran da T, Delgado V, Bertini M, Nucifora G, Vidaic J, Allman C, Holman ER, Bax JJ and Leung DY. Incremental value of 2-dimensional speckle tracking strain imaging to wall motion analysis for detection of coronary artery disease in patients undergoing dobutamine stress echocardiography. *American heart journal*. 2009;158:836-44.
30. Nagata Y, Takeuchi M, Wu VC, Izumo M, Suzuki K, Sato K, Seo Y, Akashi YJ, Aonuma K and Otsuji Y. Prognostic value of LV deformation parameters using 2D and 3D speckle-tracking echocardiography in asymptomatic patients with severe aortic stenosis and preserved LV ejection fraction. *JACC Cardiovascular imaging*. 2015;8:235-45.
31. Rhea IB, Uppuluri S, Sawada S, Schneider BP and Feigenbaum H. Incremental prognostic value of echocardiographic strain and its association with mortality in cancer patients. *Journal of the American Society of Echocardiography : official publication of the American Society of Echocardiography*. 2015;28:667-73.
32. Buss SJ, Emami M, Mereles D, Korosoglou G, Kristen AV, Voss A, Schellberg D, Zugck C, Galuschky C, Giannitsis E, Hegenbart U, Ho AD, Katus HA, Schonland SO and Hardt SE. Longitudinal left ventricular function for prediction of survival in systemic light-chain amyloidosis: incremental value compared with clinical and biochemical markers. *Journal of the American College of Cardiology*. 2012;60:1067-76.
33. Eitel I, Stiermaier T, Lange T, Rommel KP, Koschalka A, Kowallick JT, Lotz J, Kutty S, Gutberlet M, Hasenfuss G, Thiele H and Schuster A. Cardiac Magnetic Resonance Myocardial Feature Tracking for Optimized Prediction of Cardiovascular Events Following Myocardial Infarction. *JACC Cardiovascular imaging*. 2018;11:1433-1444.
34. Schneeweis C, Qiu J, Schnackenburg B, Berger A, Kelle S, Fleck E and Gebker R. Value of additional strain analysis with feature tracking in dobutamine stress cardiovascular magnetic resonance for detecting coronary artery disease. *Journal of cardiovascular magnetic resonance : official journal of the Society for Cardiovascular Magnetic Resonance*. 2014;16:72.
35. Moore CC, Reeder SB and McVeigh ER. Tagged MR imaging in a deforming phantom: photographic validation. *Radiology*. 1994;190:765-769.
36. Lima JA, Jeremy R, Guier W, Bouton S, Zerhouni EA, McVeigh E, Buchalter MB, Weisfeldt ML, Shapiro EP and Weiss JL. Accurate systolic wall thickening by nuclear magnetic resonance imaging with tissue tagging: correlation with sonomicrometers in normal and ischemic myocardium. *Journal of the American College of Cardiology*. 1993;21:1741-51.
37. Jeung M-Y, Germain P, Croisille P, ghannudi SE, Roy C and Gangi A. Myocardial Tagging with MR Imaging: Overview of Normal and Pathologic Findings. *RadioGraphics*. 2012;32:1381-1398.
38. Götte MJW, Germans T, Rüssel IK, Zwanenburg JJM, Marcus JT, van Rossum AC and van Veldhuisen DJ. Myocardial Strain and Torsion Quantified by Cardiovascular Magnetic Resonance Tissue Tagging: Studies in Normal and Impaired Left Ventricular Function. *Journal of the American College of Cardiology*. 2006;48:2002-2011.
39. Onishi T, Saha SK, Delgado-Montero A, Ludwig DR, Onishi T, Schelbert EB, Schwartzman D and Gorcsan J, 3rd. Global longitudinal strain and global circumferential strain by speckle-tracking

echocardiography and feature-tracking cardiac magnetic resonance imaging: comparison with left ventricular ejection fraction. *Journal of the American Society of Echocardiography : official publication of the American Society of Echocardiography*. 2015;28:587-96.
40. Mangion K, Carrick D, Carberry J, Mahrous A, McComb C, Oldroyd KG, Eteiba H, Lindsay M, McEntegart M, Hood S, Petrie MC, Watkins S, Davie A, Zhong X, Epstein FH, Haig CE and Berry C. Circumferential Strain Predicts Major Adverse Cardiovascular Events Following an Acute ST-Segment-Elevation Myocardial Infarction. *Radiology*. 2018:181253.
41. Romano S, Judd RM, Kim RJ, Kim HW, Klem I, Heitner JF, Shah DJ, Jue J, White BE, Indorkar R, Shenoy C and Farzaneh-Far A. Feature-Tracking Global Longitudinal Strain Predicts Death in a Multicenter Population of Patients With Ischemic and Nonischemic Dilated Cardiomyopathy Incremental to Ejection Fraction and Late Gadolinium Enhancement. *JACC Cardiovascular imaging*. 2018;11:1419-1429.
42. Claus P, Omar AMS, Pedrizzetti G, Sengupta PP and Nagel E. Tissue Tracking Technology for Assessing Cardiac Mechanics: Principles, Normal Values, and Clinical Applications. *JACC Cardiovascular imaging*. 2015;8:1444-1460.
43. Pedrizzetti G, Claus P, Kilner PJ and Nagel E. Principles of cardiovascular magnetic resonance feature tracking and echocardiographic speckle tracking for informed clinical use. *Journal of cardiovascular magnetic resonance : official journal of the Society for Cardiovascular Magnetic Resonance*. 2016;18:51.
44. Schuster A, Hor Kan N, Kowallick Johannes T, Beerbaum P and Kutty S. Cardiovascular Magnetic Resonance Myocardial Feature Tracking. *Circulation: Cardiovascular Imaging*. 2016;9:e004077.
45. Schneeweis C, Lapinskas T, Schnackenburg B, Berger A, Hucko T, Kelle S, Fleck E and Gebker R. Comparison of myocardial tagging and feature tracking in patients with severe aortic stenosis. *The Journal of heart valve disease*. 2014;23:432-40.
46. Moody WE, Taylor RJ, Edwards NC, Chue CD, Umar F, Taylor TJ, Ferro CJ, Young AA, Townend JN, Leyva F and Steeds RP. Comparison of magnetic resonance feature tracking for systolic and diastolic strain and strain rate calculation with spatial modulation of magnetization imaging analysis. *Journal of magnetic resonance imaging : JMRI*. 2015;41:1000-12.
47. Kraitchman DL, Sampath S, Castillo E, Derbyshire JA, Boston RC, Bluemke DA, Gerber BL, Prince JL and Osman NF. Quantitative ischemia detection during cardiac magnetic resonance stress testing by use of FastHARP. *Circulation*. 2003;107:2025-30.
48. Reichek N. Myocardial Strain: Still a Long Way to Go. *Circulation Cardiovascular imaging*. 2017;10.
49. Kass DA and Maughan WL. From 'Emax' to pressure-volume relations: a broader view. *Circulation*. 1988;77:1203-12.
50. Abawi D, Faragli A, Schwarzl M, Manninger M, Zweiker D, Kresoja K-P, Verderber J, Zirngast B, Maechler H, Steendijk P, Pieske B, Post H and Alogna A. Cardiac power output accurately reflects external cardiac work over a wide range of inotropic states in pigs. *BMC Cardiovascular Disorders*. 2019;19:217.
51. Fincke R, Hochman JS, Lowe AM, Menon V, Slater JN, Webb JG, LeJemtel TH and Cotter G. Cardiac power is the strongest hemodynamic correlate of mortality in cardiogenic shock: A report from the SHOCK trial registry. *Journal of the American College of Cardiology*. 2004;44:340-348.

52. Cotter G, Williams SG, Vered Z and Tan LB. Role of cardiac power in heart failure. *Curr Opin Cardiol*. 2003;18:215-22.
53. Williams SG, Cooke GA, Wright DJ, Parsons WJ, Riley RL, Marshall P and Tan LB. Peak exercise cardiac power output; a direct indicator of cardiac function strongly predictive of prognosis in chronic heart failure. *European heart journal*. 2001;22:1496-503.
54. Fincke R, Hochman JS, Lowe AM, Menon V, Slater JN, Webb JG, LeJemtel TH, Cotter G and Investigators S. Cardiac power is the strongest hemodynamic correlate of mortality in cardiogenic shock: a report from the SHOCK trial registry. *Journal of the American College of Cardiology*. 2004;44:340-8.
55. Alogna A, Manninger M, Schwarzl M, Zirngast B, Steendijk P, Verderber J, Zweiker D, Maechler H, Pieske BM and Post H. Inotropic Effects of Experimental Hyperthermia and Hypothermia on Left Ventricular Function in Pigs-Comparison With Dobutamine. *Critical care medicine*. 2015.
56. Schulz-Menger J, Bluemke DA, Bremerich J, Flamm SD, Fogel MA, Friedrich MG, Kim RJ, von Knobelsdorff-Brenkenhoff F, Kramer CM, Pennell DJ, Plein S and Nagel E. Standardized image interpretation and post processing in cardiovascular magnetic resonance: Society for Cardiovascular Magnetic Resonance (SCMR) board of trustees task force on standardized post processing. *J Cardiovasc Magn Reson*. 2013;15:35.
57. Cerqueira MD, Weissman NJ, Dilsizian V, Jacobs AK, Kaul S, Laskey WK, Pennell DJ, Rumberger JA, Ryan T and Verani MS. Standardized Myocardial Segmentation and Nomenclature for Tomographic Imaging of the Heart. 2002;105:539-542.
58. Kelly RP, Ting CT, Yang TM, Liu CP, Maughan WL, Chang MS and Kass DA. Effective arterial elastance as index of arterial vascular load in humans. 1992;86:513-521.
59. Rhea IB, Rehman S, Jarori U, Choudhry MW, Feigenbaum H and Sawada SG. Prognostic utility of blood pressure-adjusted global and basal systolic longitudinal strain. *Echo research and practice*. 2016;3:17-24.
60. Reichek N, Wilson J, St John Sutton M, Plappert TA, Goldberg S and Hirshfeld JW. Noninvasive determination of left ventricular end-systolic stress: validation of the method and initial application. *Circulation*. 1982;65:99-108.
61. Weaver B and Wuensch KL. SPSS and SAS programs for comparing Pearson correlations and OLS regression coefficients. *Behavior research methods*. 2013;45:880-95.
62. Morton G, Schuster A, Jogiya R, Kutty S, Beerbaum P and Nagel E. Inter-study reproducibility of cardiovascular magnetic resonance myocardial feature tracking. *Journal of cardiovascular magnetic resonance : official journal of the Society for Cardiovascular Magnetic Resonance*. 2012;14:43.
63. Sampath S, Parimal AS, Feng D, Chang MM, Baumgartner R, Klimas M, Jacobsen K, Manigbas E, Gsell W, Evelhoch JL and Chin CL. Quantitative MRI biomarkers to characterize regional left ventricular perfusion and function in nonhuman primates during dobutamine-induced stress: A reproducibility and reliability study. *Journal of magnetic resonance imaging : JMRI*. 2017;45:556-569.
64. Schuster A, Hor KN, Kowallick JT, Beerbaum P and Kutty S. Cardiovascular Magnetic Resonance Myocardial Feature Tracking: Concepts and Clinical Applications. *Circulation Cardiovascular imaging*. 2016;9:e004077.

65. Amzulescu MS, De Craene M, Langet H, Pasquet A, Vancraeynest D, Pouleur AC, Vanoverschelde JL and Gerber BL. Myocardial strain imaging: review of general principles, validation, and sources of discrepancies. *European Heart Journal - Cardiovascular Imaging*. 2019;20:605-619.
66. Abawi D, Faragli A, Schwarzl M, Manninger M, Zweiker D, Kresoja KP, Verderber J, Zirngast B, Maechler H, Steendijk P, Pieske B, Post H and Alogna A. Cardiac power output accurately reflects external cardiac work over a wide range of inotropic states in pigs. *BMC Cardiovasc Disord*. 2019;19:217.
67. Weidemann F, Jamal F, Kowalski M, Kukulski T, D'Hooge J, Bijnens B, Hatle L, De Scheerder I and Sutherland GR. Can strain rate and strain quantify changes in regional systolic function during dobutamine infusion, B-blockade, and atrial pacing--implications for quantitative stress echocardiography. *Journal of the American Society of Echocardiography : official publication of the American Society of Echocardiography*. 2002;15:416-24.
68. Seemann F, Arvidsson P, Nordlund D, Kopic S, Carlsson M, Arheden H and Heiberg E. Noninvasive Quantification of Pressure-Volume Loops From Brachial Pressure and Cardiovascular Magnetic Resonance. *Circulation Cardiovascular imaging*. 2019;12:e008493.
69. Weiner RB, Weyman AE, Kim JH, Wang TJ, Picard MH and Baggish AL. The impact of isometric handgrip testing on left ventricular twist mechanics. 2012;590:5141-5150.
70. Donal E, Bergerot C, Thibault H, Ernande L, Loufoua J, Augeul L, Ovize M and Derumeaux G. Influence of afterload on left ventricular radial and longitudinal systolic functions: a two-dimensional strain imaging study. *European Journal of Echocardiography*. 2009;10:914-921.
71. Delgado M, Ruiz M, Mesa D, de Lezo Cruz Conde JS, Pan M, López J, Villanueva E and Cejudo L. Early Improvement of the Regional and Global Ventricle Function Estimated by Two-Dimensional Speckle Tracking Echocardiography after Percutaneous Aortic Valve Implantation Speckle Tracking after CoreValve Implantation. 2013;30:37-44.
72. Grabskaya E, Becker M, Altiok E, Dohmen G, Brehmer K, Hamada-Langer S, Kennes L, Marx N and Hoffmann R. Impact of Transcutaneous Aortic Valve Implantation on Myocardial Deformation. 2011;28:397-401.
73. Carasso S, Cohen O, Mutlak D, Adler Z, Lessick J, Reisner SA, Rakowski H, Bolotin G and Agmon Y. Differential effects of afterload on left ventricular long- and short-axis function: Insights from a clinical model of patients with aortic valve stenosis undergoing aortic valve replacement. *American heart journal*. 2009;158:540-545.
74. Yingchoncharoen T, Agarwal S, Popovic ZB and Marwick TH. Normal ranges of left ventricular strain: a meta-analysis. *J Am Soc Echocardiogr*. 2013;26:185-91.
75. Weiner RB, Weyman AE, Kim JH, Wang TJ, Picard MH and Baggish AL. The impact of isometric handgrip testing on left ventricular twist mechanics. *J Physiol*. 2012;590:5141-5150.
76. Lapinskas T, Grune J, Zamani SM, Jeuthe S, Messroghli D, Gebker R, Meyborg H, Kintscher U, Zaliunas R, Pieske B, Stawowy P and Kelle S. Cardiovascular magnetic resonance feature tracking in small animals - a preliminary study on reproducibility and sample size calculation. *BMC medical imaging*. 2017;17:51.
77. Lindsey ML, Kassiri Z, Virag JAI, Brás LEdC and Scherrer-Crosbie M. Guidelines for measuring cardiac physiology in mice. *American Journal of Physiology-Heart and Circulatory Physiology*. 2018;314:H733-H752.

78. Zhong J, Liu W and Yu X. Characterization of three-dimensional myocardial deformation in the mouse heart: an MR tagging study. *Journal of magnetic resonance imaging : JMRI*. 2008;27:1263-70.
79. Barreiro-Pérez M, Curione D, Symons R, Claus P, Voigt J-U and Bogaert J. Left ventricular global myocardial strain assessment comparing the reproducibility of four commercially available CMR-feature tracking algorithms. *European Radiology*. 2018;28:5137-5147.
80. Schmidt B, Dick A, Treutlein M, Schiller P, Bunck AC, Maintz D and Baeßler B. Intra- and inter-observer reproducibility of global and regional magnetic resonance feature tracking derived strain parameters of the left and right ventricle. *European Journal of Radiology*. 2017;89:97-105.
81. Swoboda PP, Larghat A, Zaman A, Fairbairn TA, Motwani M, Greenwood JP and Plein S. Reproducibility of myocardial strain and left ventricular twist measured using complementary spatial modulation of magnetization. *Journal of Magnetic Resonance Imaging*. 2014;39:887-894.
82. Schuster A, Stahnke VC, Unterberg-Buchwald C, Kowallick JT, Lamata P, Steinmetz M, Kutty S, Fasshauer M, Staab W, Sohns JM, Bigalke B, Ritter C, Hasenfuss G, Beerbaum P and Lotz J. Cardiovascular magnetic resonance feature-tracking assessment of myocardial mechanics: Intervendor agreement and considerations regarding reproducibility. *Clinical radiology*. 2015;70:989-98.
83. Helle-Valle TM, Yu W-C, Fernandes VRS, Rosen BD and Lima JAC. Usefulness of Radial Strain Mapping by Multidetector Computer Tomography to Quantify Regional Myocardial Function in Patients With Healed Myocardial Infarction. *American Journal of Cardiology*. 2010;106:483-491.
84. Schuster A, Stahnke VC, Unterberg-Buchwald C, Kowallick JT, Lamata P, Steinmetz M, Kutty S, Fasshauer M, Staab W, Sohns JM, Bigalke B, Ritter C, Hasenfuß G, Beerbaum P and Lotz J. Cardiovascular magnetic resonance feature-tracking assessment of myocardial mechanics: Intervendor agreement and considerations regarding reproducibility. *Clinical radiology*. 2015;70:989-998.
85. Schmidt B, Dick A, Treutlein M, Schiller P, Bunck AC, Maintz D and Baessler B. Intra- and inter-observer reproducibility of global and regional magnetic resonance feature tracking derived strain parameters of the left and right ventricle. *European journal of radiology*. 2017;89:97-105.
86. Liu S, Han J, Nacif MS, Jones J, Kawel N, Kellman P, Sibley CT and Bluemke DA. Diffuse myocardial fibrosis evaluation using cardiac magnetic resonance T1 mapping: sample size considerations for clinical trials. *Journal of cardiovascular magnetic resonance : official journal of the Society for Cardiovascular Magnetic Resonance*. 2012;14:90.
87. Voelkl B, Vogt L, Sena ES and Wurbel H. Reproducibility of preclinical animal research improves with heterogeneity of study samples. *PLoS biology*. 2018;16:e2003693.
88. Allgoewer A and Mayer B. Sample size estimation for pilot animal experiments by using a Markov Chain Monte Carlo approach. *Alternatives to laboratory animals : ATLA*. 2017;45:83-90.
89. Mor-Avi V, Lang RM, Badano LP, Belohlavek M, Cardim NM, Derumeaux G, Galderisi M, Marwick T, Nagueh SF, Sengupta PP, Sicari R, Smiseth OA, Smulevitz B, Takeuchi M, Thomas JD, Vannan M, Voigt J-U, Zamorano JL, From the University of Chicago CI, the University of Padua PI, Mayo Clinic SA, Hospital da Luz LP, Universite Claude Bernard Lyon LF, Federico Ii University Hospital of Naples NI, Cleveland Clinic CO, Methodist DeBakey H, Vascular Center TMHHT, the University of California IIC, Cnr Institute of Clinical Physiology PI, the University of Oslo ON, the University of Texas HT, the University of O and Environmental Health KJ. Current and Evolving Echocardiographic Techniques for the Quantitative Evaluation of Cardiac Mechanics: ASE/EAE

Consensus Statement on Methodology and Indications Endorsed by the Japanese Society of Echocardiography. *European Journal of Echocardiography*. 2011;12:167-205.
90. Tanacli R, Hashemi D, Lapinskas T, Edelmann F, Gebker R, Pedrizzetti G, Schuster A, Nagel E, Pieske B, Düngen HD and Kelle S. Range Variability in CMR Feature Tracking Multilayer Strain across Different Stages of Heart Failure. *Sci Rep*. 2019;9:16478.

5 Statutory Declaration / Declaration of own contribution

“I, Alessandro Faragli, by personally signing this document in lieu of an oath, hereby affirm that I prepared the submitted dissertation on the topic [Left ventricular strain analysis with cardiovascular magnetic resonance feature tracking (CMR-FT): a study in Landrace pigs - Analyse der linksventrikulären Strain mittels kardiovaskulärer Magnetresonanztomographie (CMR-FT): eine Studie an Landrassenchweinen], independently and without the support of third parties, and that I used no other sources and aids than those stated.

All parts which are based on the publications or presentations of other authors, either in letter or in spirit, are specified as such in accordance with the citing guidelines. The sections on methodology (in particular regarding practical work, laboratory regulations, statistical processing) and results (in particular regarding figures, charts and tables) are exclusively my responsibility.

[In the case of having conducted your doctoral research project completely or in part within a working group:] Furthermore, I declare that I have correctly marked all of the data, the analyses, and the conclusions generated from data obtained in collaboration with other persons, and that I have correctly marked my own contribution and the contributions of other persons (cf. declaration of contribution). I have correctly marked all texts or parts of texts that were generated in collaboration with other persons.

My contributions to any publications to this dissertation correspond to those stated in the below joint declaration made together with the supervisor. All publications created within the scope of the dissertation comply with the guidelines of the ICMJE (International Committee of Medical Journal Editors; www.icmje.org) on authorship. In addition, I declare that I shall comply with the regulations of Charité – Universitätsmedizin Berlin on ensuring

I declare that I have not yet submitted this dissertation in identical or similar form to another Faculty.

The significance of this statutory declaration and the consequences of a false statutory declaration under criminal law (Sections 156, 161 of the German Criminal Code) are known to me.”

Date	Signature
26.02.23	Alessandro Faragli

Declaration of your own contribution to the publications

I hereby declare that I am the sole first author of the presented publications:

Cardiovascular magnetic resonance-derived left ventricular mechanics-strain, cardiac power and end-systolic elastance under various inotropic states in swine.

Faragli et al. - J Cardiovasc Magn Reson. 2020 Nov 30;22(1):79. doi: 10.1186/s12968-020-00679-z

Cardiovascular magnetic resonance feature tracking in pigs: a reproducibility and sample size calculation study.

Faragli et al. - The International Journal of Cardiovascular Imaging 2020 doi.org/10.1007/s10554-020-01767-y

My contribution encompasses the ideation, the analysis, the revision and writing of the publications under the supervision of the two Supervisors. All the tables and the figures included were created by me and based on my statistical evaluation.

Berlin, 26.02.2023

Alessandro Faragli

_____

Signature of doctoral candidate

6 Extract from the Journal Summary List

Journal Data Filtered By: **Selected JCR Year: 2018** Selected Editions: SCIE,SSCI Selected Categories: **"CARDIAC and CARDIOVASCULAR SYSTEMS"** Selected Category Scheme: WoS

Gesamtanzahl: 136 Journale

Rank	Full Journal Title	Total Cites	Journal Impact Factor	Eigenfactor Score
1	EUROPEAN HEART JOURNAL	57,358	23.239	0.125920
2	CIRCULATION	166,484	23.054	0.211290
3	JOURNAL OF THE AMERICAN COLLEGE OF CARDIOLOGY	100,986	18.639	0.193290
4	Nature Reviews Cardiology	6,301	17.420	0.018820
5	CIRCULATION RESEARCH	52,988	15.862	0.072290
6	EUROPEAN JOURNAL OF HEART FAILURE	13,107	13.965	0.027620
7	JAMA Cardiology	3,280	11.866	0.019320
8	JACC-Cardiovascular Imaging	8,801	10.975	0.026160
9	JACC-Cardiovascular Interventions	11,555	9.544	0.033640
10	JACC-Heart Failure	3,537	8.910	0.016830
11	JOURNAL OF HEART AND LUNG TRANSPLANTATION	12,436	8.578	0.027310
12	CARDIOVASCULAR RESEARCH	21,828	7.014	0.021500
13	European Heart Journal-Cardiovascular Pharmacotherapy	442	6.723	0.001430
14	Circulation-Heart Failure	6,900	6.526	0.022830
15	BASIC RESEARCH IN CARDIOLOGY	4,137	6.470	0.005590
16	PROGRESS IN CARDIOVASCULAR DISEASES	4,055	6.162	0.008860
17	JOURNAL OF THE AMERICAN SOCIETY OF ECHOCARDIOGRAPHY	10,478	6.111	0.016060
18	EUROPACE	10,908	6.100	0.025320
19	Circulation-Cardiovascular Interventions	5,289	6.060	0.016640

Rank	Full Journal Title	Total Cites	Journal Impact Factor	Eigenfactor Score
20	Cardiovascular Diabetology	5,392	5.948	0.011550
21	Circulation-Cardiovascular Imaging	5,456	5.813	0.018480
22	European Journal of Preventive Cardiology	4,782	5.640	0.013370
23	CANADIAN JOURNAL OF CARDIOLOGY	6,710	5.592	0.018500
24	JOURNAL OF THORACIC AND CARDIOVASCULAR SURGERY	29,599	5.261	0.036950
25	European Heart Journal-Cardiovascular Imaging	5,498	5.260	0.021650
26	HEART RHYTHM	12,344	5.225	0.029030
27	REVISTA ESPANOLA DE CARDIOLOGIA	3,566	5.126	0.004640
28	HEART	18,063	5.082	0.030620
29	JOURNAL OF CARDIOVASCULAR MAGNETIC RESONANCE	5,113	5.070	0.014020
30	JOURNAL OF MOLECULAR AND CELLULAR CARDIOLOGY	14,143	5.055	0.020450
31	Circulation-Arrhythmia and Electrophysiology	6,432	4.968	0.017840
32	Clinical Research in Cardiology	3,022	4.907	0.006760
33	Circulation-Cardiovascular Genetics	3,441	4.864	0.010500
34	Journal of the American Heart Association	13,230	4.660	0.060340
35	TRENDS IN CARDIOVASCULAR MEDICINE	2,667	4.462	0.003930
36	Circulation-Cardiovascular Quality and Outcomes	4,531	4.378	0.014350
37	ATHEROSCLEROSIS	23,442	4.255	0.033500
38	CARDIOVASCULAR DRUGS AND THERAPY	2,109	4.181	0.003140
39	JOURNAL OF NUCLEAR CARDIOLOGY	3,711	4.112	0.004480

Rank	Full Journal Title	Total Cites	Journal Impact Factor	Eigenfactor Score
40	AMERICAN JOURNAL OF PHYSIOLOGY-HEART AND CIRCULATORY PHYSIOLOGY	27,828	4.048	0.022820
41	AMERICAN HEART JOURNAL	20,811	4.023	0.026780
42	EuroIntervention	6,097	4.018	0.016840
43	HEART FAILURE REVIEWS	2,598	4.015	0.005300
44	ANNALS OF THORACIC SURGERY	36,145	3.919	0.040630
45	JOURNAL OF CARDIAC FAILURE	5,339	3.857	0.009350
46	EUROPEAN JOURNAL OF CARDIO-THORACIC SURGERY	17,156	3.847	0.026410
47	European Heart Journal-Acute Cardiovascular Care	1,466	3.734	0.005330
48	INTERNATIONAL JOURNAL OF CARDIOLOGY	30,479	3.471	0.080570
49	ESC Heart Failure	680	3.407	0.002020
50	NUTRITION METABOLISM AND CARDIOVASCULAR DISEASES	5,821	3.340	0.010180
51	CURRENT PROBLEMS IN CARDIOLOGY	574	3.333	0.000700
52	Journal of Cardiovascular Computed Tomography	1,711	3.316	0.004430
53	Global Heart	881	3.238	0.003800
54	RESPIRATORY MEDICINE	11,846	3.237	0.015840
55	CIRCULATION JOURNAL	9,904	3.025	0.016510
56	JOURNAL OF THROMBOSIS AND THROMBOLYSIS	2,789	2.941	0.005860
57	JOURNAL OF CARDIOVASCULAR ELECTROPHYSIOLOGY	7,508	2.910	0.010700
58	Annals of Cardiothoracic Surgery	1,528	2.895	0.004950
59	AMERICAN JOURNAL OF CARDIOLOGY	37,275	2.843	0.044530

Rank	Full Journal Title	Total Cites	Journal Impact Factor	Eigenfactor Score
60	Journal of Cardiovascular Translational Research	1,458	2.756	0.003220
61	Cardiovascular Toxicology	1,209	2.630	0.001720
62	American Journal of Cardiovascular Drugs	1,005	2.578	0.001830
63	JOURNAL OF CARDIOVASCULAR PHARMACOLOGY AND THERAPEUTICS	1,239	2.570	0.002540
64	CATHETERIZATION AND CARDIOVASCULAR INTERVENTIONS	9,366	2.551	0.016550
65	Journal of Cardiovascular Nursing	1,997	2.510	0.003080
66	European Journal of Cardiovascular Nursing	1,648	2.497	0.002480
67	CLINICAL CARDIOLOGY	4,234	2.455	0.006620
68	Current Cardiology Reports	1,859	2.395	0.005470
69	JOURNAL OF CARDIOVASCULAR PHARMACOLOGY	5,522	2.371	0.004680
70	Archives of Cardiovascular Diseases	1,496	2.355	0.003590
71	Cardiovascular Therapeutics	1,353	2.315	0.002190
72	Journal of Cardiology	2,991	2.289	0.006360
73	Hellenic Journal of Cardiology	850	2.269	0.000840
74	International Heart Journal	1,791	2.226	0.002530
75	CardioRenal Medicine	517	2.214	0.001230
76	Cardiology Research and Practice	847	2.140	0.001360
77	JOURNAL OF INTERVENTIONAL CARDIOLOGY	1,406	2.106	0.002590
78	Heart Lung and Circulation	2,503	2.078	0.006030
79	Pulmonary Circulation	1,407	2.075	0.004170
80	CARDIOLOGY CLINICS	1,075	2.061	0.001630

Rank	Full Journal Title	Total Cites	Journal Impact Factor	Eigenfactor Score
81	Cardiovascular Ultrasound	1,022	2.043	0.001740
82	Congenital Heart Disease	1,534	2.036	0.003760
83	Cardiovascular Diagnosis and Therapy	763	2.006	0.002480
84	CURRENT OPINION IN CARDIOLOGY	2,056	1.979	0.003750
85	Netherlands Heart Journal	1,196	1.972	0.001920
86	BMC Cardiovascular Disorders	3,243	1.947	0.008320
87	Interactive Cardiovascular and Thoracic Surgery	5,544	1.931	0.010010
88	CARDIOVASCULAR AND INTERVENTIONAL RADIOLOGY	5,219	1.928	0.007850
89	Heart Failure Clinics	903	1.895	0.001840
90	JOURNAL OF CARDIOTHORACIC AND VASCULAR ANESTHESIA	5,098	1.882	0.006650
91	INTERNATIONAL JOURNAL OF CARDIOVASCULAR IMAGING	2,949	1.860	0.006790
92	HEART & LUNG	2,445	1.840	0.003060
93	Cardiovascular Engineering and Technology	447	1.776	0.000870
94	CARDIOVASCULAR PATHOLOGY	1,830	1.765	0.003290
95	Journal of Geriatric Cardiology	917	1.763	0.002450
96	Cardiology Journal	1,144	1.743	0.001920
97	Korean Circulation Journal	1,117	1.694	0.002180
98	Arquivos Brasileiros de Cardiologia	2,999	1.679	0.003300
99	Acta Cardiologica Sinica	517	1.676	0.000850
100	Kardiologia Polska	1,532	1.674	0.002140
101	HEART AND VESSELS	2,093	1.620	0.003690

7 Publications

Cardiovascular magnetic resonance-derived left ventricular mechanics-strain, cardiac power and end-systolic elastance under various inotropic states in swine.

Faragli A, Tanacli R, Kolp C, Abawi D, Lapinskas T, Stehning C, Schnackenburg B, Lo Muzio FP, Fassina L, Pieske B, Nagel E, Post H, Kelle S, Alogna A.

J Cardiovasc Magn Reson. 2020 Nov 30;22(1):79. doi: 10.1186/s12968-020-00679-z. **(Impact Factor: 5.364)**

Cardiovascular magnetic resonance feature tracking in pigs: a reproducibility and sample size calculation study.

Faragli A, Tanacli R, Kolp C, Lapinskas T, Stehning C, Schnackenburg B, Lo Muzio F-P, Perna S, Pieske B, Nagel E, Post H, Kelle S, Alogna A.

The International Journal of Cardiovascular Imaging 2020 - https://doi.org/10.1007/s10554-020-01767-y. **(Impact Factor: 2.357)**

Journal of Cardiovascular Magnetic Resonance

RESEARCH

Open Access

Cardiovascular magnetic resonance-derived left ventricular mechanics—strain, cardiac power and end-systolic elastance under various inotropic states in swine

A. Faragli[1,2,3,4], R. Tanacli[1,4], C. Kolp[1], D. Abawi[1], T. Lapinskas[4,5], C. Stehning[6], B. Schnackenburg[6], F. P. Lo Muzio[7,8], L. Fassina[9], B. Pieske[1,2,3,4], E. Nagel[10], H. Post[1,2,3,11], S. Kelle[1,2,3,4†] and A. Alogna[1,2,3*†]

Abstract

Background: Cardiovascular magnetic resonance (CMR) strain imaging is an established technique to quantify myocardial deformation. However, to what extent left ventricular (LV) systolic strain, and therefore LV mechanics, reflects classical hemodynamic parameters under various inotropic states is still not completely clear. Therefore, the aim of this study was to investigate the correlation of LV global strain parameters measured via CMR feature tracking (CMR-FT, based on conventional cine balanced steady state free precession (bSSFP) images) with hemodynamic parameters such as cardiac index (CI), cardiac power output (CPO) and end-systolic elastance (Ees) under various inotropic states.

Methods: Ten anaesthetized, healthy Landrace swine were acutely instrumented closed-chest and transported to the CMR facility for measurements. After baseline measurements, two steps were performed: (1) dobutamine-stress (Dobutamine) and (2) verapamil-induced cardiovascular depression (Verapamil). During each protocol, CMR images were acquired in the short axisand apical 2Ch, 3Ch and 4Ch views. MEDIS software was utilized to analyze global longitudinal (GLS), global circumferential (GCS), and global radial strain (GRS).

Results: Dobutamine significantly increased heart rate, CI, CPO and Ees, while Verapamil decreased them. Absolute values of GLS, GCS and GRS accordingly increased during Dobutamine infusion, while GLS and GCS decreased during Verapamil. Linear regression analysis showed a moderate correlation between GLS, GCS and LV hemodynamic parameters, while GRS correlated poorly. Indexing global strain parameters for indirect measures of afterload, such as mean aortic pressure or wall stress, significantly improved these correlations, with GLS indexed for wall stress reflecting LV contractility as the clinically widespread LV ejection fraction.

Conclusion: GLS and GCS correlate accordingly with LV hemodynamics under various inotropic states in swine. Indexing strain parameters for indirect measures of afterload substantially improves this correlation, with GLS being as good as LV ejection fraction in reflecting LV contractility. CMR-FT-strain imaging may be a quick and promising tool to characterize LV hemodynamics in patients with varying degrees of LV dysfunction.

*Correspondence: alessio.alogna@charite.de
†S. Kelle and A. Alogna contributed equally to this work
[1] Department of Internal Medicine and Cardiology, Charité-Universitätsmedizin Berlin, Campus Virchow-Klinikum, Augustenburger Platz 1, 13353 Berlin, Germany
Full list of author information is available at the end of the article

Keywords: Cardiovascular magnetic resonance, Feature tracking, Left ventricular strain, Contractile function, Porcine model, Translational studies, Hemodynamics

Background

The routine assessment of left ventricular (LV) ejection fraction (LVEF), being a measure of global systolic function, falls short in identifying regional myocardial impairment and the mechanical contraction of the heart [1, 2]. Therefore, strain imaging has emerged in the past years to better quantify myocardial LV deformation in various patient populations [3–7]. Numerous studies have validated and shown the utility of myocardial strain in the diagnosis of several pathologies, identifying subclinical myocardial changes, and even by showing an impact on the prognosis of cardiovascular pathologies [8–15]. Recently, cardiovascular magnetic resonance (CMR) feature tracking (FT) strain analysis was shown to be accurate in the detection of myocardial dysfunction as well as useful as a predictor of major adverse cardiac events, with the advantage of utilizing conventional balanced steady-state free precession (bSSFP) cine sequences [15–19]. Impaired LV systolic function and cardiac reserve can be clinically assessed by hemodynamic parameters such as cardiac index (CI), as well as by cardiac power output (CPO) at rest and during pharmacological stress. In particular, the latest has been shown to strongly correlate with the clinical outcome of chronic heart failure patients [20, 21]. Moreover, LV CPO is able to provide an assessment of the intraventricular flow as well as of its mechanics much more than other hemodynamic parameters, since it couples not only with the cardiac work, but also with the response of the vasculature [22, 23]. The invasively measured end-systolic elastance (Ees) is instead, a relatively load-independent parameter describing the LV inotropic state [24]. Recently, Seeman and colleagues successfully investigated a novel CMR method to noninvasively quantify Ees [25]. Whether or not, and to what extent CMR-FT LV strain reflects the above-mentioned hemodynamic parameters under various inotropic states has not been investigated thus far. Therefore, the aim of this study was to validate the correlation of CMR LV strain parameters against hemodynamic parameters such as CI, CPO and the Ees mentioned above, under various inotropic states in swine.

Methods

The experimental protocols were approved by the local bioethics committee of Berlin, Germany (G0138/17), and conform to the "European Convention for the Protection of Vertebrate Animals used for Experimental and other Scientific Purposes" (Council of Europe No 123, Strasbourg 1985).

Experimental setup

Female Landrace swine (n = 10, 51 ± 10 kg) were fasted overnight with free access to water, and then sedated and intubated on the day of the experiment. Anaesthesia was continued with fentanyl, midazolam, ketamine and pancuronium as needed. The anesthesia regimen included low-dose isofluorane to obtain a deeper sedation and stabilize hemodynamics without impacting much on systemic vascular resistance. Animals were ventilated (Cato, Dräger Medical, Lubeck, Germany) with a FiO2 of 0.5, an I: E-ratio of 1:1.5, the positive end-expiratory pressure was set at 5 mmHg and a tidal volume of 10 ml kg^{-1}. The respiratory rate was continuously adjusted to maintain an end-expiratory carbon dioxide partial pressure between 35 and 45 mmHg. Under fluoroscopic guidance, all animals were instrumented with a floating balloon catheter in the right atrium, as well as in the coronary sinus (Arrow Balloon Wedge-Pressure Catheters, Teleflex Inc, Wayne, Pennsylvania USA). In order to avoid CMR-artefacts, the balloon-tip was cut before introducing the catheters in the vessel. Respiratory gases (PM 8050 MRI, Dräger Medical), heart rate (HR), and invasively derived arterial blood pressure were continuously monitored (Precess 3160, InVivo, Gainesville, Florida, USA) via a sheath access surgically prepared in the internal carotid artery. Body temperature was monitored by a sublingual thermometer and was maintained at 38 °C during CMR imaging via air ventilation or infusion of cold saline solution.

Experimental protocols

After acute instrumentation, the animals were transported to the CMR facility for measurements. After baseline measurements, two steps were performed: (1) Dobutamine-stress (Dobutamine) and (2) verapamil-induced cardiovascular depression (Verapamil). Dobutamine infusion was titrated aiming at a 25% HR increase compared to baseline values, while verapamil was given as single 2.5 mg bolus, aiming at a 25% decrease of CI. This protocol was established beforehand with a small pilot study (data not shown), in which the titration of dobutamine and verapamil was assessed by LV invasive conductance measurements according to previous publications by our group [26]. The cumulative dose for each experiment was achieved via careful titration of

verapamil, administered as a 2.5 mg bolus in order to avoid a pronounced hypotension leading to hemodynamic instability. In the pilot experiments CI was continuously assessed online via a Swan-Ganz catheter in the pulmonary artery (Edwards Lifesciences CCO connected to Vigilance I, Edwards Lifesciences, Irvine, California, USA). In the CMR study, after the first bolus, we estimated stroke volume via short-axis cine imaging after reaching a hemodynamic steady state (around 5 min after bolus injection). In case CI was not decreased as much as 25%, we proceeded with a further bolus of verapamil. Between the different protocol steps there was a washout period of 30 min. The anaesthesia regimen included low dose isoflurane to obtain a deeper sedation and stabilize hemodynamics without impacting much on systemic vascular resistance. This protocol was established beforehand with a small pilot study (data not shown), in which the titration of dobutamine and verapamil was assessed by LV invasive conductance measurements according to previous publications by our group [26]. At each protocol step, CMR images were acquired in the short axis (SAx), two-chamber (2Ch), three-chamber (3Ch) and four-chamber (4Ch) views. At the end of the measurements, animals were transported back to the operating room for sacrifice. Sacrifice was performed with an intracoronary 80 mmol potassium bolus.

Cardiovascular magnetic resonance

All CMR images were acquired in a supine position using a 3 T CMR scanner (Ingenia, Philips Healthcare, Best, The Netherlands) CMR scanner with an anterior- and a built-in posterior coil element, where up to 30 coil elements were employed, depending on the individual anatomy. All animals were scanned using identical comprehensive imaging protocol. The study protocol included initial scouts to determine cardiac imaging planes. Cine images were acquired using electrocardiogram (ECG)-gated bSSFP cine sequence in three LV long-axis (2Ch, 3Ch, 4Ch) planes. The ventricular 2Ch and 4Ch planes were used to plan stack of SAx slices covering entire LV. The following imaging parameters were used: repetition time (TR) = 2.9 ms, echo time (TE) = 1.45 ms, flip angle = 45°, measured voxel size = $1.9 \times 1.9 \times 8.0$ mm^3, reconstructed voxel size $1.0 \times 1.0 \times 8 mm^3$, and 40 cardiac phases.

Image analysis

All images were analyzed offline using a commercially available software (Medis Suite, version 3.1, Leiden, The Netherlands) in accordance with a recent consensus document for quantification of LV function using CMR [27]. A numeric code was assigned to the sequences of different measurements steps and the observers were therefore blinded to the pharmacological interventions. Given the excellent inter-observer reproducibility, we averaged values obtained by several measurements from one observer.

On SAx view, the outline of the endocardial border of the LV was manually traced on all slices of each phase. Volumes were computed by Simpson method of disks summation, whereby the sum of cross-sectional areas was multiplied by slice thickness (8 mm). The LVEF was calculated using the Simpson method. The LV outflow tract was included as LV blood volume. Papillary muscles and trabeculation were included as LV volume. The ascending aorta was outlined in all the images and flow calculation was performed in the corresponding velocity-encoded phase images. The average flow velocity (cm/s) was multiplied by the area of the vessel (cm^2) to obtain the flow (ml/s) and integrated over one cardiac cycle to obtain the stroke volume (SV). Then, the cardiac output (CO) is indirectly calculated as the product of SV and HR. Finally, the CI is calculated as the CO divided by the body surface area (BSA) [28]. For the strain analysis 2Ch, 3Ch and 4Ch cine images, and respectively, 3 preselected mid-ventricle slices from the LV SAx stack were included. The endocardial and epicardial contours drawn on cine images with QMass (version 8.1, Medis Medical) were transferred to QStrain RE (version 2.0, Medis Medical) where after the application of tissue tracking algorithm, endocardial and epicardial borders were detected throughout all the cardiac cycle (Fig. 1a, d). These long-axis cine images were further used to compute myocardial global longitudinal strain (GLS), and SAx images were used to compute global circumferential strain (GCS) and global radial strain (GRS) and strain-rate (Fig. 1b, e). The global values were obtained by averaging the values of systolic peak strain according to an AHA 17 segments model, apex being excluded, as follows: GCS from averaging circumferential strain for 6 basal, 6 mid and 4 apical segmental individual values; GLS from 2Ch, 3Ch and 4Ch averaging 6 basal, 6 mid and 4 apical segments using a bull-eye view (Fig. 1c, f, g, h, i). Data on strain rate are presented in Table 3. In line with the global strain parameters, dobutamine increased peak systolic SR. Verapamil significantly decreased peak systolic SR compared to dobutamine but not to baseline values.

Hemodynamic parameters

Systolic blood pressure (SBP), diastolic blood pressure (DBP) and mean aortic pressure (mAoP) were invasively measured throughout the entire protocol study via a sheath access surgically prepared in an internal carotid artery.

The systemic vascular resistance was calculated as follows:

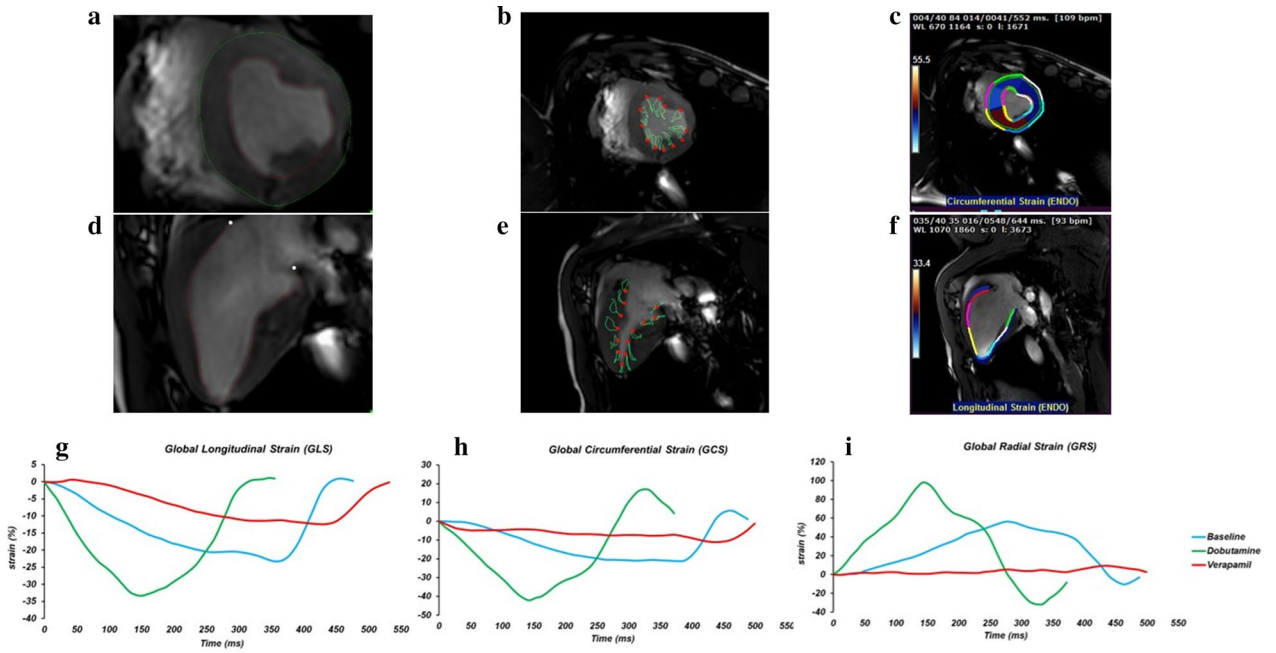

Fig. 1 Global strain analysis via Qstrain and representative left ventricular (LV) strain curves from one experiment. **a** Short axis endocardial and epicardial contouring; **b** circumferential strain measured with Qstrain, the lower end of the scale bar is equal to zero and it is not represented in the original window from MEDIS; **c** circumferential strain measured at end-systole time-to-peak; **d** longitudinal axis endocardial contouring; **e** longitudinal strain measured with Qstrain, the lower end of the scale bar is equal to zero and it is not represented in the original window from MEDIS; **f** longitudinal strain measured at end-systole time-to-peak; **g** global longitudinal strain (GLS), **h** global circumferential strain (GCS), and **i** global radial strain (GRS) representative curves from one animal measured during Baseline, Dobutamine (Dob) and Verapamil (Ver) (mean values of all segments)

$$SVR_{mmHg/L} = \frac{Mean\,Arterial\,Pressure(MAP) - Right\,Atrial\,Pressure}{Cardiac\,Output(CO)}$$

CPO, CI and Ees were calculated as follows:

$$CPO = \frac{CO \times mAoP}{451}$$

$$CI = \frac{CO}{BSA}$$

$$Ees = \frac{LVP_{sys}}{V_{LVP_{max}} - V_0}$$

where:

$$LVP_{sys} = \frac{2}{3}Systolic\,Blood\,Pressure + \frac{1}{3}Diastolic\,Blood\,Pressure$$

$$V_{LVP_{max}} = End - Systolic\,Volume$$

$$V_0 = 0$$

as described in the work by Kelly et al [29].

GLS, GCS and GRS were indexed to the measured mAoP adapting the formula from the previous study by Rhea et al. [30] as follows:

$$\frac{Global\,Strain \times mAoP}{avg(mAoP)}$$

where Global Strain was the global value of either longitudinal (GLSi), circumferential (GCSi) or radial (GRSi) strain and avg(mAoP) was the average of the mAoP measured for each protocol step, namely at baseline, dobutamine and verapamil (Table 1).

Table 1 Systemic hemodynamics and cardiac mechanics parameters during BL, Dob and Ver steps

	Baseline	Dobutamine	Verapamil
HR (bpm)	106 ± 15	146 ± 12*	98 ± 19*,§
LVEF (%)	59 ± 8	77 ± 7*	39 ± 9*,§
CO (L/min)	6 ± 1	9 ± 2*	4 ± 1*,§
CI (L/min/m^2)	2.5 ± 0.2	3.8 ± 0.5*	1.7 ± 0.7*,§
CPO (W)	1.2 ± 0.3	2.0 ± 0.6*	0.7 ± 0.2*,§
SVR (dyn s cm^{-5})	15 ± 5	11 ± 4*	19 ± 9*,§
mAoP (mmHg)	90 ± 12	98 ± 19	70 ± 10*,§
Wall stress (mmHg)	0.12 ± 0.02	0.16 ± 0.04*	0.10 ± 0.02§

HR heart rate, *LVEF* left ventricular ejection fraction, *CO* cardiac output, *CI* cardiac index, *CPO* cardiac power output, *SVR* systemic vascular resistance, *mAoP* mean aortic pressure

*p < 0.05 vs. Baseline; §p < 0.05 vs. Dobutamine

Meridional wall stress was calculated via the following formula [31]:

$$LV\ wall\ stress = \frac{\left(0.334 \times LVP_{sys} \times LVESD\right)}{PWT \times [1 + PWT/LVID]}$$

where LVESD = left ventricular end-systolic diameter and PWT = posterior wall thickness as described in the paper by Reichek et al. [31]. PLT was measured by averaging three separate measurements in the basal short axis sequence.

GLS, GCS and GRS were indexed to the measured wall stress adapting the formula from the study by Reichek et al. [31] as follows:

$$\frac{Global\ Strain \times LV\ wall\ stress}{avg(LV\ wall\ stress)}$$

where Global Strain was the global value of either global longitudinal (GLSw), global circumferential (GCSw) or global radial (GRSw) strain. The average for both LV wall stress were calculated for each step, namely at baseline, dobutamine and verapamil (Table 1).

Statistical analysis

All data are presented as mean ± SD. The association between strain data and hemodynamic data was assessed by linear regression analysis. The condition (baseline, dobutamine, verapamil) was included as a regressor into the linear regression model. To verify whether the linear regressions were significantly different (p-value < 0.05), using custom-made scripts in MATLAB (release R2020a; The MathWorks, Inc., Natick, Massachusetts, USA), we compared slopes, intercepts as well as correlation coefficients: (i) via t-test (for slopes and intercepts) and (ii) via the Fisher's r-to-z transformation followed by z-test (for correlation coefficients), as previously described by Weaver and Wuensch [32]. Data between groups at different inotropic states were analysed by one-way ANOVA for repeated measurements. Post-hoc testing was performed by Tukey's test. A p-value < 0.05 was considered significant. For statistical calculations, we used the software Sigmastat (Version 4.0, Systat Software, Inc., Cranes Software, Karnataka, India) and SPSS (Version 23.0, Statistical Package for the Social Sciences, International Business Machines, Inc., Armonk, New York, USA).

Results

The dose of dobutamine needed to induce a 25% HR increase was 6.4 ± 2.5 μg/kg/min, while the dose of verapamil needed to decrease CI significantly was 5 ± 2 mg.

Systemic hemodynamics

Systemic hemodynamic data are summarized in Table 1. mAoP was not affected by Dobutamine, but significantly decreased during Verapamil. Dobutamine increased baseline HR, CO and LVEF, while Verapamil decreased them. Systemic vascular resistance (SVR) substantially decreased during Dobutamine, while increased during Verapamil. CPO and CI both increased during Dobutamine and decreased during Verapamil. Ees, the slope of the end-systolic pressure–volume relationship, increased during Dobutamine and decreased during Verapamil infusion (Fig. 2).

Global strain parameters

Strain parameters are summarized in Table 2a, b and c. GLS as well as GCS increased during Dobutamine, while decreased during Verapamil. GRS was not significantly affected by Dobutamine, while decreased significantly during Verapamil.

Systolic strain rate

Data on strain rate (SR) are presented in Table 3. In line with the global strain parameters, Dobutamine increased peak systolic SR. Verapamil significantly decreased peak systolic SR compared to Dobutamine but not to baseline values.

Indexing strain parameters for indirect measures of afterload

Indexing global strain parameters for either mAoP (Table 2b) or for meridional wall stress (Table 2c) did not significantly impact the above-described changes induced by Dobutamine and Verapamil.

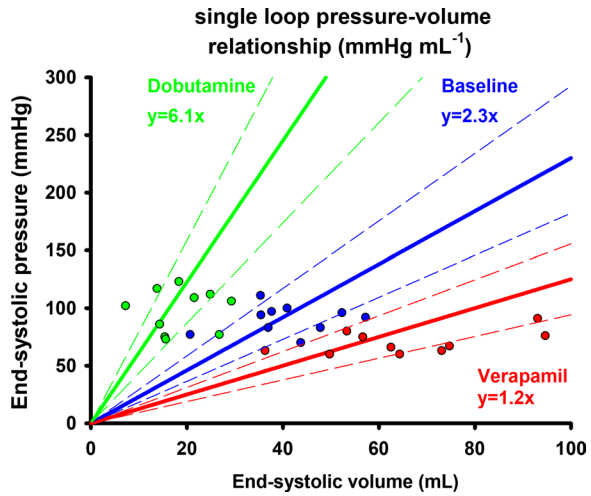

Fig. 2 Averaged end-systolic pressure–volume relationship at baseline, during dobutamine and verapamil. Single-loop derived by the LV end-systolic pressure–volume relationship (ESPVR) is plotted under various inotropic states. The green line corresponds to the averaged ESPVR during dobutamine infusion, the blue line represents the averaged ESPVR at baseline, while the red one represented the averaged ESPVR at verapamil. A steeper increase in ESPVR during dobutamine and a relevant decrease during verapamil are observed. The equation for each ESPVR is displayed in the graph. Data points are plotted for each animal during different inotropic states. The dashed lines represent the 95% confidence intervals

Table 2 Global strain and indexed global strain values measured at different inotropic states

	Baseline	Dobutamine	Verapamil
(A)			
GLS (%)	− 23 ± 4	− 45 ± 9*	− 16 ± 3*,§
GCS (%)	− 31 ± 8	− 53 ± 10*	− 17 ± 5*,§
GRS (%)	72 ± 19	88 ± 36	30 ± 12*,§
(B)			
GLSi (%)	− 23 ± 4	− 45 ± 10*	− 16 ± 4*,§
GCSi (%)	− 30 ± 8	− 52 ± 8*	− 16 ± 5*,§
GRSi (%)	71 ± 19	84 ± 23	30 ± 13*,§
(C)			
GLSw (%)	− 23 ± 5	− 44 ± 10*	− 16 ± 3*,§
GCSw (%)	− 31 ± 9	− 52 ± 13*	− 17 ± 17*,§
GRSw (%)	71 ± 20	90 ± 54	35 ± 27*,§

(A) Global strain: *GLS* global longitudinal strain, *GCS* global circumferential strain, *GRS* global radial strain; (B) Global strain indexed for mean aortic pressure (mAoP): *GLSi* global longitudinal strain indexed for mAoP, *GCSi* global circumferential strain indexed for mAOP, *GRSi* global radial strain indexed for mAoP; (C) Global strain indexed for meridional wall stress: *GLSw* global longitudinal strain indexed for wall stress, *GCSw* global circumferential strain indexed for wall stress, *GRSw* global radial strain indexed for wall stress. *$p < 0.05$ vs. baseline; §$p < 0.05$ vs. Dobutamine

Table 3 Global peak systolic strain rates values measured at different inotropic states

	Baseline	Dobutamine	Verapamil
GLS peak systolic SR (s-1)	− 2.5 ± 0.6	− 6.4 ± 1.5*	− 2.1 ± 1.1§
GCS peak systolic SR (s-1)	− 3.2 ± 2.2	− 8.7 ± 2.5*	− 2.0 ± 1.3§
GRS peak systolic SR (s-1)	2.7 ± 1.0	5.5 ± 0.9	2.2 ± 1.5§

Strain Rate (SR). *$p < 0.05$ vs. Baseline; §$p < 0.05$ vs. Dobutamine

Correlation between global strain, LVEF and LV hemodynamic parameters

Linear regression analysis showed a moderate correlation between GLS, GCS and CPO, while a poor one was observed between GRS and CPO (Fig. 3a). A similar correlation was observed between GLS, GCS and CI (Fig. 3b), with GRS worst performing. A moderate correlation was observed between GLS, GCS and Ees, while a poor one was observed between GRS and Ees (Fig. 3c). Indexing global strain parameters either for mAoP or for wall stress improved their correlations with CPO (Figs. 4a and 5a), with CI (Figs. 4b and 5b) as well as with Ees (Figs. 4c and 5c). LVEF moderately correlated with CI and CPO ($r^2 = 0.81$ and $r^2 = 0.69$, respectively) as GLSw with CI and CPO ($r^2 = 0.74$ and $r^2 = 0.72$, respectively). GLSw moderately correlated with Ees as well as LVEF with Ees ($r^2 = 0.74$ versus $r^2 = 0.74$). The above-mentioned correlations were both statistically significant with a $p < 0.0001$.

Relative change of mechanics under various inotropic states

In Fig. 6, we plotted the relative change of mechanics (global LV strain parameters) as well as hemodynamic parameters during Dobutamine and Verapamil in comparison to baseline.

Among global strain parameters, GLS showed a higher relative change than GRS during both Dobutamine and Verapamil, while the same was valid for GCS during dobutamine only. Moreover, the impact of Dobutamine was more prominently expressed by GLS than by CI, while the impact of Verapamil on GRS was negligible when in comparison to CI. The impact of Dobutamine and Verapamil on the rest of the mechanic and hemodynamic parameters was comparable.

Discussion

CMR strain imaging is an established technique to quantify myocardial deformation. However, to what extent LV systolic strain, and therefore LV mechanics, reflects classical hemodynamic parameters under various inotropic states is still not completely clear. In the current study, we set out to investigate the correlation of LV global strain parameters measured via CMR-FT with hemodynamic

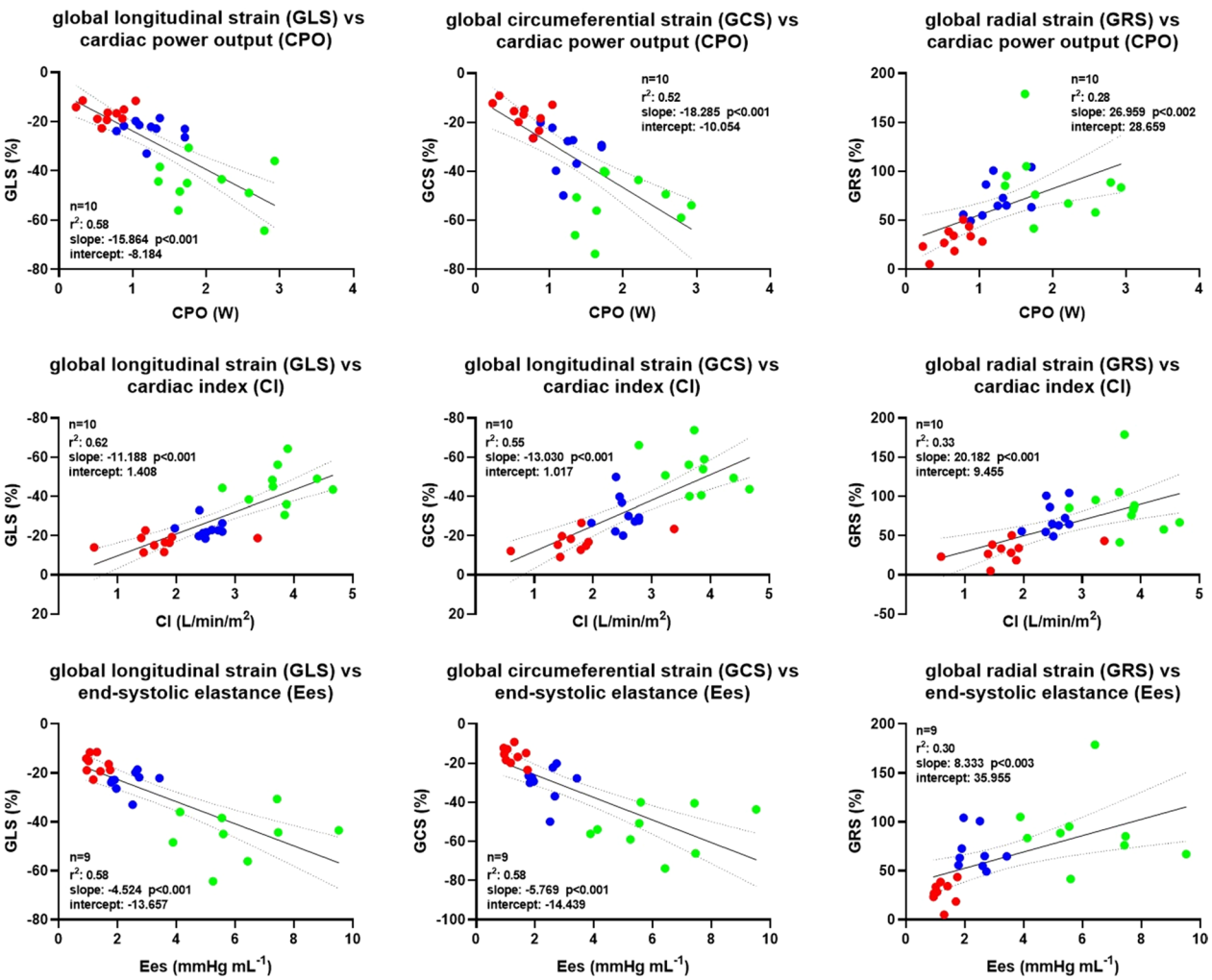

Fig. 3 Correlation between global strain and different invasive parameters of hemodynamics. **a** Linear regression analysis showing a moderate correlation between GLS, GCS, and CI; and a poor correlation between GRS and CI. **b** Linear regression analysis showing a moderate correlation between GLS, GCS and CPO; and a poor correlation between GRS and CPO. **c** Linear regression analysis showing a moderate correlation between GLS, GCS, and Ees; and a poor correlation between GRS and Ees. Blue dots represent *BL* baseline, green dots represent *Dob* dobutamine, red dots represent *Ver* verapamil

parameters under various inotropic states in swine. We observed a moderate correlation of global strain parameters with LV hemodynamics. Interestingly, indexing strain parameters for indirect measures of afterload substantially improved this correlation, with GLS indexed for wall stress reflecting LV contractility as the clinically widespread LVEF.

Correlation between global strain, LVEF and LV hemodynamic parameters

Numerous studies have reported a significant diagnostic as well as a prognostic role of LV strain in the assessment of LV mechanics in various study populations [10, 11], including patients with heart failure with preserved ejection fraction, coronary artery disease, diabetes mellitus, hypertensive heart disease, hypertrophic cardiomyopathy, and arrhythmia [1–7]. Recently, CMR-FT strain analysis was shown to be accurate in the detection of myocardial dysfunction and as well useful as a predictor of major adverse cardiac events in ischemic or non-ischemic cardiomyopathy [18], with the advantage of utilizing simple bSSFP cine sequences [15–19, 33, 34]. However, notwithstanding the multitude of published papers assessing the clinical usefulness of strain, there is a notable lack of in-vivo validation studies [35]. Whether CMR-FT LV strain represents a valid tool to assess the cardiac mechanics of the myocardium, and how this varies under different inotropic states, is still unclear. In this

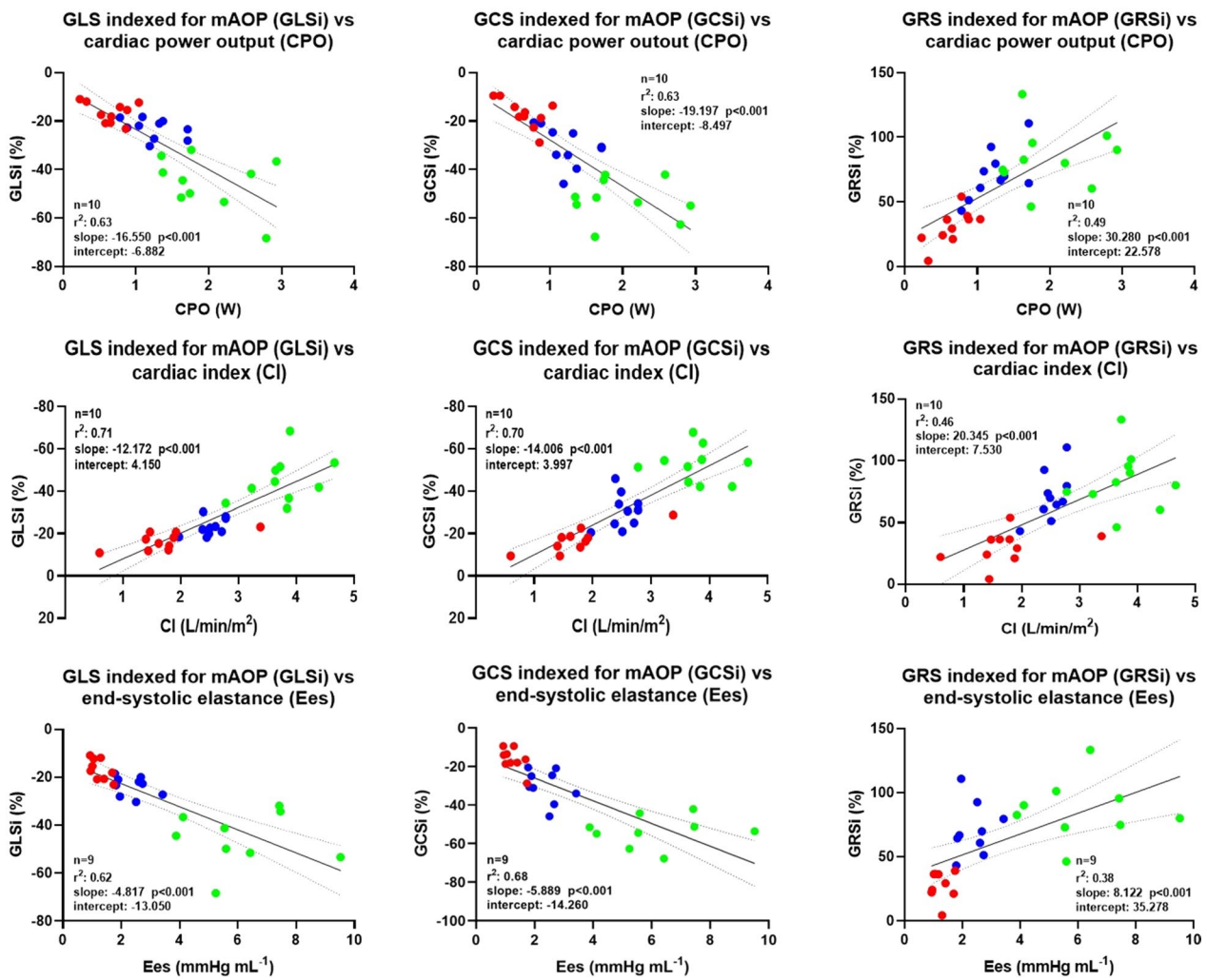

Fig. 4 Correlation between global strain indexed for mean aortic pressure and different invasive parameters of hemodynamics. Linear correlation between GLSi, GCSi, GRSi; and CI (**a**), CPO (**b**), and Ees (**c**), after adjusting strain values for mean aortic pressure (mAoP), according to the following formula (Global Strain × mAOP/avg (mAoP). Blue dots represent *BL* baseline, green dots represent *Dob* dobutamine, red dots represent *Ver* verapamil. *GLSi* global longitudinal strain indexed for mAoP, *GCSi* global circumferential strain indexed for mAoP, *GRSi* global radial strain indexed for mAoP

work, we could show a role of CMR LV strain as a surrogate of classic hemodynamic parameters such as CI, CPO, and a load-independent parameter of cardiac contractility such as Ees, which are established parameters to describe the hydraulic and mechanical role of the heart as a pump [22, 24]. Previous in vivo studies concentrated on the role of 2D and 3D speckle tracking echocardiography (STE) [35]. The main validation studies analysed the correlation of STE with the sonomicrometry technique in open-chest large animal models, showing an overall good agreement of the two techniques [35]. Similarly to our study, Weidemann et al. showed the ability of strain as well as strain rate to reflect swine LV-contractility under different inotropic states and independently of heart rate [36]. The invasively measured Ees, the slope of the end-systolic pressure–volume relationship, is a relatively load-independent parameter describing the LV inotropic state [24]. A recent study by Seeman et al. established a reliable method to assess Ees via CMR imaging [25]. In the current work, we showed a moderate to good correlation between both GLS, GCS, and Ees. The accuracy of GLS in reflecting Ees improved when indexing for wall stress. In line with our data, Yotti et al [8] showed a moderate correlation between echocardiographic assessed GCS and invasive pressure–volume catheterization data, while on the opposite, GLS correlated poorly. The authors

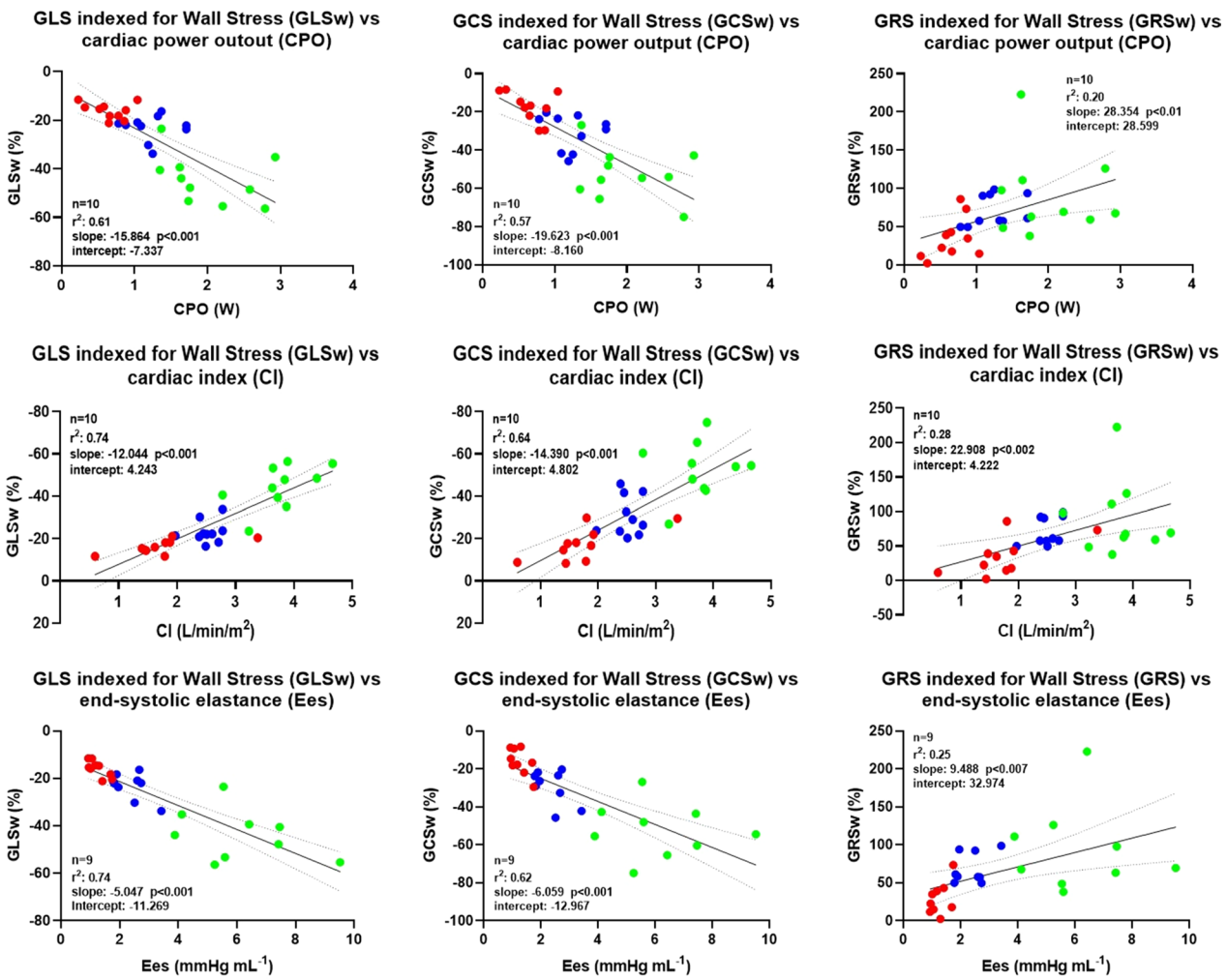

Fig. 5 Correlation between global strain indexed for wall stress and different invasive parameters of hemodynamics. Linear correlation between GLSw, GCSw, GRSw, LVEF; and CI (**a**), CPO (**b**), and Ees (**c**), after adjusting strain values for meridional Wall Stress, according to the following formula (Global Strain × Wall Stress / avg (Wall Stress). Blue dots represent *BL* baseline, green dots represent *Dob* dobutamine, red dots represent *Ver* verapamil

highlighted how the GCS measurements, as opposed to the GLS, did not change in patients with aortic stenosis or hypertension. They hypothesized this could be related to a lower load-dependency [8] of the first in comparison to the latter ones, but the different methodology of strain assessment in comparison to our study is probably playing a role as well.

Indexing strain parameters for indirect measures of afterload

In the current study, in order to minimize the load-dependency of the strain measurements, we indexed all the global strain values for indirect measures of afterload, such as the invasively measured mAoP as well as the meridional wall stress, as already described by Rhea et al. and Reichek et al [30, 31]. Correcting the strain measurements, as mentioned above, improved the ability of strain parameters to reflect LV hemodynamics. Yingchoncharoen et al. already demonstrated that blood pressure adjustment of strain is advisable in patients with large deviations of SBP from the normal-reference value [37]. Furthermore, in a study by Weiner et al. on the impact of isometric handgrip testing on LV twist mechanics, it was shown that longitudinal strain is influenced by blood pressure [38]. Finally, in line with our study, Rhea et al. showed an improved accuracy of pressure-adjusted GLS in predicting cardiac events and mortality [30].

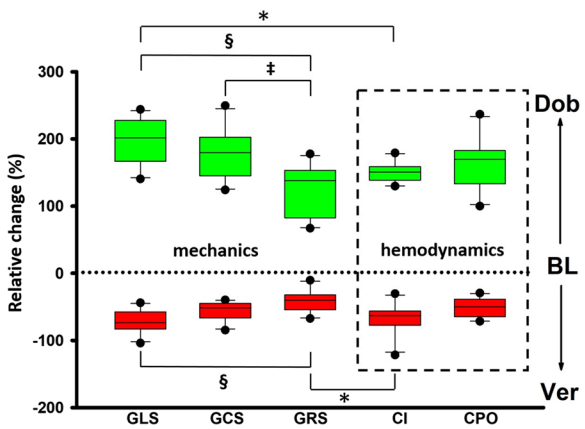

Fig. 6 Relative change of global strain and cardiac mechanics parameters from baseline to dobutamine or verapamil. The schematic representation above shows the relative change of global strain values and invasive hemodynamic parameters (dashed box) from baseline (BL, dashed horizontal line) to dobutamine (Dob, green boxes) and from BL to verapamil (Ver, red boxes), respectively. *$p < 0.05$ vs CI, §$p < 0.05$ vs GLS, ‡$p < 0.05$ vs GCS

Relative change of mechanics under various inotropic states

In order to investigate to what extent global LV strain parameters reflect hemodynamic changes we plotted the relative change of these parameters during Dobutamine and Verapamil compared to baseline. The relative change of GLS during Dobutamine was higher than the one of CI, while the impact of Verapamil on GRS was negligible when compared to CI, overall in line with the poor reproducibility of GRS measurements. The impact of Dobutamine and Verapamil on the rest of the mechanic and hemodynamic parameters was comparable. In line with previous reproducibility studies [39–42], we showed that radial strain is a poorly reproducible and inaccurate measurement. In this study we did not show the inter- and intra-observer reproducibility because it was already assessed in a previous work from our group based on the same cohort [43]. Our analysis showed that measurements at baseline were good to excellent (good ICC 0.60–0.74; excellent ICC > 0.74) for GLS, GCS and GRS, but that only GLS and GCS displayed good reproducibility during both dobutamine and verapamil steps, whereas radial strain was highly variable [43].

Clinical and translational perspective

In this in vivo study, we could show that CMR-FT strain parameters, such as GLS and GCS, reflect classic hemodynamic parameters such as CI, CPO, as well as a load-independent parameter of cardiac contractility such as Ees. LV strain has indeed emerged in the past year as a valid technique to assess LV deformation with high reproducibility. However, the spread of this technique in the clinical routine is limited by the often lengthy post-processing of the sequences, confining this important resource to the mere research field [44]. FT-strain, in particular, possesses the advantage of a quick assessment, being based on conventional bSSFP cine sequences [15–19], and seems to be therefore a promising technique to allow a more extensive clinical use of LV strain. Furthermore, indexing the global strain values for indirect measures of afterload, such as the invasively measured mAoP as well as the meridional wall stress, improves the ability of strain parameters to reflect LV hemodynamics. After accounting for meridional wall stress, GLS performed as good as LVEF in reflecting LV contractility, expressed as Ees, confirming the potential role of this novel parameter in the clinical arena. These results suggest that implementing strain measurements with pressure-derived variables may add accuracy to the evaluation of the mechanical and contractile function of the heart, improving the impact of LV strain in the clinical routine and helping to overcome the limitations of LVEF as a surrogate parameter of LV systolic function. In daily clinical routine, this could be potentially achieved even with a standard sphygmomanometer, as shown in the paper by Seeman at al [25].

Finally, we envision a promising role for CMR-FT LV strain investigation of chronic heart failure patients. In particular heart failure with preserved ejection fraction patients seem that they would benefit the most from this assessment, since previous studies have already shown a diagnostic and prognostic impact of strain measurements [2].

Limitations

Specific limitation of the study are related to the fact that animals were investigated under general anaesthesia, in order to minimize the animals' distress and to obtain stable hemodynamic conditions. Due to easier housing and milder behaviour, all the animals were females. We therefore cannot draw any relevant conclusions on the role of gender on strain variability. A limitation regarding the strain analysis is that only endocardial values of strain were analysed. Moreover, an inter-vendor software variability should be considered if looking at the absolute strain values. Another limitation is that the animals were healthy, and even if conditions of hyper-contractility and hypo-contractility were induced, these were only transient and acutely assessed. We believe the data to be representative enough for the clinical translation, however further studies are needed in a clinical setting.

In conclusion, CMR-FT derived LV strain parameters, such as GLS and GCS, correlate accordingly with

LV hemodynamics in swine under various inotropic states. Indexing strain parameters for indirect measures of afterload substantially improves this correlation, with GLS being as good as LVEF in reflecting LV contractility. CMR-FT strain imaging may be a quick and promising tool to characterize LV hemodynamics in patients with a various degree of LV dysfunction.

Abbreviations

2Ch: Two chambers; 3Ch: Three chambers; 4Ch: Four chambers; BSA: Body surface area; bSSFP: Balanced steady-state free precession; CI: Cardiac index; CMR: Cardiovascular magnetic resonance; CMR-FT: Cardiovascular magnetic resonance feature tracking; CO: Cardiac output; CPO: Cardiac power output; DBP: Diastolic blood pressure; ECG: Electrocardiogram; Ees: End-systolic elastance; ESPVR: End-systolic pressure–volume relationship; FT: Feature tracking; GCS: Global circumferential strain; GCSi: Global circumferential strain indexed for mAoP; GCSw: Global circumferential strain indexed for meridional wall stress; GLS: Global longitudinal strain; GLSi: Global longitudinal strain indexed for mAoP; GLSw: Global longitudinal strain indexed for meridional wall stress; GRS: Global radial strain; GRSi: Global radial strain indexed for mAoP; GRSw: Global radial strain indexed for meridional wall stress; HR: Heart rate; LV: Left ventricle/left ventricular; LVEF: Left ventricular ejection fraction; LVESD: Left ventricular end-systolic diameter; LVP: Left ventricular pressure; mAoP: Mean aortic pressure; PWT: Posterior wall thickness; SAx: Short axis; SBP: Systolic blood pressure; SR: Strain rate; STE: Speckle tracking echocardiography; SVR: Systemic vascular resistance; TE: Echo time; TR: Repetition time.

Aknowledgements

Not applicable.

Authors' contributions

AA, SK, HP conceived the experiment, AF, AA, SK, CK, CS conducted the experiments, AF, RT, DA, AA, SP, CS, FPLM, LF analyzed the results. All authors revised the manuscript. All authors read and approved the final manuscript.

Funding

Open Access funding enabled and organized by Projekt DEAL. Alessandro Faragli, Heiner Post, Sebastian Kelle and Alessio Alogna received funding from DZHK (c) and by the BMBF (German Ministry of Education and Research). Sebastian Kelle is supported by a grant from Philips Healthcare.

Availability of data

Not applicable

Ethics approval and consent to participate

Not applicable.

Consent for publication

Not applicable.

Competing interests

Apart from Alessandro Faragli, Heiner Post, Sebastian Kelle and Alessio Alogna, who declare to have received funding in the Funding section, none of the other authors reports a relationship with industry and other relevant entities—financial or otherwise—that might pose a conflict of interest in connection with the submitted article. The following authors report financial activities outside the submitted work: Burkert Pieske reports having received consultancy and lecture honoraria from Bayer Daiichi Sankyo, MSD, Novartis, Sanofi-Aventis, Stealth Peptides and Vifor Pharma; and editor honoraria from the Journal of the American College of Cardiology.

Author details

[1] Department of Internal Medicine and Cardiology, Charité-Universitätsmedizin Berlin, Campus Virchow-Klinikum, Augustenburger Platz 1, 13353 Berlin, Germany. [2] Berlin Institute of Health (BIH), Berlin, Germany. [3] DZHK (German Centre for Cardiovascular Research), partner site, Berlin, Germany. [4] Department of Internal Medicine/Cardiology, Deutsches Herzzentrum Berlin, Augustenburger Platz 1, 13353 Berlin, Germany. [5] Department of Cardiology, Medical Academy, Lithuanian University of Health Sciences, Eiveniu Street 2, 50161 Kaunas, Lithuania. [6] Clinical Science, Philips Healthcare, Röntgenstr. 24, 22335 Hamburg, Germany. [7] Department of Surgery, Dentistry, Paediatrics and Gynaecology, University of Verona, Via S. Francesco 22, 37129 Verona, Italy. [8] Department of Medicine and Surgery, University of Parma, Via Gramsci 14, 43126 Parma, Italy. [9] Department of Electrical, Computer and Biomedical Engineering (DIII), Centre for Health Technologies (CHT), University of Pavia, Via Ferrata 5, 27100 Pavia, Italy. [10] Institute of Experimental and Translational Cardiac Imaging, DZHK Centre for Cardiovascular Imaging, Goethe University Hospital Frankfurt, Frankfurt am Main, Germany. [11] Department of Cardiology, Contilia Heart and Vessel Centre, St. Marien-Hospital Mülheim, 45468 Mülheim, Germany.

Received: 17 November 2019 Accepted: 6 October 2020
Published online: 30 November 2020

References

1. Stanton T, Leano R, Marwick TH. Prediction of all-cause mortality from global longitudinal speckle strain: comparison with ejection fraction and wall motion scoring. Circ Cardiovasc Imaging. 2009;2:356–64.
2. Stokke TM, Hasselberg NE, Smedsrud MK, Sarvari SI, Haugaa KH, Smiseth OA, Edvardsen T, Remme EW. Geometry as a confounder when assessing ventricular systolic function: comparison between ejection fraction and strain. J Am Coll Cardiol. 2017;70:942–54.
3. Kraigher-Krainer E, Shah AM, Gupta DK, Santos A, Claggett B, Pieske B, Zile MR, Voors AA, Lefkowitz MP, Packer M, McMurray JJ, Solomon SD, Investigators P. Impaired systolic function by strain imaging in heart failure with preserved ejection fraction. J Am Coll Cardiol. 2014;63:447–56.
4. Hasselberg NE, Haugaa KH, Sarvari SI, Gullestad L, Andreassen AK, Smiseth OA, Edvardsen T. Left ventricular global longitudinal strain is associated with exercise capacity in failing hearts with preserved and reduced ejection fraction. Eur Heart J Cardiovasc Imaging. 2015;16:217–24.
5. Smedsrud MK, Sarvari S, Haugaa KH, Gjesdal O, Orn S, Aaberge L, Smiseth OA, Edvardsen T. Duration of myocardial early systolic lengthening predicts the presence of significant coronary artery disease. J Am Coll Cardiol. 2012;60:1086–93.
6. Yang H, Sun JP, Lever HM, Popovic ZB, Drinko JK, Greenberg NL, Shiota T, Thomas JD, Garcia MJ. Use of strain imaging in detecting segmental dysfunction in patients with hypertrophic cardiomyopathy. J Am Soc Echocardiogr. 2003;16:233–9.
7. Fang ZY, Yuda S, Anderson V, Short L, Case C, Marwick TH. Echocardiographic detection of early diabetic myocardial disease. J Am Coll Cardiol. 2003;41:611–7.
8. Yotti R, Bermejo J, Benito Y, Sanz-Ruiz R, Ripoll C, Martinez-Legazpi P, del Villar CP, Elizaga J, Gonzalez-Mansilla A, Barrio A, Banares R, Fernandez-Aviles F. Validation of noninvasive indices of global systolic function in patients with normal and abnormal loading conditions: a simultaneous echocardiography pressure-volume catheterization study. Circ Cardiovasc Imaging. 2014;7:164–72.
9. Gorcsan J 3rd, Tanaka H. Echocardiographic assessment of myocardial strain. J Am Coll Cardiol. 2011;58:1401–13.
10. Dahlslett T, Karlsen S, Grenne B, Eek C, Sjoli B, Skulstad H, Smiseth OA, Edvardsen T, Brunvand H. Early assessment of strain echocardiography can accurately exclude significant coronary artery stenosis in suspected non-ST-segment elevation acute coronary syndrome. J Am Soc Echocardiogr. 2014;27:512–9.
11. Ng AC, Sitges M, Pham PN, da Tran T, Delgado V, Bertini M, Nucifora G, Vidaic J, Allman C, Holman ER, Bax JJ, Leung DY. Incremental value of 2-dimensional speckle tracking strain imaging to wall motion analysis for detection of coronary artery disease in patients undergoing dobutamine stress echocardiography. Am Heart J. 2009;158:836–44.
12. Nagata Y, Takeuchi M, Wu VC, Izumo M, Suzuki K, Sato K, Seo Y, Akashi YJ, Aonuma K, Otsuji Y. Prognostic value of LV deformation parameters using 2D and 3D speckle-tracking echocardiography in asymptomatic patients with severe aortic stenosis and preserved LV ejection fraction. JACC Cardiovasc Imaging. 2015;8:235–45.

13. Rhea IB, Uppuluri S, Sawada S, Schneider BP, Feigenbaum H. Incremental prognostic value of echocardiographic strain and its association with mortality in cancer patients. J Am Soc Echocardiogr. 2015;28:667–73.
14. Buss SJ, Emami M, Mereles D, Korosoglou G, Kristen AV, Voss A, Schellberg D, Zugck C, Galuschky C, Giannitsis E, Hegenbart U, Ho AD, Katus HA, Schonland SO, Hardt SE. Longitudinal left ventricular function for prediction of survival in systemic light-chain amyloidosis: incremental value compared with clinical and biochemical markers. J Am Coll Cardiol. 2012;60:1067–76.
15. Eitel I, Stiermaier T, Lange T, Rommel KP, Koschalka A, Kowallick JT, Lotz J, Kutty S, Gutberlet M, Hasenfuss G, Thiele H, Schuster A. Cardiac magnetic resonance myocardial feature tracking for optimized prediction of cardiovascular events following myocardial infarction. JACC Cardiovasc Imaging. 2018;11:1433–44.
16. Onishi T, Saha SK, Delgado-Montero A, Ludwig DR, Onishi T, Schelbert EB, Schwartzman D, Gorcsan J 3rd. Global longitudinal strain and global circumferential strain by speckle-tracking echocardiography and feature-tracking cardiac magnetic resonance imaging: comparison with left ventricular ejection fraction. J Am Soc Echocardiogr. 2015;28:587–96.
17. Mangion K, Carrick D, Carberry J, Mahrous A, McComb C, Oldroyd KG, Eteiba H, Lindsay M, McEntegart M, Hood S, Petrie MC, Watkins S, Davie A, Zhong X, Epstein FH, Haig CE, Berry C. Circumferential strain predicts major adverse cardiovascular events following an acute ST-segment-elevation myocardial infarction. Radiology. 2018. https://doi.org/10.1148/radiol.2018181253.
18. Romano S, Judd RM, Kim RJ, Kim HW, Klem I, Heitner JF, Shah DJ, Jue J, White BE, Indorkar R, Shenoy C, Farzaneh-Far A. Feature-tracking global longitudinal strain predicts death in a multicenter population of patients with ischemic and nonischemic dilated cardiomyopathy incremental to ejection fraction and late gadolinium enhancement. JACC Cardiovasc Imaging. 2018;11:1419–29.
19. Schneeweis C, Qiu J, Schnackenburg B, Berger A, Kelle S, Fleck E, Gebker R. Value of additional strain analysis with feature tracking in dobutamine stress cardiovascular magnetic resonance for detecting coronary artery disease. J Cardiovasc Magnc Reson. 2014;16:72.
20. Williams SG, Cooke GA, Wright DJ, Parsons WJ, Riley RL, Marshall P, Tan LB. Peak exercise cardiac power output; a direct indicator of cardiac function strongly predictive of prognosis in chronic heart failure. Eur Heart J. 2001;22:1496–503.
21. Fincke R, Hochman JS, Lowe AM, Menon V, Slater JN, Webb JG, LeJemtel TH, Cotter G, Investigators S. Cardiac power is the strongest hemodynamic correlate of mortality in cardiogenic shock: a report from the SHOCK trial registry. J Am Coll Cardiol. 2004;44:340–8.
22. Cotter G, Williams SG, Vered Z, Tan LB. Role of cardiac power in heart failure. Curr Opin Cardiol. 2003;18:215–22.
23. Abawi D, Faragli A, Schwarzl M, Manninger M, Zweiker D, Kresoja K-P, Verderber J, Zirngast B, Maechler H, Steendijk P, Pieske B, Post H, Alogna A. Cardiac power output accurately reflects external cardiac work over a wide range of inotropic states in pigs. BMC Cardiovasc Disord. 2019;19:217.
24. Kass DA, Maughan WL. From 'Emax' to pressure-volume relations: a broader view. Circulation. 1988;77:1203–12.
25. Seemann F, Arvidsson P, Nordlund D, Kopic S, Carlsson M, Arheden H, Heiberg E. Noninvasive quantification of pressure-volume loops from brachial pressure and cardiovascular magnetic resonance. Circ Cardiovasc Imaging. 2019;12:e008493.
26. Alogna A, Manninger M, Schwarzl M, Zirngast B, Steendijk P, Verderber J, Zweiker D, Maechler H, Pieske BM, Post H. Inotropic effects of experimental hyperthermia and hypothermia on left ventricular function in pigs-comparison with dobutamine. Crit Care Med. 2016;44:e158–67.
27. Schulz-Menger J, Bluemke DA, Bremerich J, Flamm SD, Fogel MA, Friedrich MG, Kim RJ, von Knobelsdorff-Brenkenhoff F, Kramer CM, Pennell DJ, Plein S, Nagel E. Standardized image interpretation and post processing in cardiovascular magnetic resonance: Society for Cardiovascular Magnetic Resonance (SCMR) board of trustees task force on standardized post processing. J Cardiovasc Magn Reson. 2013;15:35.
28. Carlsson M, Andersson R, Bloch KM, Steding-Ehrenborg K, Mosén H, Stahlberg F, Ekmehag B, Arheden H. Cardiac output and cardiac index measured with cardiovascular magnetic resonance in healthy subjects, elite athletes and patients with congestive heart failure. J Cardiovasc Magn Reson. 2012;14:51.
29. Kelly RP, Ting CT, Yang TM, Liu CP, Maughan WL, Chang MS, Kass DA. Effective arterial elastance as index of arterial vascular load in humans. Circulation. 1992;86:513–21.
30. Rhea IB, Rehman S, Jarori U, Choudhry MW, Feigenbaum H, Sawada SG. Prognostic utility of blood pressure-adjusted global and basal systolic longitudinal strain. Echo Res Pract. 2016;3:17–24.
31. Reichek N, Wilson J, John Sutton M, Plappert TA, Goldberg S, Hirshfeld JW. Noninvasive determination of left ventricular end-systolic stress: validation of the method and initial application. Circulation. 1982;65:99–108.
32. Weaver B, Wuensch KL. SPSS and SAS programs for comparing Pearson correlations and OLS regression coefficients. Behav Res Methods. 2013;45:880–95.
33. Scatteia A, Baritussio A, Bucciarelli-Ducci C. Strain imaging using cardiac magnetic resonance. Heart Fail Rev. 2017;22:465–76.
34. Schuster A, Hor KN, Kowallick JT, Beerbaum P, Kutty S. Cardiovascular magnetic resonance myocardial feature tracking: concepts and clinical applications. Circ Cardiovasc Imaging. 2016;9:e004077.
35. Amzulescu MS, De Craene M, Langet H, Pasquet A, Vancraeynest D, Pouleur AC, Vanoverschelde JL, Gerber BL. Myocardial strain imaging: review of general principles, validation, and sources of discrepancies. Eur Heart J Cardiovasc Imaging. 2019;20:605–19.
36. Weidemann F, Jamal F, Kowalski M, Kukulski T, D'Hooge J, Bijnens B, Hatle L, De Scheerder I, Sutherland GR. Can strain rate and strain quantify changes in regional systolic function during dobutamine infusion, B-blockade, and atrial pacing—implications for quantitative stress echocardiography. J Am Soc Echocardiogr. 2002;15:416–24.
37. Yingchoncharoen T, Agarwal S, Popovic ZB, Marwick TH. Normal ranges of left ventricular strain: a meta-analysis. J Am Soc Echocardiogr. 2013;26:185–91.
38. Weiner RB, Weyman AE, Kim JH, Wang TJ, Picard MH, Baggish AL. The impact of isometric handgrip testing on left ventricular twist mechanics. J Physiol. 2012;590:5141–50.
39. Bouchez S, Heyde B, Barbosa D, Vandenheuvel M, Houle H, Wang Y, D'Hooge J, Wouters PF. In-vivo validation of a new clinical tool to quantify three-dimensional myocardial strain using ultrasound. Int J Cardiovasc Imaging. 2016;32:1707–14.
40. Barreiro-Pérez M, Curione D, Symons R, Claus P, Voigt J-U, Bogaert J. Left ventricular global myocardial strain assessment comparing the reproducibility of four commercially available CMR-feature tracking algorithms. Eur Radiol. 2018;28:5137–47.
41. Swoboda PP, Larghat A, Zaman A, Fairbairn TA, Motwani M, Greenwood JP, Plein S. Reproducibility of myocardial strain and left ventricular twist measured using complementary spatial modulation of magnetization. J Magn Reson Imaging. 2014;39:887–94.
42. Schmidt B, Dick A, Treutlein M, Schiller P, Bunck AC, Maintz D, Baeßler B. Intra- and inter-observer reproducibility of global and regional magnetic resonance feature tracking derived strain parameters of the left and right ventricle. Eur J Radiol. 2017;89:97–105.
43. Faragli A, Tanacli R, Kolp C, Lapinskas T, Stehning C, Schnackenburg B, Lo Muzio FP, Perna S, Pieske B, Nagel E, Post H, Kelle S, Alogna A. Cardiovascular magnetic resonance feature tracking in pigs: a reproducibility and sample size calculation study. Int J Cardiovasc Imaging. 2020;36:703–12.
44. Reichek N. Myocardial strain: still a long way to go. Circ Cardiovasc Imaging. 2017. https://doi.org/10.1161/CIRCIMAGING.117.007145.

Publisher's Note

The International Journal of Cardiovascular Imaging
https://doi.org/10.1007/s10554-020-01767-y

ORIGINAL PAPER

Cardiovascular magnetic resonance feature tracking in pigs: a reproducibility and sample size calculation study

A. Faragli[1,2,3] · R. Tanacli[4] · C. Kolp[1] · T. Lapinskas[4,5] · C. Stehning[6] · B. Schnackenburg[6] · F. P. Lo Muzio[7,8] · S. Perna[9] · B. Pieske[1,2,3,4] · E. Nagel[10] · H. Post[1,2,3,11] · S. Kelle[1,2,3] · A. Alogna[1,2,3]

Received: 1 November 2019 / Accepted: 2 January 2020

Abstract
Cardiovascular magnetic resonance feature tracking (CMR-FT) is a novel technique for non-invasive assessment of myocardial motion and deformation. Although CMR-FT is standardized in humans, literature on comparative analysis from animal models is scarce. In this study, we measured the reproducibility of global strain under various inotropic states and the sample size needed to test its relative changes in pigs. Ten anesthetized healthy Landrace pigs were investigated. After baseline (BL), two further steps were performed: (I) dobutamine-induced hyper-contractility (Dob) and (II) verapamil-induced hypocontractility (Ver). Global longitudinal (GLS), circumferential (GCS) and radial strain (GRS) were assessed. This study shows a good to excellent inter- and intra-observer reproducibility of CMR-FT in pigs under various inotropic states. The highest inter-observer reproducibility was observed for GLS at both BL (ICC 0.88) and Ver (ICC 0.79). According to the sample size calculation for GLS, a small number of animals could be used for future trials.

Keywords Cardiovascular magnetic resonance · Feature tracking · Left ventricular strain · Reproducibility · Sample size · Porcine model

Introduction

Myocardial strain has been demonstrated as an effective method for the assessment of the regional myocardial function and deformation, and in particular, the cardiovascular magnetic resonance (CMR) tissue tracking approach has

S. Kelle and A. Alogna have equally contributed to this work.

✉ A. Alogna
alessio.alogna@charite.de

1 Department of Internal Medicine and Cardiology, Charité – Universitätsmedizin Berlin, Campus Virchow-Klinikum, Augustenburgerplatz 1, 13353 Berlin, Germany

2 Berlin Institute of Health (BIH), Berlin, Germany

3 DZHK (German Centre for Cardiovascular Research), partner site, Berlin, Germany

4 Department of Internal Medicine / Cardiology, Deutsches Herzzentrum Berlin, Augustenburger Platz 1, 13353 Berlin, Germany

5 Department of Cardiology, Medical Academy, Lithuanian University of Health Sciences, Eiveniu Street 2, 50161 Kaunas, Lithuania

6 Clinical Science, Philips Healthcare, Röntgenstr. 24, 22335 Hamburg, Germany

7 Department of Surgery, Dentistry, Paedriatics and Gynaecology, University of Verona, Via S. Francesco 22, 37129 Verona, Italy

8 Department of Medicine and Surgery, University of Parma, Via Gramsci 14, 43126 Parma, Italy

9 Department of Biology, College of Science, University of Bahrain, Sakhir Campus, P.O. Box 32038, Zallaq, Bahrain

10 Institute of Experimental and Translational Cardiac Imaging, DZHK Centre for Cardiovascular Imaging, Goethe University Hospital Frankfurt, Theodor-Stern-Kai 7, 60590 Frankfurt, Germany

11 Department of Cardiology, Contilia Heart and Vessel Centre, St. Marien-Hospital Mülheim, Kaiserstraße 50, 45468 Mülheim, Germany

Published online: 16 January 2020

been established as a technique comparable to the highly validated speckle tracking echocardiography [19]. CMR feature tracking (CMR-FT) is a relatively novel technique that focuses on endocardial and epicardial contouring and is able to detect the contrast between myocardium and blood pool [4, 14]. CMR-FT has been validated against myocardial tagging technique for the assessment of regional myocardial motion in humans [8, 12, 17]. As every new technique CMR-FT has been widely tested for reproducibility, and what has been already shown in human is the excellent inter- and intra-observer reproducibility, for different parameters and at different field strength MRI scanners [13, 20, 21]. However, since CMR is becoming widely utilized in animal research, there is a lack of standardization, a lack of reference databases and a lack of reproducibility studies. For this reason, a previous study from our group demonstrated the high reproducibility of strain measurements through feature tracking in a model of small animals (mice) which has already been acknowledged in the recent guidelines for animal research [9, 10]. Nonetheless, the main limitation of this previous study was indeed the model, recognized to be not translational enough for a comparison with the humans, in particular regarding the assessment of myocardial function. Large animals, such as Landrace pigs, are instead more suited to investigate myocardial function under various pharmacological interventions given a cardiac anatomy and physiology closer to humans. There is only one study in the literature that has assessed the reproducibility of myocardial deformation parameters in large animals (macaque) [15] and no studies have performed such an analysis in pigs. Accordingly, we performed this preliminary study to evaluate inter- and intra-observer reproducibility of CMR-FT derived strain measurements in a porcine model of pharmacologically induced hyper- and hypo-contractility. Furthermore, we performed a sample size calculation based on global strain values useful to define the number of animals required for future studies.

Methods

Data from ten landrace pigs were selected from an ongoing experiment at our center. The experimental protocols were approved by the local bioethics committee of Berlin, Germany (G0138/17), and conform to the "European Convention for the Protection of Vertebrate Animals used for Experimental and other Scientific Purposes" (Council of Europe No 123, Strasbourg 1985).

Experimental setup

Briefly, female Landrace pigs (n = 10, 51 ± 10 kg) were fasted overnight with free access to water, sedated and intubated on the day of the experiment. Anesthesia was continued with isoflurane, fentanyl, midazolam, ketamine and pancuronium. Pigs were ventilated (Cato, Dräger Medical, Germany) with a FiO2 of 0.5, an I: E-ratio of 1:1.5, the positive end-expiratory pressure was set at 5 mmHg and a tidal volume (VT) of 10 ml kg^{-1}. The respiratory rate was adjusted constantly to maintain an end-expiratory carbon dioxide partial pressure between 35 and 45 mmHg. Under fluoroscopic guidance all animals were instrumented with a floating balloon catheter in the right atrium as well as in the coronary sinus (Arrow Balloon Wedge-Pressure Catheters, Teleflex Inc USA). In order to avoid MRI artefacts, the balloon-tip was cut before introducing the catheters in the vessel. Respiratory gases (PM 8050 MRI, Dräger Medical, Germany), heart rate and arterial blood pressure continuously monitored. Body temperature was monitored by a sublingual thermometer and was maintained at 38 °C during CMR imaging via air ventilation and/or infusion of cold saline solution. The experimental setup can be visualized in Fig. 1a, b.

Experimental protocols

After acute instrumentation the animals were transported to the MRI facility for measurements, pigs were ventilated with an MRI compatible machine (Titus, Dräger Medical, Germany) (see Fig. 1c, d). After baseline measurements (BL), two steps were performed: (I) dobutamine-induced hypercontractility (Dob) and (II) verapamil-induced hypocontractility (Ver). At each protocol, MRI images were acquired at short axis (SAX), two chambers (2Ch), three chambers (3Ch) and four chambers (4Ch) views. After the MRI measurements were concluded the animals were transported back to the operating room for sacrifice.

Cardiac magnetic resonance

All CMR images were acquired in a supine position using a 3 Tesla (3 T) (Achieva, Philips Healthcare, Best, The Netherlands) MRI scanner with an anterior- and the built-in posterior coil element, where up to 30 coil elements were employed, depending on the respective anatomy. All animals were scanned using identical comprehensive imaging protocol. The study protocol included initial scouts to determine cardiac imaging planes. Cine images were acquired using ECG-gated balanced steady state free precession (bSSFP) sequence in three left ventricular (LV) long-axis (two-chamber, three-chamber and four-chamber) planes. The ventricular two-chamber and four-chamber planes were used to plan stack of short-axis slices covering entire LV. The following imaging parameters were used: repetition time (TR) = 2.9 ms, echo time (TE) = 1.45 ms, flip angle = 45°, voxel size = 1.9 × 1.9 × 8.0 mm3 and 40 phases per cardiac cycle.

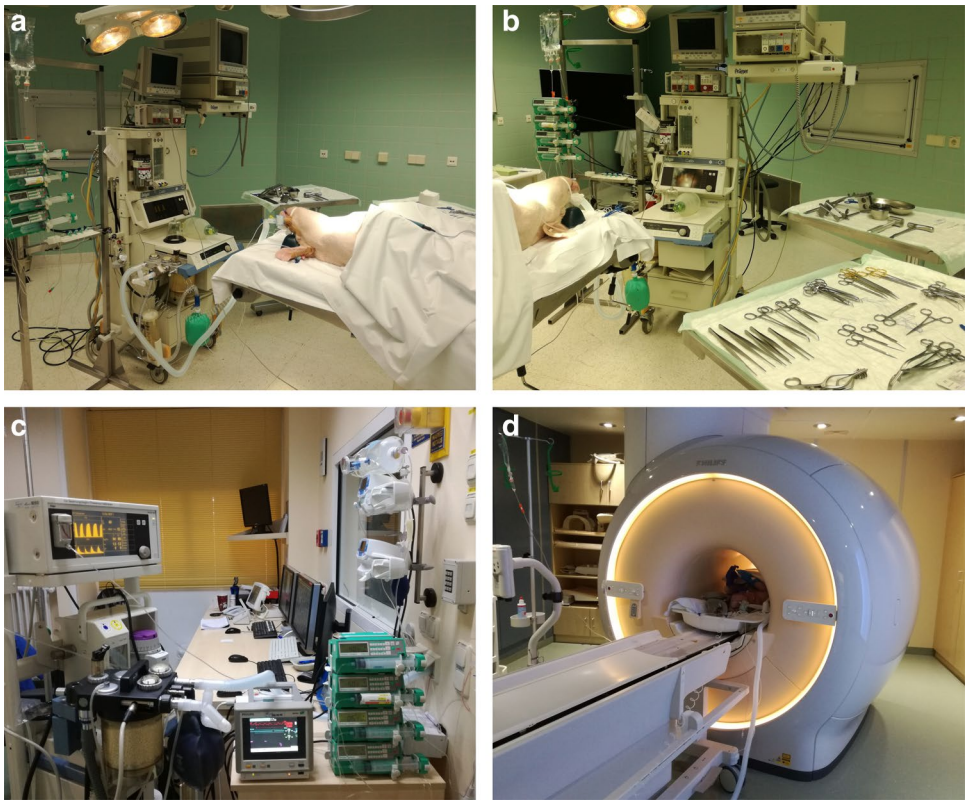

Fig. 1 The experimental setting. The animals were acutely instrumented closed chest in the operating room (**a**, **b**) and then transported to the MRI facility where anesthesia and monitoring was maintained during the whole experimental protocol (**c**, **d**)

Image analysis

All images were analyzed offline using commercially available software (Medis Suite, version 3.1, Leiden, The Netherlands) in accordance to recent consensus document for quantification of LV function using CMR. In the strain analysis were included 2Ch, 3Ch and 4Ch cine images, and respectively, three preselected mid-ventricle slices from the LV short-axis stack. The endocardial and epicardial contours drawn on cine images with QMass version 8.1 were transferred to QStrain RE version 2.0, where after the application of tissue tracking algorithm endocardial and epicardial borders were detected throughout all the cardiac cycle. These long-axis cine images were further used to compute global myocardial longitudinal (GLS) strain and short-axis images were used to compute circumferential (GCS) and radial (GRS) strain and strain-rate. The global values were obtained through averaging the values according to an AHA 17 segments model, apex being excluded, as follows: GCS and GRS from averaging CS and RS for 6 basal, 6 mid and 4 apical segmental individual values; GLS from 2Ch, 3Ch and 4Ch averaging 6 basal, 6 mid and 4 apical segments using a bull-eye view.

Statistical analysis

Data were analyzed using Microsoft Excel and IBM SPSS Statistics version 23.0 software (SPSS Inc., Chicago, IL, USA) for Windows. Figures 1, 2, 3, 4 were made with Microsoft PowerPoint version 17, while Figs. 2, 3 were made with GraphPad Prism version 8. All data are presented as mean ± SD. Data between groups at different inotropic states were analyzed by one-way ANOVA for repeated measurements. Post-hoc testing was performed by Tukey's test. A p-value < 0.05 was considered significant.

Reproducibility testing

Data are expressed as mean ± standard deviation (SD). The Shapiro–Wilk test was used to determine whether the data were normally distributed. Nonparametric variables were compared using the Wilcoxon test. A p-value of < 0.05 was considered statistically significant. Inter- and intra-observer reproducibility was quantified using intra-class correlation coefficient (ICC) and Bland–Altman analysis (13). Agreement was considered excellent for ICC > 0.74, good for ICC 0.60–0.74, fair for ICC 0.40–0.59, and poor for ICC < 0.40

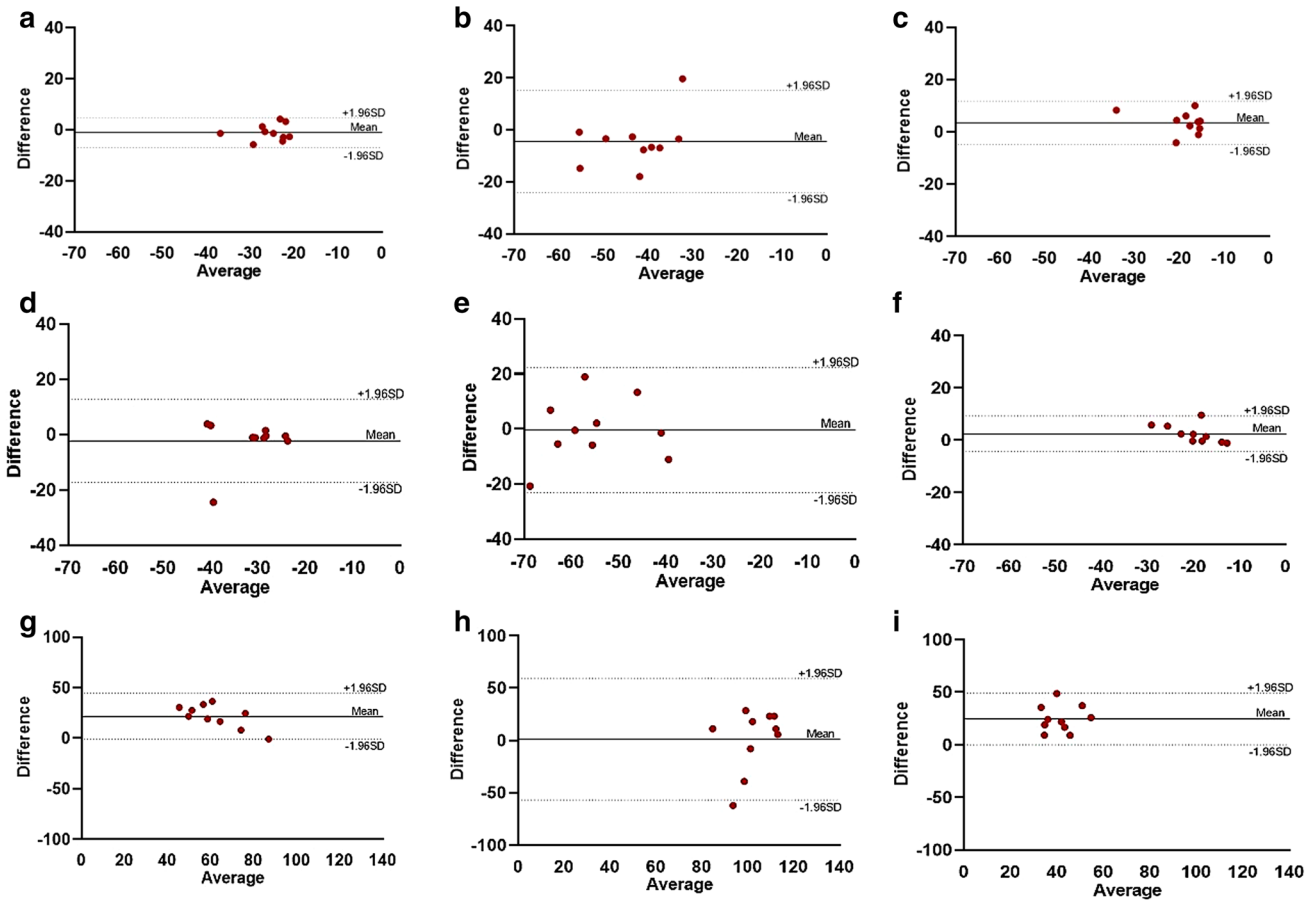

Fig. 2 Bland–Altman plots for inter-observer reproducibility of global strain values. Bland–Altman plots showing inter-observer reproducibility for GLS (top row, panels **a**–**c**), GCS (middle row, panels **d**–**f**) and GRS analysis (bottom row, panels **g**–**i**) during BL, Dob and Ver steps respectively. *BL* baseline, *Dob* Dobutamine, *Ver* Verapamil, *GLS* global longitudinal strain, *GCS* global circumferential strain, *GRS* global radial strain

(14). To assess intra-observer agreement data analysis was repeated after 4 weeks. All the operators took the measurements twice and the average values were taken.

Sample size calculation

Study sample size required to detect a relative 5, 8 and 10% change in strain with power of 80% and significance of 5% was calculated as follows (15):

$$n = f(\alpha, P)\sigma 2/\delta$$

where n is the sample size, α the significance level, P the study power required and f the value of the factor for different values of α and P (f = 10.5 for α = 0.05 and p = 0.080), with σ the standard deviation of differences in measurements between two studies and δ the desired difference to be detected. Sample size calculation was performed for baseline values only.

Results

The volumetric and functional parameters of study population are summarized in Table 1. All studies were completed, and image quality was sufficient to perform CMR-FT analysis. Table 2 demonstrates CMR-FT derived strain parameters obtained by two independent investigators.

Inter-observer and intra-observer reproducibility

Mean differences ± SD, limits of agreement and ICC for strain parameters are given in Table 3. There was an excellent inter-observer reproducibility for GLS during BL and Ver steps, while during Dob the observed reproducibility was good. Regarding the GCS analysis, there was a good reproducibility during BL and Ver steps; while during Dob, the reproducibility was only fair. The GRS analysis showed, instead, an excellent reproducibility for BL, while during Dob and Ver steps the reproducibility was poor. Concerning the intra-observer analysis, the level of reproducibility was

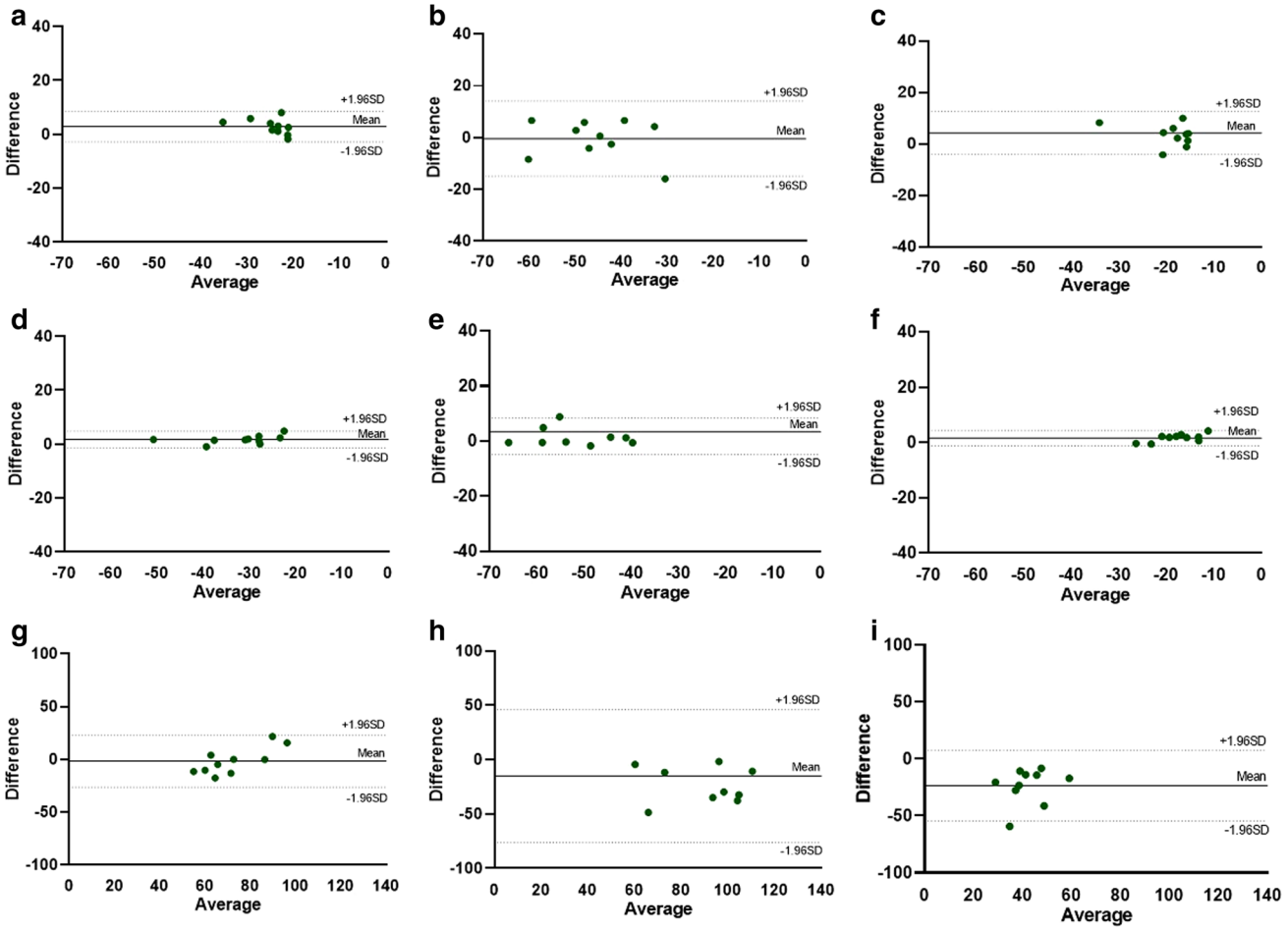

Fig. 3 Bland–Altman plots for intra-observer reproducibility of global strain values. Bland–Altman plots showing intra-observer reproducibility for GLS (top row, panels **a**–**c**), GCS (middle row, panels **d**–**f**) and GRS analysis (bottom row, panels **g**–**i**) during BL, Dob and Ver steps respectively. *BL* baseline, *Dob* Dobutamine, *Ver* Verapamil, *GLS* global longitudinal strain, *GCS* global circumferential strain, *GRS* global radial strain

generally excellent for most of the measurements. GLS and GCS showed an excellent reproducibility for all steps, while GRS showed an excellent reproducibility during BL, a good one during Dob and a poor one during Ver. Bland–Altman plots demonstrate inter-observer and intra-observer reproducibility for GLS, GCS and GRS analysis during BL, Dob and Ver steps (see Figs. 2, 3).

Sample size calculation for baseline values

The change in reproducibility has an impact on the sample size required to detect significant differences in strain parameters. Table 4 lists the required sample sizes for each strain-derived parameter. For example, to show a relative 10% change in GLS in pigs would require five animals (not measures—Fig. 4). In contrast, 20 pigs are required to detect a 5% change in GLS with CMR-FT (power of 80% and α error of 0.05).

Discussion

While studies analyzing reproducibility of CMR-FT in humans are already present in the literature [3, 16], works on the reproducibility of myocardial deformation parameters of large animal models are, instead, lacking. The current study was designed, therefore, to assess the inter-observer and intra-observer reproducibility of CMR-FT for the analysis of global LV strain in a porcine model of hyper- and hypo-contractility. Here we show a good to excellent inter- and intra-observer reproducibility of CMR-FT technique in pigs under different inotropic states. Furthermore, sample size calculation demonstrates that for GLS analysis a small number of animals could be enough for future trials. A previous study from our group has demonstrated a high reproducibility in the LV strain measurements in a murine model [9]. This current study provides a more extensive analysis in pigs and confirms the previous one regarding the most reproducible parameters derived from

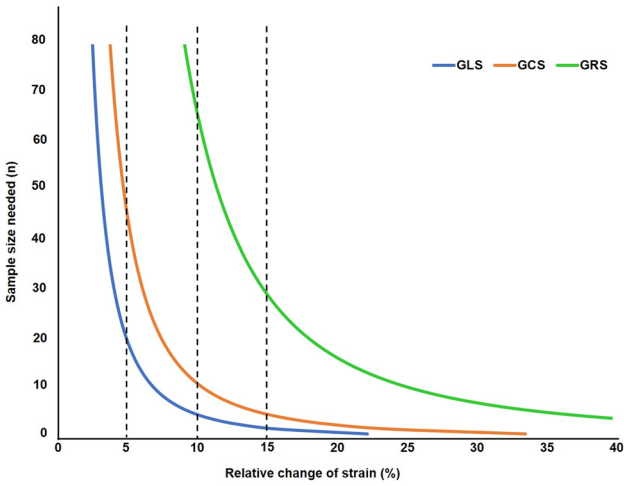

Fig. 4 Graphical representation of the sample size calculation for global strain values. Representation of the sample size calculation for GLS (blue), GCS (red) and GRS (green) baseline measurements to detect the desired % relative change of strain with 80% power and α error of 0.05. Dashed lines represent the relative change of strain at 5%, 10% and 15% respectively. *GLS* global longitudinal strain, *GCS* global circumferential strain, *GRS* global radial strain

Table 1 Volumetric and functional characteristics of study subjects

Parameter	Value	
Study population		10
LV EDV (ml)	BL	101 ± 24
	Dob	83 ± 21*
	Ver	108 ± 25†
LV ESV (ml)	BL	41 ± 10
	Dob	19 ± 7*
	Ver	66 ± 18*†
LV SV (ml)	BL	60 ± 19
	Dob	64 ± 18
	Ver	42 ± 12*†
LV EF (%)	BL	59 ± 8
	Dob	77 ± 7*
	Ver	39 ± 9*†
Cardiac output (l/min)	BL	6 ± 1
	Dob	9 ± 2*
	Ver	4 ± 1*†
Heart rate (bpm)	BL	106 ± 15
	Dob	146 ± 12*
	Ver	98 ± 19†
LV Mass (g)		81 ± 20

Results are reported as mean ± standard deviation

BL baseline, *Dob* Dobutamine, *EDV* end-diastolic volume, *EF* ejection fraction, *ESV* end-systolic volume, *LV* left ventricle/ventricular *SV* stroke volume, *Ver* Verapamil

*p-value < 0.05 versus BL

†p-value < 0.05 versus Dob

CMR-FT. Good to excellent inter-observer reproducibility was found for global longitudinal and global circumferential strain, whereas radial strain confirms, instead, to be highly variable between repeated measurements, in particular when considering the inter-observers measurements. The weak reproducibility of radial strain has also been reported in previous studies [2, 16, 23, 28]. While global longitudinal strain was the most reproducible parameter during the inter-observer analysis, the intra-observer reproducibility was predictably higher for most of the strain values and excellent for global circumferential strain, as already described in previous studies [13, 22]. In a previous study from our group, we were able to show the positive additional role of LV strain analysis during dobutamine stress in a group of patients with coronary artery disease [18]. A good reproducibility and a low inter-observer variability of dobutamine stress Echo and CMR has been previously observed in human [21, 26] and animal studies [15]. However, only few studies concentrated on the reproducibility of LV strain in hyper- and hypo-contractility model. With this study, we were able to assess the reproducibility of the LV strain measurements under various inotropic states. During the infusion of dobutamine, aiming at an increase of at least 25% of the baseline HR, we were able to observe a clinically significant increase in LV EF and LV cardiac output. In our study, the high HR obtained during dobutamine infusion (mean 146 ± 12 bpm) was, however, detrimental to the reproducibility of the measurements when measured by another observer. This can be explained by a worse resolution of the MRI processed images and by an increase in frame rates under such fast heart beats, as already described in other studies [7, 15]. In one of the studies by Schuster et al. a high reproducibility of CMR-FT in a group of ischemic cardiomyopathy patients after dobutamine infusion for stress test was observed [21]. Nevertheless, it is worth to mention that in that study no reference to the heart rate at which the sequences were recorded was mentioned, making the comparison with our model not consistent. In our study, we were able to show that at lower heart rates, such as during baseline state and verapamil infusion, the reproducibility was generally higher for all the strain values. With the advent, development and availability of computers, large datasets can be used in statistical analysis to calculate the sample sizes necessary for clinical studies. Sample size calculation is an important aspect of study design and enables determination of how large the study sample should be. Estimates of required sample size depend on the variability of the population—the greater the variability, the larger the required sample size. This is particularly relevant for CMR studies, where the role of sample size is extremely useful to test the reliability of new imaging techniques [11, 16]. The same should be applicable to animal studies, where the reduction of the numbers of animals used is of extreme value [25]. In some cases, by using previously published studies, the use of animals can be totally avoided by eliminating unnecessary replications [1]. Modern

Table 2 Comparison of CMR-FT derived average of global strain parameters obtained by observers in ten pigs during BL, Dob and Ver steps

Measurements obtained by two observers (inter-observer level)		
	First observer	Second observer
BL (%)		
GLS	−26.1 ± 5	−25.1 ± 4
GCS	−32.7 ± 8	−30.4 ± 6
GRS	73.3 ± 9	51.5 ± 17
Dob (%)		
GLS	−45.1 ± 11*	−40.6 ± 7*
GCS	−55.1 ± 12	−54.7 ± 10*
GRS	103.0 ± 20	101.8 ± 14*
Ver (%)		
GLS	−20.8 ± 6†	−17.3 ± 5*†
GCS	−18.6 ± 4†	−21.0 ± 6*†
GRS	53.9 ± 10†	29.1 ± 9*†
Measurements obtained by one observer (intra-observer level)		
	First measurement	Second measurement
BL (%)		
GLS	−26.1 ± 5	−23.3 ± 4
GCS	−32.7 ± 8	−31.0 ± 8
GRS	73.3 ± 9	71.7 ± 19
Dob (%)		
GLS	−45.1 ± 11 *	−45.6 ± 9*
GCS	−55.1 ± 12	−53.3 ± 11*
GRS	103.0 ± 20	87.9 ± 36
Ver (%)		
GLS	−20.8 ± 6†	−16.5 ± 3*†
GCS	−18.6 ± 4†	−16.9 ± 5*†
GRS	53.9 ± 10†	30.3 ± 13*†

All the operators took the measurements twice and the average values were taken

BL baseline, *Dob* Dobutamine, *GCS* global circumferential strain, *GLS* global longitudinal strain, *GRS* global radial strain, *Ver* Verapamil

*p-value < 0.05 versus BL

†p value < 0.05 versus Dob

imaging techniques in conjunction with new statistical analysis methods also allow reductions in the numbers of animals used, for example, by providing greater information per animal [27]. Too small sample size can miss the real effect, whereas too large sample size leads to unnecessary waste of time and resources (animals) [1, 25, 27]. In the already published pilot study on sample size calculation and variability in small animals by our study group, we demonstrated that the number of animals needed to test a hypothesis could be reduced if the effect of animal-to-animal variation on the measurement is eliminated or highly reduced [9]. With the present study, we were able to show that in this cohort a relatively small sample size of animals (not measures) is required to detect a 5, 10 and 15% change in strain parameters for global longitudinal strain. We also observed that a higher sample size is necessary for circumferential strain, and particularly high for radial strain.

The ability to apply human-like settings to model animals increases the chances of translation of new effective diagnostic and therapeutic interventions [24]. The importance of large animal research in the field of human diseases is evident in most medical settings, however, this holds particularly true for cardiology where in terms of anatomy, physiology and size, large animals such as pigs represent the closest comparison to humans [24]. In the European Union, the Directive 2010/63/EU voted in 2010 has been implemented in 2013 in the European Medicines Agency (EMA) guidelines, resulting in restrictions in the use of nonhuman primates in biomedical research (EMA 2014) and promoting instead the utilization of non-rodents species such as pigs and sheep that should be chosen based on their similarity to humans with regard to in vitro metabolic profile [6]. In order to appropriately assure translational success and safety, at least two animal species that are

Table 3 Inter-observer and intra-observer reproducibility for GLS, GCS and GRS

	Parameter	Steps	Mean difference ± SD	Limits of agreement	ICC (95% CI)
Inter-observer variability	GLS	BL	− 1.0 ± 3.0	− 6.9 to 4.8	0.88 (0.57–0.97)
		Dob	− 4.5 ± 10.0	− 24.1 to 15.1	0.60 (− 0.35 to 0.89)
		Ver	3.5 ± 4.2	− 4.7 to 11.7	0.79 (0.10–0.95)
	GCS	BL	− 2.2 ± 7.6	− 17.2 to 12.6	0.66 (− 0.21 to 0.92)
		Dob	− 0.4 ± 11.5	− 23.0 to 22.2	0.51 (− 0.23 to 0.87)
		Ver	2.4 ± 3.4	− 4.3 to 9.2	0.61 (− 0.40 to 0.90)
	GRS	BL	21.7 ± 11.6	− 0.9 to 44.5	0.80 (0.21–0.95)
		Dob	1.2 ± 29.6	− 56.9 to 59.3	− 1.60 (− 9.47 to 0.35)
		Ver	24.7 ± 12.6	0.1 to 49.4	0.24 (− 2.03 to 0.81)
Intra-observer variability	GLS	BL	2.8 ± 2.9	− 2.8 to 8.5	0.81 (0.41–0.95)
		Dob	− 0.4 ± 7.3	− 14.8 to 14.0	0.87 (0.45–0.96)
		Ver	4.3 ± 4.3	− 4.1 to 12.7	0.75 (0.01–0.94)
	GCS	BL	1.7 ± 1.5	− 1.3 to 4.7	0.98 (0.77–0.99)
		Dob	1.8 ± 3.4	− 4.8 to 8.4	0.97 (0.89–0.99)
		Ver	1.6 ± 1.4	− 1.1 to 4.4	0.95 (0.36–0.99)
	GRS	BL	− 1.5 ± 12.7	− 26.4 to 23.3	0.79 (0.15–0.94)
		Dob	− 15.1 ± 31.1	− 76.0 to 45.8	0.62 (− 0.50 to 0.90)
		Ver	− 23.6 ± 15.7	− 54.4 to 7.2	0.14 (− 2.43 to 0.78)

Results are reported as mean ± standard deviation

BL baseline, *CI* confidence interval, *Dob* Dobutamine, *GCS* global circumferential strain, *GLS* global longitudinal strain, *GRS* global radial strain, *ICC* intra-class correlation coefficient, *Ver* Verapamil

Table 4 Sample size calculation for GLS, GCS and GRS (baseline measurements) to detect the desired % relative change with 80% power and α error of 0.05

	Mean difference ± SD pooled	Sample size (n)		
		5%	10%	15%
GLS	− 1.1 ± 4.9	20	5	2
GCS	− 2.3 ± 7.4	45	11	5
GRS	21.7 ± 17.9	NA	68	30

The mean difference is calculated from the inter-observer mean difference analysis. The pooled SD has been obtained by applying Cohen formula: $SD_{pooled} = \sqrt{(SD_1^2 + SD_2^2)^{-1}}$

GCS global circumferential strain, *GLS* global longitudinal strain, *GRS* global radial strain, *SD* standard deviation

phylogenetically somewhat apart like a rodent and a non-rodent species are necessary. Without necessarily requiring closeness to man, this is the general rule supported by the current international guidelines like the International Council for Harmonization of Technical Requirements for Pharmaceuticals for Human Use, Guidance M3 (Revision 2; 2009) [6]. Nonetheless, the employment of large animal models carries ethical problems and higher costs, mainly because of the size of the animals and husbandry needed when compared to smaller models [24]. It is evident that all the necessary methods should be introduced to reduce, refine and replace the unnecessary animal experiments [5]. In accordance with the 3Rs principles on animal use (Directive 2010/63/EU), a scientifically satisfactory method or testing strategy, not entailing the use of live animals, should be used wherever possible [6]. For this reason, our preliminary study could be paving the road to the realization of an open access database of cardiovascular magnetic resonance data that could be of great need for future laboratory experiments, to reduce the number of animal experiments performed and to be utilized as a platform for simulation and testing of novel compounds. The experiments were performed during anesthesia, being a possible confounder for reproducibility of the measurements. The animals were not awake limiting the translation to clinical settings. The study is limited due to the small number of animals and larger sample size may be required to detect more subtle differences. The addition of a 25% dropout rate (proportion of eligible subjects who will not complete the study or provide only partial information) before planning a study will further increase the final sample size.

Conclusion

Global LV strain parameters analyzed by CMR-FT analyzed in a large animal model (pig) of hyper- and hypocontractility are highly reproducible. The most reproducible measures are global circumferential and global longitudinal strain, whereas reproducibility of radial strain is weak.

Sample size calculation are an essential tool that could help to reduce the number of animal experiments and databases on large animals can be used as a platform to test the effect of novel compounds.

Acknowledgements Open Access funding provided by Projekt DEAL. Burkert Pieske reports having received consultancy and lecture honoraria from Bayer Daiichi Sankyo, MSD, Novartis, Sanofi-Aventis, Stealth Peptides and Vifor Pharma; and editor honoraria from the Journal of the American College of Cardiology.

Author contributions AA, SK, HP conceived the experiment, AF, AA, SK, CK, CS conducted the experiments, AF, RT, AA, SP, CS, analyzed the results. All authors revised the manuscript.

Funding Alessandro Faragli, Heiner Post, Alessio Alogna and Sebastian Kelle received funding from DZHK (German Centre for Cardiovascular Research—Grant Number: 81X2100305).

Compliance with ethical standards

Conflict of interest All authors declare that they have no conflict of interest.

Ethical approval All institutional and national guidelines for the care and use of laboratory animals were followed and approved by the appropriate institutional committees. The experimental protocols were approved by the local bioethics committee of Berlin, Germany (G0138/17), and conform to the "European Convention for the Protection of Vertebrate Animals used for Experimental and other Scientific Purposes" (Council of Europe No 123, Strasbourg 1985).

References

1. Allgoewer A, Mayer B (2017) Sample size estimation for pilot animal experiments by using a Markov Chain Monte Carlo approach. Alter Lab Anim 45:83–90
2. Barreiro-Pérez M, Curione D, Symons R et al (2018) Left ventricular global myocardial strain assessment comparing the reproducibility of four commercially available CMR-feature tracking algorithms. Eur Radiol 28:5137–5147
3. Barreiro-Perez M, Curione D, Symons R et al (2018) Left ventricular global myocardial strain assessment comparing the reproducibility of four commercially available CMR-feature tracking algorithms. Eur Radiol 28:5137–5147
4. Claus P, Omar AMS, Pedrizzetti G et al (2015) Tissue tracking technology for assessing cardiac mechanics: principles, normal values, and clinical applications. JACC Cardiovasc Imaging 8:1444–1460
5. Flecknell P (2002) Replacement, reduction and refinement. Altex 19:73–78
6. Heining P, Ruysschaert T (2016) The use of minipig in drug discovery and development: pros and cons of minipig selection and strategies to use as a preferred nonrodent species. Toxicol Pathol 44:467–473
7. Helle-Valle TM, Yu W-C, Fernandes VRS et al (2010) Usefulness of radial strain mapping by multidetector computer tomography to quantify regional myocardial function in patients with healed myocardial infarction. Am J Cardiol 106:483–491
8. Kraitchman DL, Sampath S, Castillo E et al (2003) Quantitative ischemia detection during cardiac magnetic resonance stress testing by use of FastHARP. Circulation 107:2025–2030
9. Lapinskas T, Grune J, Zamani SM et al (2017) Cardiovascular magnetic resonance feature tracking in small animals—a preliminary study on reproducibility and sample size calculation. BMC Med Imaging 17:51
10. Lindsey ML, Kassiri Z, JaI V et al (2018) Guidelines for measuring cardiac physiology in mice. Am J Physiol Heart Circ Physiol 314:H733–H752
11. Liu S, Han J, Nacif MS et al (2012) Diffuse myocardial fibrosis evaluation using cardiac magnetic resonance T1 mapping: sample size considerations for clinical trials. J Cardiovasc Magn Res 14:90
12. Moody WE, Taylor RJ, Edwards NC et al (2015) Comparison of magnetic resonance feature tracking for systolic and diastolic strain and strain rate calculation with spatial modulation of magnetization imaging analysis. J Magn Res Imaging 41:1000–1012
13. Morton G, Schuster A, Jogiya R et al (2012) Inter-study reproducibility of cardiovascular magnetic resonance myocardial feature tracking. J Cardiovasc Magn Res 14:43
14. Pedrizzetti G, Claus P, Kilner PJ et al (2016) Principles of cardiovascular magnetic resonance feature tracking and echocardiographic speckle tracking for informed clinical use. J Cardiovasc Magn Res 18:51
15. Sampath S, Parimal AS, Feng D et al (2017) Quantitative MRI biomarkers to characterize regional left ventricular perfusion and function in nonhuman primates during dobutamine-induced stress: a reproducibility and reliability study. J Magn Res Imaging 45:556–569
16. Schmidt B, Dick A, Treutlein M et al (2017) Intra- and inter-observer reproducibility of global and regional magnetic resonance feature tracking derived strain parameters of the left and right ventricle. Eur J Radiol 89:97–105
17. Schneeweis C, Lapinskas T, Schnackenburg B et al (2014) Comparison of myocardial tagging and feature tracking in patients with severe aortic stenosis. J Heart Valve dis 23:432–440
18. Schneeweis C, Qiu J, Schnackenburg B et al (2014) Value of additional strain analysis with feature tracking in dobutamine stress cardiovascular magnetic resonance for detecting coronary artery disease. J Cardiovasc Magn 16:72
19. Schuster A, Hor Kan N, Kowallick Johannes T et al (2016) Cardiovascular magnetic resonance myocardial feature tracking. circulation. Cardiovasc Imaging 9:e004077
20. Schuster A, Morton G, Hussain ST et al (2013) The intra-observer reproducibility of cardiovascular magnetic resonance myocardial feature tracking strain assessment is independent of field strength. Eur J Radiol 82:296–301
21. Schuster A, Paul M, Bettencourt N et al (2015) Myocardial feature tracking reduces observer-dependence in low-dose dobutamine stress cardiovascular magnetic resonance. PLoS ONE 10:e0122858
22. Schuster A, Stahnke VC, Unterberg-Buchwald C et al (2015) Cardiovascular magnetic resonance feature-tracking assessment of

myocardial mechanics: Intervendor agreement and considerations regarding reproducibility. Clin Radiol 70:989–998
23. Swoboda PP, Larghat A, Zaman A et al (2014) Reproducibility of myocardial strain and left ventricular twist measured using complementary spatial modulation of magnetization. J Magn Res Imaging 39:887–894
24. Tsang HG, Rashdan NA, Whitelaw CBA et al (2016) Large animal models of cardiovascular disease. Cell Biochem Funct 34:113–132
25. Voelkl B, Vogt L, Sena ES et al (2018) Reproducibility of preclinical animal research improves with heterogeneity of study samples. PLoS Biol 16:e2003693
26. Yamada A, Luis SA, Sathianathan D et al (2014) Reproducibility of regional and global longitudinal strains derived from two-dimensional speckle-tracking and doppler tissue imaging between expert and novice readers during quantitative dobutamine stress echocardiography. J Am Soc Echocardiogr 27:880–887
27. Yoon SJ, Yoon DY, Cho YK et al (2017) Characteristics and quality of published animal research in the field of radiology. Acta Radiol 58:685–691
28. Zhong J, Liu W, Yu X (2008) Characterization of three-dimensional myocardial deformation in the mouse heart: an MR tagging study. J Magn Res Imaging 27:1263–1270

8 Curriculum Vitae

My curriculum vitae does not appear in the electronic version of my paper for reasons of data protection.

9 Complete list of publications including impact factors

Blood-Oxygen-Level Dependent (BOLD) T2-Mapping Reflects Invasively Measured Central Venous Oxygen Saturation in Cardiovascular Patients.

Alogna A, **Faragli A**, Kolp C, Doeblin P, Tanacli R, Confortola G, Oetvoes J, Perna S, Stehning C, Nagel E, Pieske BM, Post H, Kelle S.

JACC Cardiovasc Imaging. 2023 Feb;16(2):251-253. doi: 10.1016/j.jcmg.2022.08.020. Epub 2022 Nov 16. **(Impact Factor: 16.051)**

A cross-sectional analysis of post-acute COVID-19 symptoms.

Perna S, Abdulsattar S, Alalwan TA, Zahid MN, Gasparri C, Peroni G, **Faragli A**, La Porta E, Ali Redha A, Janahi EM, Rondanelli M.

Ann Ig. 2022 Set-Oct;34(5):478-489. doi: 10.7416/ai.2022.2508. **(Impact Factor: 2.121)**

COVID-19 Knowledge, Attitudes, and Preventive Measures of University Students in Bahrain.

Perna S, Bahar K, Alalwan TA, Zahid MN, Gasparri C, Peroni G, **Faragli A**, La Porta E, Ali Redha A, Janahi EM, Ibrahim S, Rondanelli M.

Ann Ig. 2022 Jul-Aug;34(4):398-409. doi: 10.7416/ai.2022.2507. **(Impact Factor: 2.121)**

Brief Research Report: Quantitative Analysis of Potential Coronary Microvascular Disease in Suspected Long-COVID Syndrome.

Doeblin P, Steinbeis F, Scannell CM, Goetze C, Al-Tabatabaee S, Erley J, **Faragli A**, Pröpper F, Witzenrath M, Zoller T, Stehning C, Gerhardt H, Sánchez-González J, Alskaf E, Kühne T, Pieske B, Tschöpe C, Chiribiri A, Kelle S.

Front Cardiovasc Med. 2022 May 31;9:877416. doi: 10.3389/fcvm.2022.877416. eCollection 2022. **(Impact Factor: 5.846)**

The role of kidney dysfunction in COVID-19 and the influence of age.

La Porta E, Baiardi P, Fassina L, **Faragli A**, Perna S, Tovagliari F, Tallone I, Talamo G, Secondo G, Mazzarello G, Esposito V, Pasini M, Lupo F, Deferrari G, Bassetti M, Esposito C.

Sci Rep. 2022 May 23;12(1):8650. doi: 10.1038/s41598-022-12652-0. **(Impact Factor: 4.379)**

Predicting visceral adipose tissue in older adults: A pilot clinical study.

Perna S, **Faragli A**, Spadaccini D, Peroni G, Gasparri C, Al-Mannai MA, Casali PM, La Porta E, Kelle S, Alogna A, Rondanelli M.

Clin Nutr. 2022 Apr;41(4):810-816. doi: 10.1016/j.clnu.2022.02.008. Epub 2022 Feb 17. **(Impact Factor: 7.634)**

The Ketogenic Diet: Is It an Answer for Sarcopenic Obesity?

Ilyas Z, Perna S, A Alalwan T, Zahid MN, Spadaccini D, Gasparri C, Peroni G, **Faragli A**, Alogna A, La Porta E, Ali Redha A, Negro M, Cerullo G, D'Antona G, Rondanelli M.

Nutrients. 2022 Jan 30;14(3):620. doi: 10.3390/nu14030620. **(Impact Factor: 6.706)**

COVID-19 vs. Classical Myocarditis Associated Myocardial Injury Evaluated by Cardiac Magnetic Resonance and Endomyocardial Biopsy.

Tanacli R, Doeblin P, Götze C, Zieschang V, **Faragli A**, Stehning C, Korosoglou G, Erley J, Weiss J, Berger A, Pröpper F, Steinbeis F, Kühne T, Seidel F, Geisel D, Cannon Walter-Rittel T, Stawowy P, Witzenrath M, Klingel K, Van Linthout S, Pieske B, Tschöpe C, Kelle S.

Front Cardiovasc Med. 2021 Dec 24;8:737257. doi: 10.3389/fcvm.2021.737257. eCollection 2021. **(Impact Factor: 5.846)**

Out-of-Hospital Care of Heart Failure Patients During and After COVID-19 Pandemic: Time for Telemedicine?

Faragli A, La Porta E, Campana C, Pieske B, Kelle S, Koehler F, Alogna A.

Front Digit Health. 2020 Nov 12;2:593885. doi: 10.3389/fdgth.2020.593885. eCollection 2020.

In-hospital Heart Rate Reduction With Beta Blockers and Ivabradine Early After Recovery in Patients

With Acute Decompensated Heart Failure Reduces Short-Term Mortality and Rehospitalization.

Faragli A, Di Tano G, De Carlini C, Nassiacos D, Gori M, Confortola G, Lo Muzio FP, Rapis K, Abawi D, Post H, Kelle S, Pieske B, Alogna A, Campana C.

Front. Cardiovasc. Med., 30 July 2021, https://doi.org/10.3389/fcvm.2021.665202 **(Impact Factor: 5.846)**

Non-invasive CMR-Based Quantification of Myocardial Power and Efficiency Under Stress and Ischemic Conditions in Landrace Pigs

Faragli A, Alogna A, Lee CB, Zhu M, Ghorbani N, Lo Muzio FP, Schnackenburg B, Stehning C, Kuehne T, Post H, Goubergrits L, Nagel E, Pieske B, Kelle S, Kelm M.

Front. Cardiovasc. Med., 26 July 2021 | https://doi.org/10.3389/fcvm.2021.689255 **(Impact Factor: 5.846)**

Volume Balance in Chronic Kidney Disease: Evaluation Methodologies and Innovation Opportunities.

La Porta E, Lanino L, Calatroni M, Caramella E, Avella A, Quinn C, **Faragli A,** Estienne L, Alogna A, Esposito P.

Kidney Blood Press Res. 2021 Jul 7:1-15. doi: 10.1159/000515172. **(Impact Factor: 2.687)**

The non-invasive assessment of myocardial work by pressure-strain analysis: clinical applications.

Abawi D, Rinaldi T, **Faragli A**, Pieske B, Morris DA, Kelle S, Tschöpe C, Zito C, Alogna A.

Heart Fail Rev. 2021 May 26. doi: 10.1007/s10741-021-10119-4. **(Impact Factor: 4.214)**

The "TIDE"-Algorithm for the Weaning of Patients With Cardiogenic Shock and Temporarily Mechanical Left Ventricular Support With Impella Devices. A Cardiovascular Physiology-Based Approach.

Tschöpe C, Spillmann F, Potapov E, **Faragli A**, Rapis K, Nelki V, Post H, Schmidt G, Alogna A.

Front Cardiovasc Med. 2021 Feb 19;8:563484. doi: 10.3389/fcvm.2021.563484. eCollection 2021. **(Impact Factor: 5.846)**

A Random Shuffle Method to Expand a Narrow Dataset and Overcome the Associated Challenges in a Clinical Study: A Heart Failure Cohort Example.

Fassina L, **Faragli A**, Lo Muzio FP, Kelle S, Campana C, Pieske B, Edelmann F, Alogna A.

Front Cardiovasc Med. 2020 Nov 20;7:599923. doi: 10.3389/fcvm.2020.599923. eCollection 2020. **(Impact Factor: 5.846)**

Cardiovascular magnetic resonance-derived left ventricular mechanics-strain, cardiac power and end-systolic elastance under various inotropic states in swine.

Faragli A, Tanacli R, Kolp C, Abawi D, Lapinskas T, Stehning C, Schnackenburg B, Lo Muzio FP, Fassina L, Pieske B, Nagel E, Post H, Kelle S, Alogna A.

J Cardiovasc Magn Reson. 2020 Nov 30;22(1):79. doi: 10.1186/s12968-020-00679-z. **(Impact Factor: 5.364)**

Case Report First-in-Man Method Description: Left Ventricular Unloading With iVAC2L During Veno-Arterial Extracorporeal Membrane Oxygenation: From Veno-Arterial Extracorporeal Membrane Oxygenation to ECMELLA to EC-iVAC®.

Tschöpe C, Alogna A, **Faragli A**, Klingel K, Schmidt G, Heilmann TW, B Bastos M, Spillmann F.

Front Cardiovasc Med. 2020 Sep 25;7:563448. doi: 10.3389/fcvm.2020.563448. eCollection 2020. **(Impact Factor: 5.846)**

Estimation of total collagen volume: a T1 mapping versus histological comparison study in healthy Landrace pigs.

Faragli A, Merz S, Muzio FPL, Doeblin P, Tanacli R, Kolp C, Abawi D, Ötvös J, Stehning C, Schnackenburg B, Pieske B, Post H, Klopfleisch R, Alogna A, Kelle S.

Int J Cardiovasc Imaging. 2020 Sep;36(9):1761-1769. doi: 10.1007/s10554-020-01881-x. Epub 2020 May 14. **(Impact Factor: 2.357)**

DXA-Derived Visceral Adipose Tissue (VAT) in Elderly: Percentiles of Reference for Gender and Association with Metabolic Outcomes.

Spadaccini D, Perna S, Peroni G, D'Antona G, Iannello G, **Faragli A**, Infantino V, Riva A, Petrangolini G, Negro M, Gasparri C, Rondanelli M.

Life (Basel). 2020 Aug 24;10(9):163. doi: 10.3390/life10090163. **(Impact Factor: 3.817)**

The role of non-invasive devices for the telemonitoring of heart failure patients.

Faragli A, Abawi D, Quinn C, Cvetkovic M, Schlabs T, Tahirovic E, Düngen HD, Pieske B, Kelle S, Edelmann F, Alogna A.

Heart Fail Rev. 2020 Apr 27. doi: 10.1007/s10741-020-09963-7. **(Impact Factor: 4.214)**

Control of ventricular unloading using an electrocardiogram-synchronized pulsatile ventricular assist device under high stroke ratios.

Magkoutas K, Rebholz M, Sündermann S, Alogna A, **Faragli A**, Falk V, Meboldt M, Schmid Daners M.

Artif Organs. 2020 Apr 22. doi: 10.1111/aor.13711. **(Impact Factor: 3.094)**

Cardiovascular magnetic resonance feature tracking in pigs: a reproducibility and sample size calculation study.

Faragli A, Tanacli R, Kolp C, Lapinskas T, Stehning C, Schnackenburg B, Lo Muzio F-P, Perna S, Pieske B, Nagel E, Post H, Kelle S, Alogna A.

The International Journal of Cardiovascular Imaging 2020 - https://doi.org/10.1007/s10554-020-01767-y. **(Impact Factor: 2.357)**

Thermodilution vs estimated Fick cardiac output measurement in an elderly cohort of patients: A single-centre experience.

Kresoja K-P, **Faragli A**, Abawi D, Paul O, Pieske B, Post H, Alogna A.

PLoS ONE 2019 - 14(12): e0226561. https://doi.org/10.1371/journal.pone.0226561. **(Impact Factor: 3.240)**

Cardiac power output accurately reflects external cardiac work over a wide range of inotropic states in pigs.

Abawi D, **Faragli A**, Schwarzl M, Manninger M, Zweiker D, Kresoja K, Verdeber J, Zirngast B, Maechler H, Steendijk P, Pieske B, Post H, Alogna A.

BMC Cardiovasc Disord. 2019 Oct 15;19(1):217. doi: 10.1186/s12872-019-1212-2. **(Impact Factor: 2.298)**

The CardioMEMS system in the clinical management of end-stage heart failure patients: three case reports.

Tschöpe C, Alogna A, Spillmann F, **Faragli A**, Schmidt G, Blaschke F, Kühl U, Hertel E, Willner M, Morris D, Post H, Noutsias M, Pieske B, Krackhardt F.

BMC Cardiovasc Disord. 2018 Jul 31;18(1):155. doi: 10.1186/s12872-018-0883-4. **(Impact Factor: 2.298)**

Cardiovascular screening in low-income settings using a novel 4-lead smartphone-based electrocardiograph (D-Heart®).

Maurizi N, **Faragli A**, Imberti J, Briante, N., Targetti, M., Baldini, K, Sall, A, Cisse A, Berzolari FG, Borrelli P, Avvantaggiato F, Perlini, S, Marchionni N, Cecchi F, Parigi GB, Olivotto I.

International Journal of Cardiology 2017 http://dx.doi.org/10.1016/j.ijcard.2017.02.027. **(Impact Factor: 4.164)**

Neuroinflammation, immune system and Alzheimer disease: searching for the missing link.

Guerriero F, Sgarlata C, Francis M, Maurizi N, **Faragli A**, Perna S, Rondanelli M, Rollone M, Ricevuti G.

Aging Clin Exp Res. 2017 Oct;29(5):821-831. doi: 10.1007/s40520-016-0637-z. Epub 2016 Oct 7. **(Impact Factor: 3.636)**

Arrhythmogenic right ventricular cardiomyopathy: Clinical course and predictors of arrhythmic risk.

Mazzanti A, Ng K, **Faragli A**, Chiodaroli E, Maragna R, Orphanou N, Monteforte N, Memmi M, Gambelli P, Novelli V, Bloise R, Catalano O, Moro G, Tibollo V, Morini M, Bellazzi R, Napolitano C, Bagnardi V, Priori SG.

J Am Coll Cardiol. 2016 Dec 13;68(23):2540-2550. doi: 10.1016/j.jacc.2016.09.951. **(Impact Factor: 24.094)**

Gene-Specific Therapy with Mexiletine reduces Arrhythmic Events in patients with Long QT Syndrome Type 3.

Mazzanti A, Maragna R, **Faragli A,** Monteforte N, Bloise R, Memmi M, Novelli V, Baiardi P, Bagnardi V, Etheridge SP, Napolitano C, Priori SG.

J Am Coll of Cardiol. 2016 Mar 8;67(9):1053-8. doi: 10.1016/j.jacc.2015.12.033. **(Impact Factor: 24.094)**

Is there a role for genetics in the prevention of sudden cardiac death?

Faragli A, Underwood K, Priori SG, Mazzanti A.

Journal of Cardiovasc. Electrophysiol, 2016 Jun 9. doi: 10.1111/jce.13028. **(Impact Factor: 2.693)**

10 Acknowledgements

I would like to thank my supervisors: Prof. Sebastian Kelle and Dr. Alessio Alogna. Thank you for being my mentors, I have learnt how to be a better scientist and a better clinician. A big thank to all my collegues at the Experimental Cardiology Lab at Charitè, to the FEM at Charitè, to the MRI team at DHZB and to the MRI Core Lab for working together all these years. In specific, I would like to thank: Carolin Kolp, Jens Ötvöes, Radu Tanacli, Christian Stehning, Patrick Doeblin, Alexander Berger, Corinna Else, Gudrun Grosser. Moreover, I would like to thank one of my first mentors that helped me to start all this: Dr. Heiner Post.

A great thank for the support and patience in all these years of work and research goes to my wife, Aneta. This work is dedicated to the memory of my father, to my mother and to the love for my children.